Boletín de la Sociedad Geológica del Perú

Journal Homepage: www.sgp.org.pe ISSN 0079-1091

Lithofacies Patterns and Paleogeography of the Miocene Chilcatay and lower Pisco Depositional Sequences (East Pisco Basin, Peru)

Thomas J. DeVries[1], Nathan A. Jud[2]

[1] Burke Museum of Natural History and Culture, University of Washington, Box 353010, Seattle, WA 98195, USA (tomdevrie@aol.com)
[2] L.H. Bailey Hortorium, Department of Plant Biology, 412 Mann Library Building, Cornell University, Ithaca, NY 14853, USA (nathan.jud@cornell.edu)

ABSTRACT

The Chilcatay and Pisco depositional sequences consist of marine forearc sediments of Oligocene to Pliocene age in the East Pisco Basin of southern Peru. Both sequences are notable for their content of vertebrate and invertebrate fossils. Attention is focused here on four early and middle Miocene stratigraphic intervals defined temporally with radiometric ages and microfossils. During these four intervals, three lithofacies – lag deposits of bioclasts, igneous-rock boulders, and lithoclasts; massive bioturbated sands with paired valves of venerids and transported palm tree debris; and bioclastic sand and oyster-barnacle coquina – were deposited in four geographically distinct coastal areas: in waters facing an open shoreline, within an archipelago, and within two embayments. Intervening periods when deposition of fine-grained sediments, pelagic diatoms, benthic foraminifera, and sardine scales prevailed are not the subject of this study. Ravinement and forced-regression surfaces between major sequences and lesser parasequences correlate with global sea-level excursions during the latest Oligocene, early Miocene, and early middle Miocene. Evidence indicates that soon after the Chilcatay transgression commenced, a tsunami produced a backwash debris flow with large boulders of crystalline basement rock and odontocete carcasses. Sets of clinoform beds attributed to sub-aqueous marine deltas formed during the late early Miocene, but only on the eastern side of the embayments. An early phase of the middle Miocene Pisco transgression is recorded within one embayment. A second and more significant phase quickly ensued, spreading sand across most of the East Pisco Basin. Contemporaneous shallow subtidal sand flats and lagoons developed in the lee of a high-angle normal fault east of one embayment and behind hills of crystalline basement rock farther north in the basin. Evidence for a Miocene "Golfo de Pisco" is weak, but evidence for a seaward landmass during the middle Eocene exists, so the possibility remains of such a landmass during the Miocene.

RESUMEN

Las secuencias deposicionales Pisco y Chilcatay consisten en sedimentos de antearco correspondientes del Oligoceno al Plioceno, de la Cuenca Pisco Este, al sur del Perú. Ambas secuencias son notables por su contenido en fósiles de vertebrados e invertebrados. La atención acá se focaliza en cuatro niveles estratigráficos del Mioceno temprano-medio, definidos por edades radiométricas y microfósiles. Durante estos cuatro intervalos, tres litofacies - depósitos retardados de bioclastos, cantos rodados de rocas ígneas y litoclastos; arenas con alta bioturbación con conchas de venéridos presentando ambas valvas articuladas y restos de palmas transportados; y arena bioclástica con coquinas compuestas de percebes y ostras - fueron depositadas en cuatro áreas costeras geográficamente diferentes: aguas de un límite costero abierto, dentro de un archipiélago y entre dos embalsamientos. Los periodos que intercalan con deposición predominante de sedimentos de grano fino, diatomeas pelágicas, foraminíferos bénticos y escamas de sardinas no son sujeto de este estudio. Superficies de regresión

forzadas y tipo barranco, entre las secuencias mayores y las parasecuencias menores se correlacionan con las variaciones en el nivel global del mar durante el final del Oligoceno, el Mioceno temprano y el Mioceno medio inferior. La evidencia indica que poco después del inicio de la transgresión Chilcatay, un tsunami produjo un retrolavado con flujo de grandes rocas cristalinas de basamento y carcasas de cetáceos dentados. Series de camas clinoformicas atribuidas a deltas marinos sub-acuíferos fueron formadas hacia el fin del Mioceno temprano, pero solo en el lado este de los embalsamientos. Una fase temprana de las transgresiones del Mioceno medio, pero solo en una de las bahías. Una segunda y mucha más notoria fase surgió, depositando arena a lo largo de toda la Cuenca Pisco Este. Contemporáneamente llanos de arena y lagunas marinas se desarrollaron en el límite de una falla angular aguda, al este de una bahía y detrás de las colinas de roca cristalina, mucho más al norte de la cuenca. La evidencia para un "Golfo de Pisco" durante el Mioceno es débil, pero evidencia para una masa de tierra durante el Eoceno medio existe; sugiriendo su continuidad durante el Mioceno.

Palabras claves: Stratigraphy, lithofacies, Miocene, Chilcatay, Pisco, Peru, East Pisco Basin

1. Introduction

The Chilcatay and Pisco depositional sequences comprise marine bioclastic sandstone and diatomaceous and tuffaceous silty sandstone of two like-named formations in the East Pisco Basin of southern Peru (DeVries, 1998) (Figure 1A). Together, the two sequences span the latest Oligocene to Pliocene (DeVries, 1998) (Figure 1B). Chilcatay and Pisco beds are most noted for their fossil sharks (Ehret et al., 2012), cetaceans (Muizon, 1988; Lambert et al., 2010, Bianucci et al., 2015), seals (Varas-Malca and Valenzuela-Toros, 2011), penguins (Stucchi, 2007; Clarke et al, 2007, 2010), and seabirds (Stucchi, 2003; Stucchi et al., 2016), but they also host a diverse molluscan fauna (DeVries, 1995, 2003, 2007, 2008, 2016a, 2016b).

This paper is an overview of the lithofacies patterns prevalent in the East Pisco Basin and the associated paleogeography during Chilcatay and early Pisco time (Figure 1C). Attention is given to four time slices (Figure 1B): (1) the latest Oligocene to earliest Miocene, when the Chilcatay transgression was just underway; (2) the middle early Miocene, when the waters of the East Pisco Basin experienced a shoaling event; (3) the late early Miocene, when the Chilcatay transgression was at its maximum and clinoform allosequences were locally developed; and (4) the early middle Miocene, when the Pisco transgression was in its early stages. These time intervals were characterized by the deposition of coarse-grained, bioclastic, mollusk-bearing sediments. Intervening periods were characterized by the deposition of silty sand with diatoms, foraminifera, and scales of neritic and pelagic fishes, but few preserved mollusks.

2. Methods

2.1. Procedures

The observations presented in this paper represent over thirty years of fieldwork in the East Pisco Basin. Localities were once located on 1:100,000 quadrangle maps of the Peru's Instituto Geográfico Militar (now the Instituto Geográfico Nacional). For the past fifteen years, localities have been recorded with GPS coordinates and mapped to Google Earth imagery. Localities cited in the text and figure captions are listed with latitudes and longitudes in Appendix I. DeVries localities noted in the text have the prefix "DV." Localities of José Macharé, visited in the 1980s, have a two number year code followed the prefix "JM."

Sections were measured using standard field techniques, a Brunton compass, and Jacob's staff. Molluscan faunas were compared with those described in Chile by Philippi (1887) and Nielsen (2003) and in Peru by Olsson (1932), among others. Place names were taken from quadrangle maps, where names existed, and informal place names were created when needed (Figures 1D, 1E, 1F). Samples for diatoms were collected in the 1980s by the author and by Hans Schrader and Peter Rønning, both then with the Oppgave Geologisk Institutt Avdeling B, Universitetet I, in Bergen, Norway. Age ranges of specific diatom taxa have been re-stated using current biostratigraphic interpretations. Ash samples were collected in 1987 and analyzed for ^{40}Ar-^{39}Ar ages by Lawrence Snee, then with the Department of Geological Sciences, Oregon State University, Corvallis, Oregon, USA. Representative molluscan samples have been deposited with the Departamento de Paleontología de Vertebrados, Museo de Historia Natural Javier Prado, Universidad Nacional Mayor de San Marcos, in Lima, Peru.

From a hand sample of wood from locality DV 8087-1, thin sections were prepared by one author (N. Jud) using standard thin-sectioning techniques (Haas and Rowe, 1999). Wafers cut in transverse section were mounted onto slides using epoxy and then ground down to ~30 μm thick. Canada Balsam and cover slips were applied and the slides were examined using light microscopy. Images of microscopic features were captured with Canon EOS digital camera mounted on a Nikon compound microscope and were processed with Adobe Photoshop (San Jose, California, USA). The descriptions and terminology of the palm follow the recommendations of Thomas and De Franceschi (2013). The specimens and slides are housed at the Florida Museum of Natural History Paleobotanical Collections, Gainesville, Florida, USA.

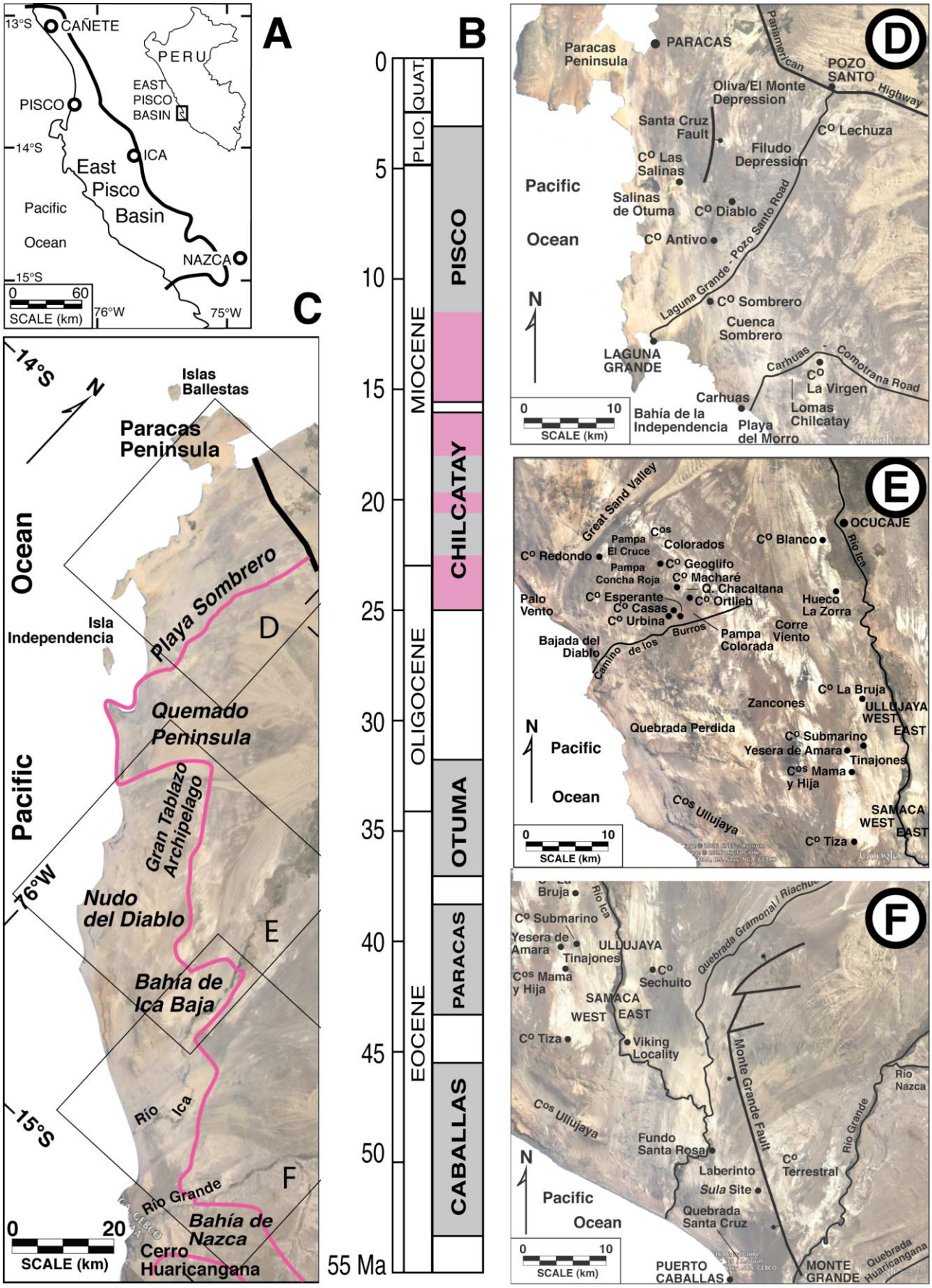

Figure 1. *Geography, stratigraphy, and paleogeography of the East Pisco Basin. A. Location of the East Pisco Basin. B. Stratigraphic column of Cenozoic sequences/formations in the East Pisco Basin (DeVries, 1998, 2004, 2017; DeVries and Schrader, 1997; DeVries et al., 2006, 2017). Rose-colored bands mark the four time intervals discussed in detail in this paper. C. Paleogeography of the East Pisco Basin during the early to middle Miocene. Lithofacies along Playa Sombrero, in the Gran Tablazo Archipelago, Bahía de Ica Baja, and Bahía de Nazca, are discussed in the text, as is the complexity of the geology in the Nudo del Diablo and scarcity of outcrop covering the Quemado Peninsula. D. Published and informally introduced place names between the town of Paracas and the Carhuas-Comotrana Road. E. Published and informally introduced place names between Cerros Colorados and the reach of the Río Ica known as Samaca. F. Published and informally introduced place names between Cerro La Bruja and Puerto Caballas.*

2.2. Lithostratigraphy vs. sequence stratigraphy in the East Pisco Basin

Traditional lithostratigraphic principles were employed by Petersen (1954) and Newell (1956) in the description of the Paracas (Eocene) and Pisco (Miocene and Pliocene) formations of the East Pisco Basin. Dunbar et al. (1990) departed from previous practice by applying separate formational names to the basal Eocene sandstone (Los Choros) and the overlying silty Eocene sandstone (Yumaque). They chose not to apply the same naming convention to the Pisco or Chilcatay formations.

The usefulness of traditional lithostratigraphic nomenclature in the East Pisco Basin is debatable (DeVries et al., 2017). All formations in the basin exhibit two predominant lithologies: yellow-orange, massive or bioclastic and bedded sandstone, typically basal but also intermittently appearing at higher levels; and white weathering silty sandstone, often diatomaceous or tuffaceous, in the upper part of the formations. It is not uncommon for Chilcatay and Pisco or even Paracas and Chilcatay basal sandstones to be contiguous. Two such sandstones, therefore, could unhelpfully be construed to constitute one lithostratigraphic unit, despite having an age difference of 10^6 to 10^7 years.

Employing stratigraphic units defined by bounding unconformities is more useful for reconstructing the geological history of the East Pisco Basin. Whether the unconformities should be inferred to represent erosional and flooding surfaces related to basin-wide or global sea-level change, as is true for sequence stratigraphy, or are assigned no *a priori* genetic significance, as is the case for allostratigraphy, is an enduring discussion (van Wagoner et al., 1988; Posamentier and James, 1993; Bhattacharya, 2005; Catuneanu et al., 2009). For purposes of this study, thick packages (10^2 m) of unconformity-bound, genetically related, successive strata, typically with increasingly fine-grained lithologies up-section that represent increasingly deeper-water marine environments, are referred to as depositional sequences, with names (Paracas, Otuma, Chilcatay, Pisco) that match traditionally employed formational names (Dunbar et al., 1990; Montoya et al., 1994; DeVries, 1998; DeVries, 2017; DeVries et al., 2017). Sequences at the smallest scale, i.e., clinoform sets in the upper Chilcatay depositional sequence, are termed allosequences, recognizing that the geographic restriction of clinoform sets to the heavily faulted Ica valley indicates that their bounding unconformities might not result from basin-wide or global sea level changes. Sequences of intermediate scale (10^2 km^2, thicknesses of 10^1 m), termed allosequences by Di Celma et al. (2017), are referred to as parasequences, i.e., their bounding unconformities are inferred to have formed in response to basin-wide or global sea-level changes.

3. Background

3.1. History and overview

The name "Pisco Formation" was introduced by Adams (1906, 1909) and further described by Steinmann (1930). The Miocene and Pliocene strata were differentiated from Eocene strata, first by Rüegg (1948) and Gutiérrez (1948), who introduced the designation "Paracas Formation," and subsequently by Stainforth and Rüegg (1953) and Rüegg (1956). Further treatments of the Pisco Formation (*sensu strictu*) soon followed (Petersen, 1954; Newell, 1956; Rivera, 1957), with additional studies coming much later (Muizon and DeVries, 1985; Marocco and Muizon, 1988; Dunbar et al., 1990; DeVries and Schrader, 1997; DeVries, 1998; Brand et al., 2011; Esperante et al., 2015; Di Celma et al., 2017). Exposures extend from north of Pisco south to Nazca (Figure 1A).

The Pisco depositional sequence consists of bioclastic pale yellow sandstone or massive, bioturbated, orange sandstone overlain by tuffaceous and diatomaceous white silty sandstone, a pair of successive lithofacies that can repeat more than once within the sequence (Di Celma et al., 2017). Pisco strata are usually separated by a disconformable or unconformable forced regression surface from underlying silty sandstone of the Chilcatay depositional sequence (Figures 2A, 2B, 2C, 2D) or, rarely, tree trunk-bearing marine sandstone of early Oligocene Otuma beds (Figure 2E). Near Ocucaje, Cerro Sechuito (Figures 1F, 2F) and east of Quebrada Riachuelo (Figure 2G), Pisco sandstones and coquinas nonconformably onlap a rugged and often precipitous paleo-terrain of crystalline basement rock (CBR).

A lithostratigraphic unit of uppermost Oligocene to lower Miocene age, distinct from the Pisco Formation, was first identified by José Macharé (Macharé, 1987; Macharé and Fourtanier, 1988; Macharé et al., 1988). Its original name, "Caballas," was already in use for a lower Eocene formation in the East Pisco Basin (Dávila 1989; Dávila et al., 1987), so in 1989 the name "Chilcatay Formation" was adopted and a type section designated in the Lomas Chilcatay (DeVries, 1988b; Dunbar et al., 1990; DeVries, 2017).

The Chilcatay depositional sequence consists of basal transgressive sandstone – orange, medium- to coarse-grained, massive, bioturbated, in places conglomeratic and bioclastic – and a thicker overlying interval of silty sandstone with varying contributions of ash and diatoms (DeVries, 1998). Chilcatay outcrops, which extend as far north as the Oliva/El Monte Depression (Figure 1D), are separated by an angular unconformity from underlying lower Oligocene silty sandstones of the Otuma sequence (Figures 3A, 3B, 3C) or by a nonconformity from underlying CBR (Lomas Chilcatay, Pampa de Poroma) (DeVries, 1998; DeVries et al., 2017; Figures 3C, 3D). In the lower Ica Valley, Chilcatay sandstone beds locally lie in angular unconformity over sandstone of the middle Eocene Los Choros Member of the Paracas Formation (Figure 3E).

3.2. Age of the Chilcatay and lower Pisco depositional sequences

Existing microfossil data and $^{40}Ar/^{39}Ar$ ages are sufficient to create a temporal framework for the development of the Chilcatay and lower Pisco sequences. Some of these data have been published or referenced in Dunbar et al. (1990), DeVries and Schrader (1997), DeVries (1998), and the Masters thesis of Rønning (1990) and PhD dissertation of Marty (1989). Other information is published here for the first time.

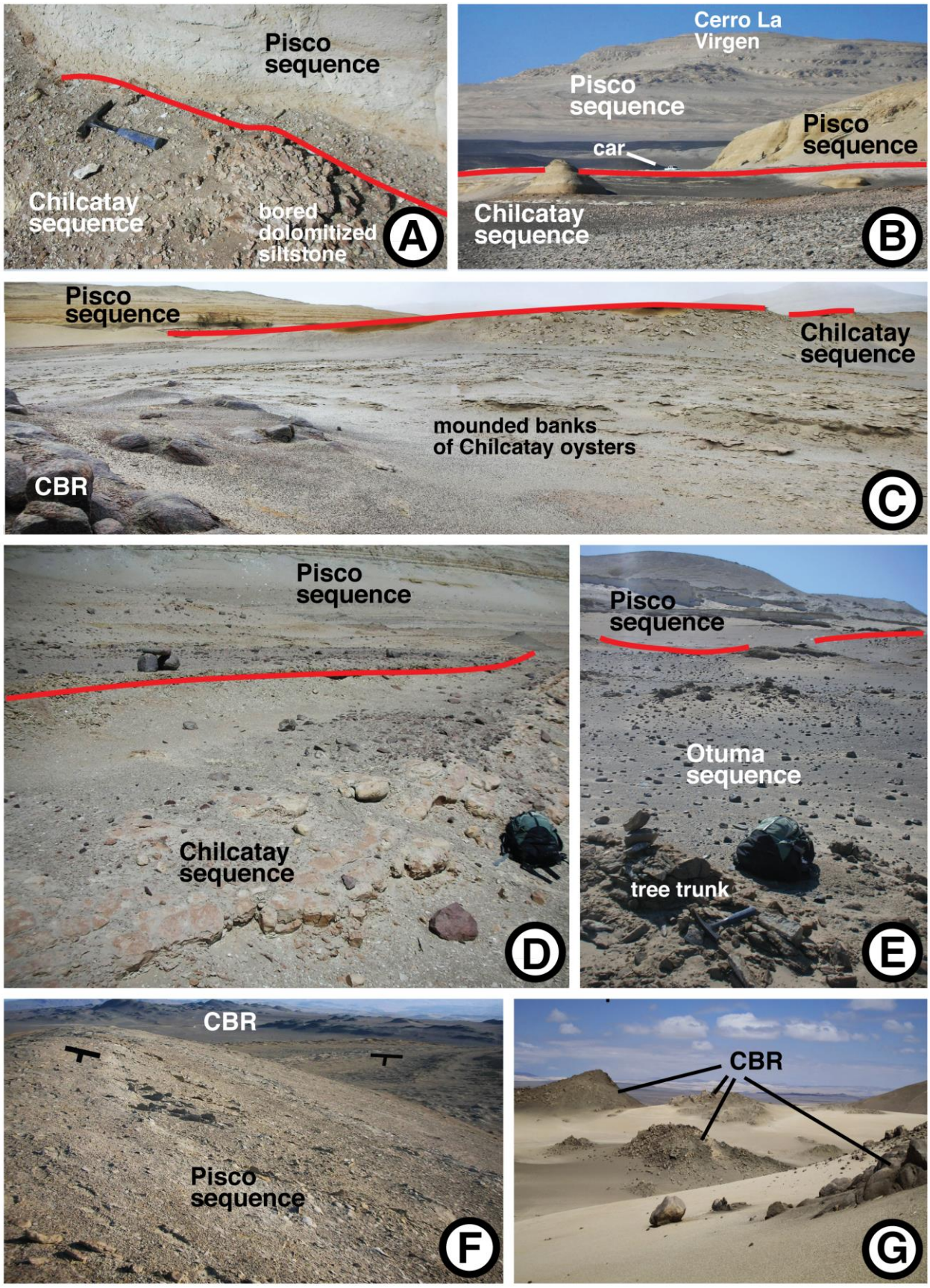

Figure 2. *Ravinement surfaces and nonconformities at the base of the Pisco depositional sequence. Red lines mark sequence boundaries. A. Ravinement surface with bored dolomite of underlying upper Chilcatay depositional sequence at Cerros Colorados (DV 2231). B. Ravinement surface near Cerro La Virgen (DV 397). Car for scale. C. Ravinement surface at southwestern foot of Cerro La Virgen (DV 4017). CBR (= crystalline basement rock) outcrop, which is about five meters across, is draped with banks of cup-and-flange Chilcatay oysters. D. Ravinement surface at northern edge of Yesera de Amara (DV 4109). Day pack for scale. E. Ravinement surface on southern face of Cerro Redondo (DV 3021; see Figure 1E). Pisco sequence lies unconformably over Otuma sequence. Day pack and hammer for scale. F. Nonconformity near Cerro Sechuito (DV 2012). Beds of Pisco depositional sequence dipping toward foreground; contact with CBE in mid-ground. Footprints in foreground for scale. G. Nonconformity east of Quebrada Riachuelo on the footwall of the Monte Grande Fault (DV 1230). White beds are late Miocene barnacle and shell banks. Boulder in center foreground is about one meter in diameter.*

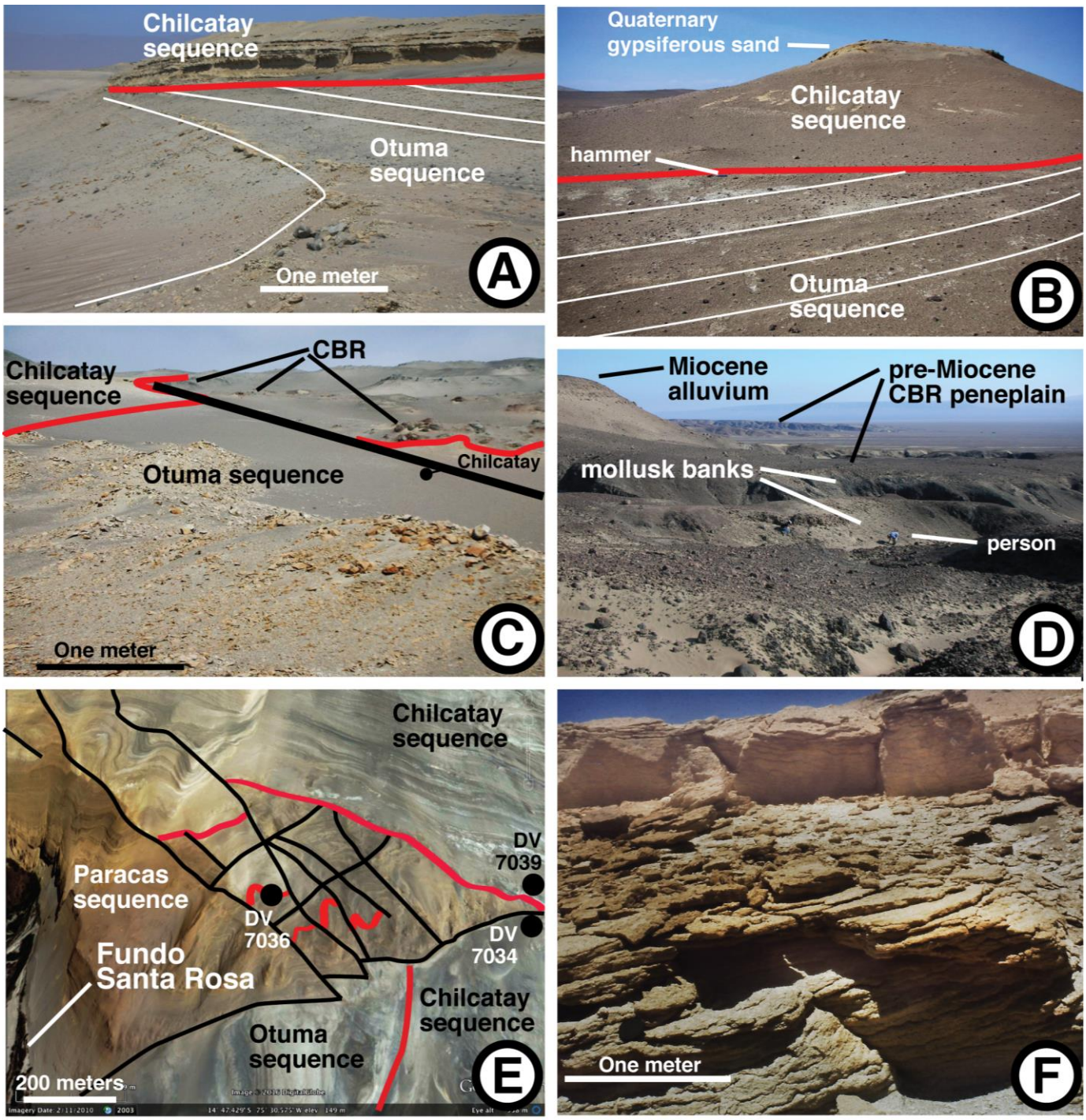

Figure 3. *Ravinement surfaces and nonconformities at the base of the Chilcatay depositional sequence. Red lines mark sequence boundaries. A. Ravinement surface and angular unconformity on the overland road to Samaca West (DV 2001). Thin white lines mark bedding planes in Otuma depositional sequence. B. Ravinement surface and angular unconformity at southeastern end of Pampa El Cruce (DV 2249). Thin white lines mark bedding planes in Otuma sequence. Knoll has an indurated cap of Quaternary gypsum-cemented sand. Hammer for scale. C. Chilcatay sequence overlying both Otuma strata and basement of CBR, south end of Lomas Chilcatay. View is 100 meters east of DV 441. D. Nonconformity on Pampa de Poroma (DV 1970). Several meters of marine bioclastic sandstone and conglomerate are overlain by Miocene alluvium. Person for scale. E. Google Earth imagery showing angular unconformity between Paracas and Chilcatay sequences. DV 7034 with outcrop of mid-Chilcatay boulder bed; DV 7039 with measured section of basal and lower Chilcatay depositional sequence, not the Pisco P0 parasequence attributed to locality by Marx et al. (2017). F. Crossbedded bioclastic sandstone with Chilcatay-age mollusks, 20 km south of Caravelí, southern Peru (DV 1256).*

Three lines of evidence support a ~25 Ma age for the onset of the Chilcatay transgression. First, two ashes from a crossbedded bioclastic marine sandstone, several meters thick, cropping out near Caravelí, 350 kilometers south of the East Pisco Basin, yielded $^{40}Ar/^{39}Ar$ dates at 24.5 +/- 0.8 Ma and 25.5 +/- 1.0 Ma (Noble et al., 1985). The marine sandstone beds (DV 1256, 1258, 1259, 1260; Figure 3F) are sandwiched between thick continental deposits (Pecho, 1983); their molluscan fauna includes Miocene gastropods (*Acanthina katzi*, *Testallium cepa*, *Olivancellaria tumorifera*) also found in the Chilcatay sequence of the East Pisco Basin (Vermeij and DeVries, 1997; DeVries, 1998, 2003). Molluscan species from the Caravelí beds that are listed and assigned to the Eocene by Pecho (1983) are incorrectly identified.

Further evidence of a late Oligocene age for the onset of the Chilcatay transgression is provided by planktonic foraminifera found by Ibaraki (1993) in silty sandstone on the southwestern flank of Cerros Las Salinas (Ibaraki sample Pe-88-7-8; Figure 1D), about 50 meters above basal Chilcatay sandstone (DV 1130, 1131) that contain index Chilcatay mollusks. The foram assemblage (*Globigerina ciperoensis*, *Paragloborotalia kugleri*, *P. pseudokugleri*) was assigned by Ibaraki (1993) to foraminiferal zones P22 to lower N4, i.e., about 23-25 Ma (Leckie et al., 1993; Berggren et al., 1995; Anthonissen and Ogg, 2012; see Clemens et al. (2016) for first and last occurrences of the three foraminiferal taxa).

The third line of evidence comes from beds of silty sandstone 25 meters above the base (DV 441-15) and 40 to 50 meters above the base (DV 395-6, 395-7) of the Chilcatay sequence in the composite Chilcatay type section (Figures 4A, 4B). These samples contain diatoms assigned by H. Schrader (December 1986, written communication) to the early Miocene silicoflagellate *Naviculopsis lata* Zone (DV 441-15) or the diatom *Rocella gelida* Zone (DV 395-6, 395-7; Barron, 1985), or, in current usage, the *Rocella gelida* Partial-Range Zone (27.6 Ma to about 24/24.5 Ma; see Baldauf and Barron, 1991). The age of basal Chilcatay beds is constrained at its oldest by the presence in DV 395-7 of *Bogorovia veniamini*, which has a first occurrence (FO) of about 26-28 Ma (Barron et al., 1985; Fourtanier, 1991; Barron et al., 2004), and *Rocella gelida*, which has a FO of 26 Ma (Barron et al., 2004; Clemens, 2016), the presence in DV 395-6 and 395-7 of *Raphidodiscus marylandicus*, with a FO in the Southern Ocean of about 20-22 Ma (Ramsey and Baldauf, 1999), and the presence in DV 441-15 of *Rossiella palacea*, with a FO in the Indian Ocean of 22.7 Ma (Fourtanier, 1991). (The latter two species indicate a zonal assignment younger than that cited by Schrader.) The age of the Chilcatay transgression is constrained at its youngest at DV 395-7 by the presence of *Rocella gelida*, with a last occurrence (LO) of 20-24 Ma (Ramsey and Baldauf, 1999; Barron et al., 2004) and *B. veniamini*, with a LO of 20-21 Ma (Fourtanier, 1991; Barron, 2006; Clemens et al., 2016); the latter species also occurs in the middle of the composite Chilcatay type section (DV 441-16, 441-17).

An age of about 25 Ma for the lower sequence boundary of the Chilcatay depositional sequence, as indicated by radiometric ages at Caravelí and the ages of diatoms and foraminifera from deeper-water deposits of the lower Chilcatay type section, correlates well with the major global seismic sequence boundary at 24-25 Ma proposed by Haq et al. (1987), Hardenbol et al. (1998), and Miller et al. (2005), as well as seismic sequence boundaries on the coastal plain of New Jersey (Miller et al., 1998).

One sample from close to the faulted juncture of CBR with the Otuma depositional sequence and the overlying base of the Chilcatay sequence (DV 441-4) contains diatoms identified by H. Schrader (written communication, 1986) that are a mix of Oligocene species (*Cestodiscus robustus*, *Melosira architecturalis*; Barron et al., 2004) and early Miocene species (*B. veniamini*, *R. marylandicus*), indicating reworking or contamination with the underlying Otuma depositional sequence or the presence of late Oligocene strata not recognized elsewhere in the basin (DV 4006, 4007, 8031).

Diatoms collected at intervals through the composite Chilcatay type section (Figure 4A) and identified by H. Schrader show successively younger biostratigraphic events involving tropical and Southern Ocean species (Ramsey and Baldauf, 1999; Barron, 2006): the LO of *B. veniamini* at about 20-21 Ma (Barron, 2006; DV 441-17), the FO of *T. fraga* at about 19-21 Ma (Harwood and Maruyama, 1992; Ramsey and Baldauf, 1999; Barron, 2006; DV 443-8), the FO of *N. maleinterpretaria* at about 17-19 Ma (Ramsey and Baldauf, 1999; Barron, 2006; DV 443-10), and the LO of *T. fraga* at about 15-18 Ma (Harwood and Maruyama, 1992; Ramsey and Baldauf, 1999; DV 443-13). Also within this section, just above 250 meters in the composite type Chilcatay section (Figure 4A), sample 84JM 407-1 contains diatoms (*N. maleinterpretaria*, *R. marylandicus*, *T. fraga*) that indicate an age of 19-17 Ma (Macharé et al., 1988).

Diatoms identified by H. Schrader from four samples provide evidence for the youngest age of Chilcatay strata. In the composite Chilcatay type section, the co-occurrence of *N. maleinterpretaria* and *T. fraga* 40 meters below the Chilcatay/Pisco unconformity (DV 397-3) indicates an age of about 19.5-15 Ma (Barron, 2006). Near the head of the canyon at Quebrada Gramonal, the occurrence of *R. marylandicus* just five meters below the Chilcatay/Pisco unconformity (DV 574-P180) indicates an age older than 16.7 Ma (Barron, 1983, 1985; Andrews, 1988; Clemens et al., 2016). Near the juncture of the Río Ica and Quebrada Gramonal, above the uppermost clinoform bioclastic sandstone and below the Chilcatay/Pisco unconformity (DV 574-P184), the co-occurrence of *Actinocyclus ingens* and *T. fraga* indicates a Southern Ocean age of about 17.5-16.8 Ma (Barron, 1985; Ramsey and Baldauf, 1999). At Yesera de Amara, four meters below the Chilcatay/Pisco unconformity (DV 542a-P105; Figure 4C), the co-occurrence of *A. ingens* and *Synedra jouseana* in tuffaceous sandstone indicates an age of 17.5-14.5 Ma (Ramsey and Baldauf, 1999). An ash bed three meters above DV 542a-P105 (Figure 4C) has yielded an $^{40}Ar/^{39}Ar$ age of 17.7 +/- 0.24 Ma (Belia et al., 2015; Belia and Nick, 2016). The latter authors mis-assign the ash bed (DV 484, 1183) to the basal Pisco Formation, which it underlies by one meter, and misattribute an older age (late Oligocene to early Miocene) to strata 20 meters below the ash bed based on nannofossils, which are likely reworked from the base of the Chilcatay Formation. Alternatively, a sliver of basal

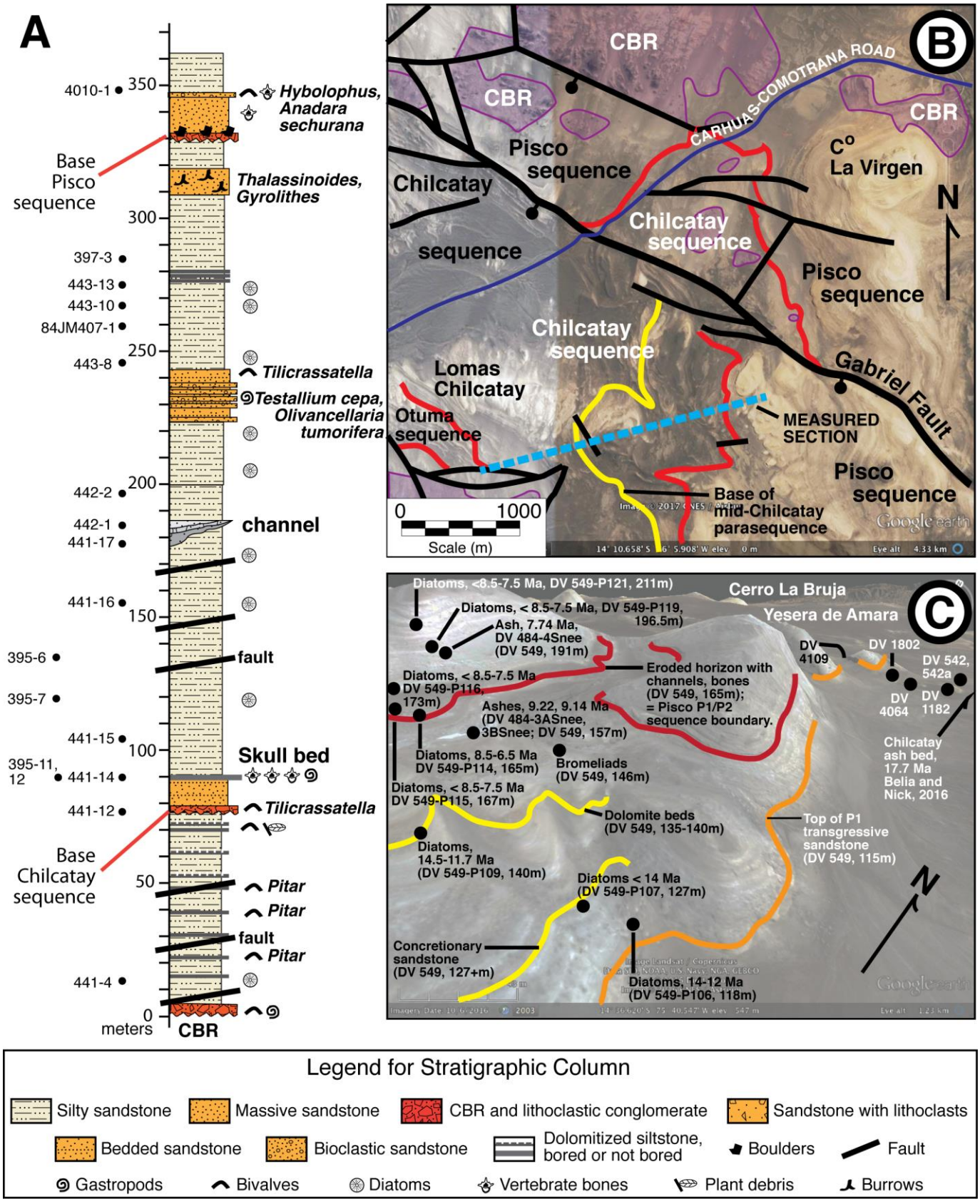

Figure 4. *Measured and mapped sections. A. Composite measured section of Chilcatay and lower Pisco sequences, Lomas Chilcatay to Cerro La Virgen. Samples from measured section (84JM407-1, DV 397-3, DV 441 series, DV 442 series, and DV 443 series and samples from nearby correlative outcrops of DV 395 series) listed at left of section. Selected molluscan and ichnofossil taxa listed at right of section. Channel and "skull bed" discussed in text. Faulted lower 50 meters of section probably with Otuma and Chilcatay beds. B. Location of measured composite section in Figure 4A mapped on a Google Earth image. Sequence boundaries are red lines. The base of the mid-Chilcatay shoaling event/parasequence is a yellow line. A NW-SE extensional structure is informally named the "Gabriel Fault." Measure section is dashed blue line. C. Oblique Google Earth image of Cerros Mama y Hija and Yesera de Amara showing radiometric and biostratigraphic data from measured section DV 549. Additional DV localities shown to north and east. Scoured surface recently designated Pisco P1/P2 sequence boundary by Di Celma et al. (2017) shown as red line.*

Chilcatay beds may crop out in the highly faulted Río Ica valley.

Evidence for the age of the lower Pisco sequence is also provided by diatoms (DeVries and Schrader, 1997). In Pisco sediments that overlie the Chilcatay type section near Cerro La Virgen (DV 480-1, 480-2, 480-4, 480-5; Figures 1D, 4A), the presence of *Denticulopsis hustedtii* throughout the lower Pisco section confirms an age younger than about 14.5 Ma, a conclusion supported by the absence of *S. jouseana* (Ramsey and Baldauf, 1999). *Denticulopsis hustedtii* also occurs at Cerro Lechuza (DV 417-3). The presence of both *Mediaria splendida* and *D. hustedtii* in samples near Cerro La Virgen (DV 480-1, 480-2, 480-4) indicates that lower Pisco sediments are older than about 11 Ma (Shipboard Scientific Party, ODP Leg 186, 2000; Barron et al., 2013; Clemens et al., 2016).

Near Yesera de Amara, silty sandstone low on the east-facing slope of Cerro Mama y Hija (DV 549-P106; Figure 4C) contains both *D. hustedtii* and *S. jouseana* (DeVries and Schrader, 1997), indicating an age of about 14.5 Ma (Ramsey and Baldauf, 1999). Eight meters higher in the section and 30 meters below two ash beds with $^{40}Ar/^{39}Ar$ ages of 9.14 +/-0.04 Ma and 9.22 +/- 0.04 Ma (L. Snee, 1987, written communication), sample DV 549-P107 contains *D. hustedtii*, *M. splendida*, and *Nitzschia porteri*. The presence of the first two species indicates an age of 14.5 to 11 Ma, whereas the presence of *N. porteri* restricts the age to 13.6-11 Ma (Niitsuma et al., 2006). About eight meters above the two dated ashes, a silty sandstone bed (DV 549-P114) associated with an erosional surface (the base of Di Celma et al.'s (2017) Pisco P2 allosequence) contains *Thalassiosira antiqua* and *Rouxia californica*, indicating an age of 8.5-6.5 Ma (Akiba, 1986; Barron, 1992; Maruyama, 2000). Samples DV 549-P115 and DV 549-P116, two and eight meters, respectively, above the erosional surface also contain *T. antiqua*, which indicates an age younger than 8.5 Ma. Eighteen meters higher in the section, an ash bed yielded an $^{40}Ar/^{39}Ar$ age of 7.74 +/-0.15 Ma (L. Snee, 1987, written communication).

4. Results

4.1. Coastal physiography

The coastal physiography of the East Pisco Basin was most complex early during the Chilcatay transgression, following an extended period of emergence and tectonism from about 32 to 25 Ma (DeVries, 1998; DeVries et al., 2017). During that transgression, the coast of the East Pisco Pasin presented four physiographic zones (Figure 1C). They were, from northwest to southeast:

1. An exposed shoreface, "Playa Sombrero," carved from soft substrates of underlying Paracas and Otuma silty sandstones (DV 841, 1129, 1403) with limited relief created by CBR (DV 1101, 1126). Farther inland, upper Chilcatay beds are exposed on the floor of the Filudo Depression beneath the Chilcatay/Pisco unconformity (DV 937). The fine-grained and dolomitic Chilcatay sediments show no lithologic influence of the seaward highlands of Cerros Diablo and Antivo, indicating that those highlands did not yet exist during early Miocene time.

At the southeastern end of Playa Sombrero, abutting the uplifted "Quemado Peninsula" (DeVries et al., 2017), lower Chilcatay strata lapped onto a broad, faulted, coastal peneplain composed of both CBR and Otuma silty sandstone and dolomite. Evidence from the foot of Lomas Chilcatay (DV 4007, 8031) indicates no more than a few meters of relief along the paleo-shoreline produced by outcrops of CBR or ridges of Otuma dolomitized and indurated silty sandstone.

2. An area of elongate longshore islands, the "Gran Tablazo Archipelago." Evidence for an archipelago geography consists of beds of boulders and cobbles of CBR and beds of oyster-barnacle coquina and gravelly sandstone lapping onto fault-bounded blocks of CBR from all quadrants of the compass, including the landward-facing eastern side (DV 2240, 4048, 4049, 5120, 8048, 8056, 8057, 8061). Among the paleo-islands of the Gran Tablazo Archipelago are the modern informally named Cerro Geoglifo, Cerro Macharé, Cerro Ortlieb, Cerro Urbina, Cerro Casas, and Cerro Esperante (Figure 1E).

3. A reentrant, the "Bahía de Ica Baja." The reentrant was narrowest during the early middle Miocene, with a boundary to the east defined by paleo-coastal plain outcrops of CBR extending from Ullujaya (300 m south of DV 1028; also DV 8141) to Cerro Sechuito (DV 2013) and towards Quebrada Gramonal (east of DV 4022, 4023). The eastern coastal plain was backed by paleo-cliffs formed by pre-late Miocene uplift on the Monte Grande Fault (e.g., DV 1230, 1625). The northern border of the reentrant was a coastal plain of CBR that crops out between Cerro La Bruja and the Río Ica (DV 489, 1606, 3081). To the west, the boundary of the reentrant is defined by the disappearance of the oldest Pisco strata (allosequence P0 of Di Celma et al., 2017; parasequence P0 herein) between outcrops of a boulder bed that marks the Pisco P0/P1 parasequence contact (DV 1809, 7017) and Zancones, four kilometers to the west, where younger Pisco strata (Pisco P1 of Di Celma et al., 2017) directly overlie Chilcatay strata (DV 2211, 3042).

The early early Miocene incarnation of the reentrant was similarly bounded on the west and north, but was more broadly open to the west, judging from the distribution of Chilcatay sediments west of Yesera de Amara (DV 1808, 2211, 3042). During the middle Miocene, the reentant lost its definition as Pisco sediments spread inland across the entire East Pisco Basin from Cerros Colorados to Ocucaje and southward to Cerro Terrestral.

4. A second reentrant from the Río Grande southward to Cerro Huaricangana or possibly San Juan de Marcona, the "Bahía de Nazca." This reentrant is the least studied of the four paleogeographic zones. At the southwestern end of Cerro Terrestral, Pisco sediments of P1 age or younger rest directly on highly faulted Eocene silty sandstones (DV 1456, 1965). The Chilcatay sequence appears to be absent, although in Quebrada Huaricangana, microfossils and specimens of the gastropod,*Turritella woodsi*, reported by Stock (1990; see below) indicate the presence of Chilcatay-age sediments, and at Pampa de Poroma, the presence of *Turritella woodsi* and *Testallium cepa* (DV 638, 1970) demonstrates the exceptional inland reach of the Nazca reentrant. The southern boundary of the early Miocene

Figure 5. *Ravinement surface and lag deposit lithofacies. A. Rounded and angular cobbles and boulders, base of Chilcatay sequence, western edge of Pampa el Cruce (DV 8090). B. Dolomite lithoclasts and iron-rich authigenic nodules, base of Pisco sequence, Quebrada Perdida (DV 2215). C. Bioclastic sand-filled Thalassinoides burrows penetrating from basal Chilcatay sequence across angular unconformity (red line) into Otuma strata, road to Samaca West (DV 2001). D. Iron-rich authigenic gravel and pebbles, base of Pisco sequence, lying on contact (red line) with Chilcatay sequence, southwestern foot of Cerros Colorados (DV 8077). E. In situ paired pholad bivalves in burrows, base of Chilcatay sequence at southern edge of Pampa El Cruce (DV 4071). F. Dolomitized Otuma siltstone with borings on top and side, in contact with base of Chilcatay sequence, Lomas Chilcatay (DV 4006).*

Bahía de Nazca, if one existed, has been largely erased by Quaternary uplift of Cerro Huaricangana.

By early Pisco time, sands of Playa Sombrero lay farther inland and onlapped a hilly terrain of CBR around Cerros Antivo and Diablo (Figure 1D). Sands and oyster banks largely covered islands of the Gran Tablazo Archipelago; Bahía de Ica Baja had broadened; and Bahía de Nazca became more confined to the south by CBR uplifted along the Monte Grande Fault and beneath Cerro Huaricangana (Figure 1F).

4.2. Lithofacies

The sedimentary record of the Chilcatay and Pisco depositional sequences is characterized by a limited range of lithologies that are entirely marine and predominantly siliciclastic, with varying percentages of bioclastic material. Evaporites, shales, and carbonates are exceedingly rare, and in the latter case, present principally as syndepositional diagenetic dolomite (Dunbar et al., 1990). Authigenic iron-bearing granules, pebbles, and crusts are limited to surfaces of erosion or non-deposition. Phosphatic nodules are more widely distributed throughout the basin, most often in the Pisco depositional sequence.

The East Pisco Basin siliciclastic sediments can be grouped into four lithofacies, each being an association of sedimentary textures, structures, trace fossils, and bioclasts that defines a particular depositional environment.

1. Lag deposits. Lag deposits cover all ravinement surfaces, i.e., forced regression surfaces on the scale of 10^2 to 10^3 km^2 that disconformably or unconformably truncate silty sandstone (basinward) and coarse- and medium-grained sandstone (landward) of an underlying depositional sequence; they also nonconformably cover surfaces of CBR. Lag deposits also coincide with some lower boundaries of smaller parasequences. The lags, typically ten to 30 centimeters thick, consist of one of more of following: well rounded and angular boulders and cobbles of CBR (Figure 5A) or dolomitized silty sandstone (Figure 5B), in some cases encrusted with oysters; coarse-grained and gravelly bioclastic sandstone (Figure 5C), iron-coated authigenic nodules and pebbles (Figure 5D), barnacles, oysters, echinoids, mollusks, *Discinisca* (an inarticulate brachiopod), shark teeth, cetacean bones. *Thalassinoides* and pholad bivalve burrows (*Trypanites* ichnofacies; Figure 5E) often penetrate underlying soft-weathering strata, whereas straight or curved, short, cylindrical burrows score dolomitized beds (Figure 5F). Many of these clastic components and trace fossils have previously been associated with transgressive lags (Loutit et al, 1988, authigenic nodules; van Wagoner et al., 1988, lithoclasts and cobbles; Banerjee and Kidwell, 1991, shell beds; Savrda, 1995, *Glossifungites* and *Trypanites* ichnofacies). Modern accumulations of *Discinisca* are well documented on intertidal and shallow subtidal gravelly substrates on the Pacific coast of North America (Paine, 1962), Central America (LaBarbera, 1985), Japan (Kato, 1996), and Namibia (Zettler et al., 2009) and occur in coarse-grained bioclastic sandstones and gravels close to middle Miocene (DV 1009, 1010), upper Miocene (DV 494), Pliocene (DV 517, 614), and Pleistocene (DV 467) paleo-shorelines of the East Pisco Basin and modern Peruvian shorelines (DV 1372). By their stratigraphic and paleogeographic position, their evidence of high energy, lack of fine-grained sediments, and their associated fauna, the lag deposits are interpreted to have accumulated in an intertidal or very shallow subtidal setting.

2. Massive sandstone. Massive, medium- to coarse-grained, orange sandstone usually overlies lag deposits on forced regression surfaces (Figure 6A) but can also occur as components of parasequences or allosequences within depositional sequences (Di Celma et al., 2017). The massive sandstones are several meters thick, often with *Thalassinoides* and *Gyrolithes* burrows (Figure 6B), isolated upended bioclasts (barnacles, oysters, gastropods), wood (Figure 6C), some from palm trees, articulated *in situ* lucinid and venerid bivalves (*Miltha*, *Dosinia*, *Chione*, *Chionopsis*; Figure 6D), relict laminae, and crossbedding or hummocky cross-stratification, the latter being a feature of inner shelf and shoreface environments (Dott and Bourgeois, 1982). *Gyrolithes* burrows are usually attributed to crustaceans (Dworschak and Rodrigues, 1997) active in brackish-water environments but may also reflect feeding behaviors in full marine settings (Netto et al., 2007). *Thalassinoides* burrows are typical of *Glossifungites* ichnofacies, which characterizes shallow subtidal environments (Benton and Harper, 1997). Two modern American species of *Miltha* live in fine-grained sand at depths of about 50 meters (Vokes, 1969). The venerid species are infaunal taxa that inhabit a wide range of intertidal and sublittoral marine and estuarine environments with fine- to coarse-grained substrates (Moore and López, 1970; Martinez-Córdova, 1996; Baqueiro and Aldana, 2000; Schoene et al., 2002; Vargas-Zamora and Sibaja-Cordero, 2011). Sedimentary textures and structures, ichnofossils, and invertebrate fossils indicate that the massive orange sandstones were deposited close to shore at or just below wave base.

3. Bedded bioclastic sandstone. Coarse-grained bioclastic sandstone (Figure 7A) varies from thin- to thick-bedded and contains barnacle and oyster fragments, unbroken but often abraded gastropods (including *Acanthina katzi* and *Testallium cepa*), disarticulated bivalves, including thin-shelled but generally unbroken *Chlamys* (Figure 7B) and thick-shelled *Glycymeris ibari* and *Tilicrassatella ponderosa*, and echinoderms, including echinoids, clyperasteroids, and asteroids (Figure 7C). The beds are usually horizontally deposited, most notably as elements of fining-up cycles or as intercalations between oyster-dominated coquinas lapping onto paleo-islands of CBR (Figure 7D). Bioclastic-filled *Thalassinoides* burrows often extend from bioclastic beds into underlying fine-grained deposits (Figure 7E). Bioclastic sandstone and gravel beds also occur as topset, foreset, and bottomset beds in clinoform allosequences (Figure 7F). Bedforms, grain-size, and the disarticulated heavy-shelled bivalves indicate high-energy transport. *Glycymeris* valves are the dominant constituent of crossbedded Pliocene-Pleistocene shell banks in northern Peru (DeVries, 1986) and present in late Quaternary high-stand shell banks southeast of Sacaco (and similar Quaternary deposits in Spain (Gutierrez-Mas, 2011) and Israel (Sivan et al., 2006)); their origin at

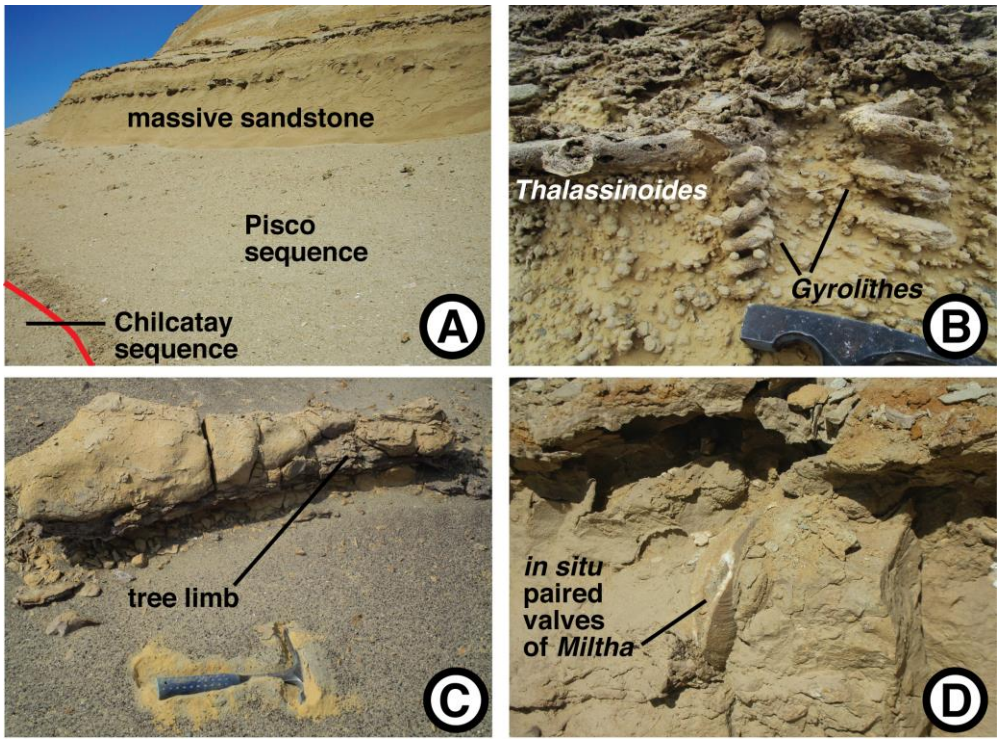

Figure 6. *Massive sandstone lithofacies. A. Lower Pisco sequence, Tinajones (DV 2202). Lower sandstone cliff about four meters thick. B. Thalassinoides and Gyrolithes trace fossils, lower Chilcatay sequence, south of Lomas Chilcatay (DV 8022). Gyrolithes burrow at left joined with Thalassinoides burrow. C. Tree limb encased in massive sandstone, lower Chilcatay sequence, western edge of Pampa El Cruce (DV 8089). D. In situ paired valves of Miltha, lower Pisco sequence, Tinajones (DV 2202). Exposed edge of bivalve is about five cm long.*

Figure 7. *Bioclastic sandstone lithofacies. A. Thick bed of bioclastic sandstone overlying massive sandstone, lower Chilcatay sequence, north of Carhuas-Comotrana Road (DV 8007). B. Oyster-barnacle bed with disarticulated valves of Chlamys, Pisco P0/P1 parasequence contact, Ullujaya West (DV 7020). C. Crossbedded bioclastic sandstone and gravel with clypeasteroid species of Abertella, lower Chilcatay sequence, north of Carhuas-Comotrana Road (DV 5015). D. Coquinas and bioclastic sandstone beds (thin black lines in background) onlapping mainland side of CBR paleo-island, Cerro Macharé, in the Gran Tablazo Archipelago (DV 8060). Day pack for scale. E. Bioclastic sand-filled Thalassinoides burrows extending down from bioclastic sandstone bed within massive sandstone lithofacies, lower Chilcatay sequence, Carhuas-Comotrana Road (DV 5021). F. Oyster-barnacle bioclastic sandstone with cup-and-flange*

shallow shelf depths and subsequent transport by storm waves can explain their presence in the bioclastic sandstone of the Chilcatay and Pisco depositional sequences. The frequent presence of unbroken fragile valves of *Chlamys* indicates that the coarse-grained substrates were stable enough to support epibenthic species living on the exposed surface or underside of rocks (Gilkinson and Gagnon, 1991).

4. Bedded silty sandstone. White-weathering silty sandstone and sandy shale, usually thin-bedded to laminated with minor scours, tiny rip-up intraclasts, and minor rippling is typically tuffaceous and/or diatomaceous and contains scales of clupeoid fishes (sardines, anchovies). Benthic foraminifera are abundant in some horizons. The soft-weathering silty sandstone, often chocolate-brown on fresh surfaces, may contain intercalations of thin- to medium-thick dolomitized horizons of silty sandstone, sometimes bored on their exposed upper surfaces. The fine-grained texture, sedimentary structures indicative of weak currents, syndiagenetic magnesium-rich carbonates, and neritic to pelagic vertebrate and microfossil content indicate an mid- to outer shelf environment comparable to that which exists today off the coast of southern Peru, where many of the same textures, structures, and fossils are preserved in Quaternary sediments formed beneath regions of coastal upwelling (DeVries, 1980; DeVries and Schrader, 1981; DeVries and Pearcy, 1982; Suess and von Huene, 1988).

Within the first three named lithofacies, boulder beds occur as single or multiple horizons. Boulders and cobbles of CBR and other lithologies vary from well rounded to angular and have diameters as great as four meters. The boulders are usually separated by several meters, but can be found stacked against or on top of one another. Their modes of occurrence are best described according to their associated lithofacies.

a. Boulders resting on ravinement surfaces of depositional sequences are blocks of CBR where the ravinement surface crosses or approaches outcrops of CBR (Figures 8A, 8B) and often lithoclasts of dolomitized silty sandstone where the ravinement surface onlaps pre-Miocene marine strata (Figure 5B).

b. Boulders of CBR, rounded or angular, occur as discrete horizons within massive orange sandstone. The boulders may be matrix supported without an accompanying lag deposit (Figure 8C) or may occur as the largest clasts, by far, that rest on a pavement, ten to 30 cm thick, of boulders, cobbles, coarse-grained bioclastic sandstone, and gravel composed of CBR (Figure 8D).

An active debate regarding paleo-tsunamis as a means for depositing large and chaotically arranged boulders and cobbles has not been resolved, as exemplified by a discussion regarding disputed Neogene tsunami deposits in northern Chile (Hartley et al., 2001; Cantalamessa and Di Celma, 2005; Spiske et al., 2014; Le Roux, 2015). Comparably thick chaotically deposited conglomerate constitutes much of the La Planchada Formation of southern Peru (DV 1265, 1266; Laharie, 1976), including poorly sorted, poorly consolidated conglomerate near Atiquipa (DV 1251) with marine mollusks and bones of terrestrial mammals (Salas et al., 2003). The proximity of steep terrain near La Planchada and Atiquipa – 200 meters of elevational gain within one kilometer and 500 meters within three kilometers – leaves open the possibility that these Pliocene conglomerates are the result of debris flows, tsunamis, or a tsunami modification of debris flows.

A boulder bed associated with massive medium-grained sandstone in the lowermost Chilcatay sequence of the East Pisco Basin, the informally termed "Piedra Negra bed," differs from the Chilean and La Planchada deposits: it is a single, thin- to medium-thick, boulder-bearing bed extending kilometers basinward from a broad coastal CBR peneplain that was accentuated by low hills and fault escarpments. The Piedra Negra bed also extends kilometers in a longshore direction. The Piedra Negra bed resembles the shallow marine boulder field deposited by ebbing flood waters of the 2004 Banda Aceh tsunami (Paris et al., 2010), including the deposition of the largest boulders farthest from the boulder source (Figure 8E).

Discrete boulder beds of lesser extent occur throughout the East Pisco Basin, especially as strata of the mid-Chilcatay (DV 1637) and lowermost Pisco (DV 574) sequences in Bahía de Ica Baja.

c. Boulders associated with coarse-grained bioclastic sandstone and conglomerate are composed of CBR and most often occur on shoreline-proximate basal unconformities of mid-scale parasequences, e.g., the base of the P1 parasequence west of Ullujaya (Figure 8F), or as a clastic component of oyster banks and intercalated bioclastic sandstone beds that encircle the paleo-islands of the Gran Tablazo Archipelago. The abundance of boulders in the archipelago beds diminishes rapidly with increasing distance (10^2 meters) from paleo-island boulder sources. In the case of the Ullujaya conglomerate on the P0/P1 parasequence boundary, rock piles, with boulders one to four meters in diameter and composed of granite or metamorphic rock (DV 1613, 1614; Figure 8F), provide evidence of a violent depositional event, whether the backwash of tsunamis (Paris et al., 2010), the result of an exceptionally energetic flash-flood-induced hyperpycnal flow (Katz et al., 2015), or a subaerial debris flow (e.g., Berti et al., 1999).

4.3. Early phase of Chilcatay transgression

4.3.1. Playa Sombrero

The shore of the latest Oligocene to early Miocene Playa Sombrero stretched for at least 24 kilometers from Chilcatay outcrops at Salinas de Otuma to the Lomas Chilcatay (Figure 1D), location of the type section of the Chilcatay Formation (Figure 4A) and just two or three kilometers from the CBR bulwark of the Quemado Peninsula. Farther inland, where upper Chilcatay strata crop out below transgressive sandstones of the lower Pisco sequence in the Oliva/El Monte and Filudo areas (DV 411, 937), the base of the Chilcatay sequence is not exposed.

The Chilcatay transgressive lag along Playa Sombrero overlies a regressive ravinement surface on silty sandstone of the Paracas and Otuma sequences. The lag consists of one or more of the following: CBR pebbles, phosphatic nodules (DV 1404), shark teeth, abraded cetacean and fish bones, barnacles, gastropods (*Turritella cruzadoi*, an index species for the base of the Chilcatay sequence (Figures 9A,

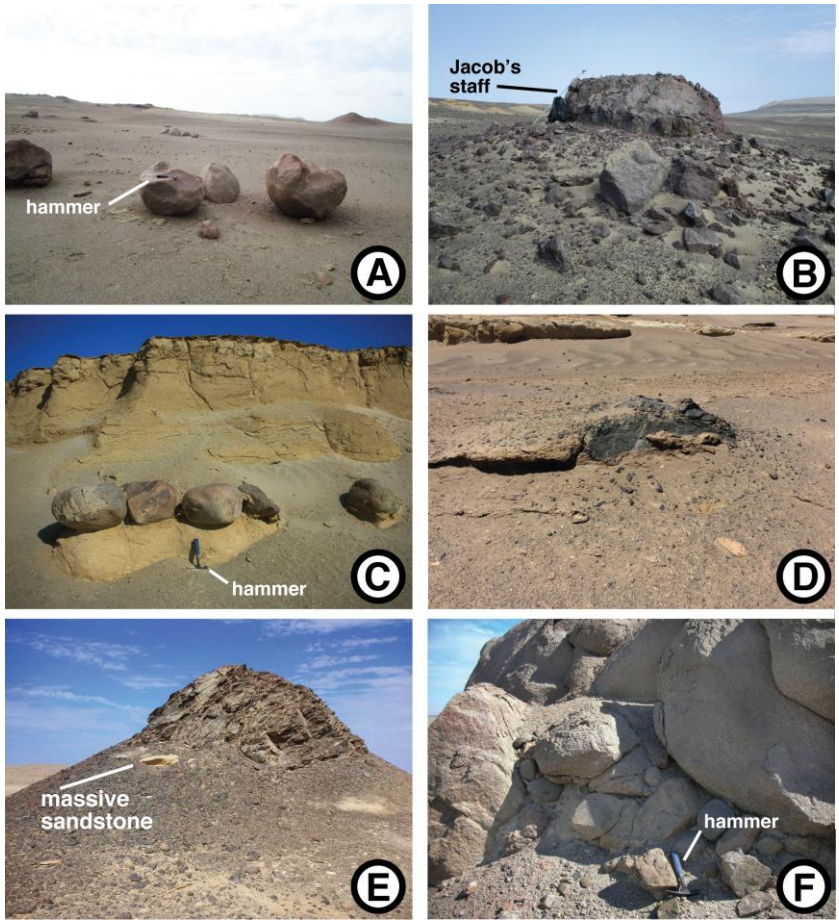

***Figure 8**. Boulder beds. A. Scattered boulders of CBR on Pisco ravinement surface, Quebrada Chacaltana (DV 8067). Hammer for scale. B. Boulder of CBR on Pisco ravinement surface, between Cerros Colorados and Cerro Geoglifo (DV 8075). Jacob's staff for scale. C. Boulders in massive sandstone lithofacies of lower Pisco sequence with no associated bioclastic bed. Tinajones, (DV 3004). Hammer for scale. D. Boulder of CBR in Piedra Negra bed, embedded in oyster-barnacle bioclastic sandstone, Samaca West (DV 8131). Boulder about 1.5 meters in diameter. E. Boulder of CBR resting on massive bioturbated sandstone at distal edge of Piedra Negra horizon between Samaca West and Cerro Tiza (DV 4031). Boulder three to four meters in diameter. F. Pile of CBR boulders of varied igneous and metamorphic lithologies, Pisco P0/P1 contact, Ullujaya West (DV 4041). Boulders rest on thin bioclastic bed with oysters, barnacles, Acanthina katzi, and Olivancellaria tumorifera. Hammer for scale.*

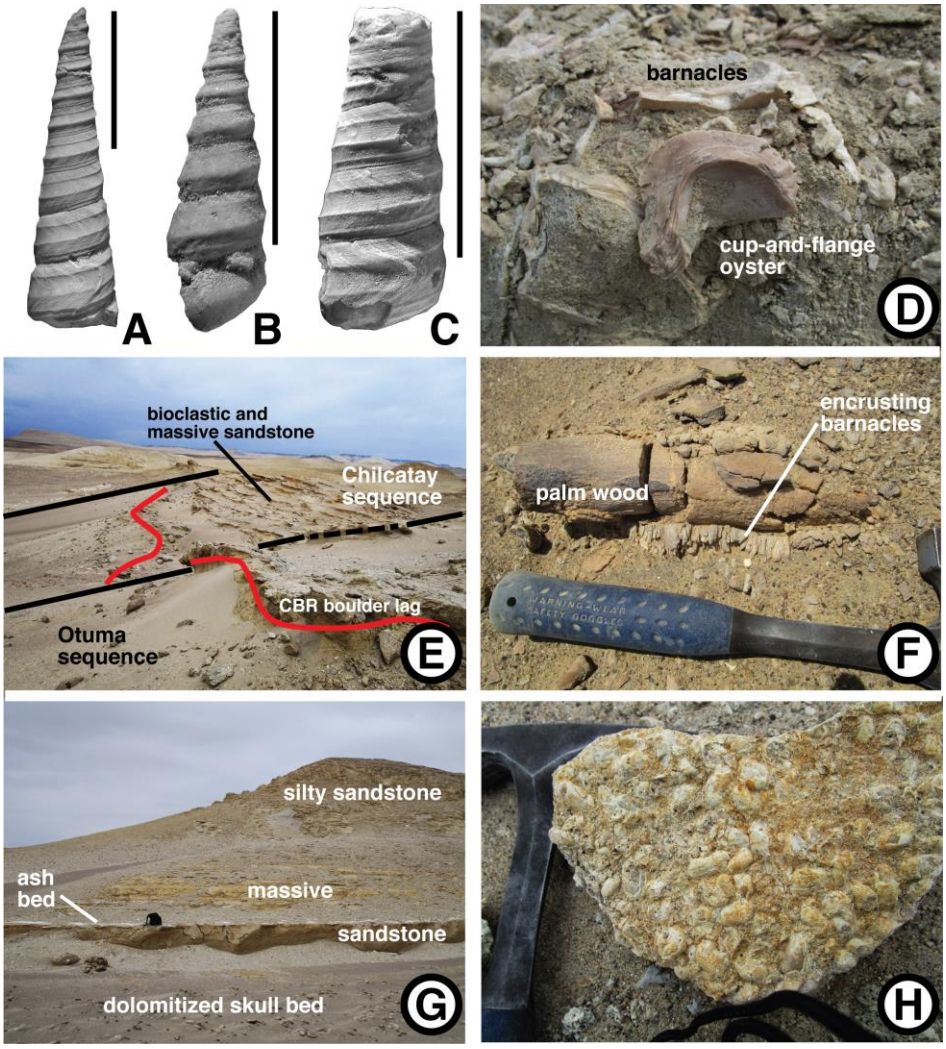

***Figure 9.** Chilcatay sequence fossils and lithofacies. A, B, C. Turritella cruzadoi DeVries, 2007, an index species for the Chilcatay sequence, most often found in basal Chilcatay massive and bioclastic sandstone. Vertical bars are one cm long. D. Undescribed cup-and-flange oyster, an index species for the Chilcatay sequence. Fragment is about three centimerters in diameter (DV 7032). E. Basal Chilcatay beds of alternating bioclastic and massive sandstone north of Carhuas-Comotrana Road (DV 5019). Lag boulders in foreground about 60 cm in diameter. F. Barnacle-encrusted and overturned piece of palm wood, lower Chilcatay massive sandstone (DV 8087). G. Lower Chilcatay sequence north of Carhuas-Comotrana Road (DV 5020). Dolomitized silstone with odontocete skulls (the "skull bed") overlain by massive sandstone with intercalated ash bed. Massive sandstone fines upward into silty sandstone in background. Day pack for scale. H. Bedding plane with small arcid bivalves typical of Chilcatay sequence, north of Carhuas-Comotrana Road (DV 5019).*

9B, 9C; DeVries, 2007) and *Testallium cepa* (DV 1129, 1130, 1131, 1132, 1133, 1403), bivalves (*Tilicrassatella* (DV 441-12; Figure 4A), *Miltha*, small mactrids and venerids), and pebble-sized iron-rich authigenic nodules (DV 841, 5012, 5021). Bioclastic sand-filled *Thalassinoides* burrows of the *Glossifungites* ichnofacies (Benton and Harper, 1997) cut into Otuma sediments (DV 2001). Where basal Chilcatay beds nonconformably lap onto CBR (DV 1101) or unconformably overlie Otuma sediments close to paleo-outcrops of CBR (DV 441, 1126, 2047, 2048; Figure 3C), the transgressive surface is strewn with boulders of CBR, lithoclasts of dolomitized sandstone, banks of "cup-and-flange" oysters (an undescribed species characteristic of the Chilcatay sequence; Figure 9D), and pebbly sandstone with broken barnacles, echinoid spines, and bryozoan-encrusted nodules, sometimes in multiple beds (DV 5019; Figure 9E).

The transgressive lag is overlain with up to eight meters of massive orange sandstone (DV 1365, 1366, 3018) with pervasive indistinct bioturbation, *Thalassinoides* and *Gyrolithes* burrows filled with bioclastic sand (DV 841, 5021; Figure 7E), a barnacle-encrusted transported stem of a palm, possibly *Palmoxylon* (DV 8087; Figure 9F; see Section 4.9), and an ash bed near Cuenca Sombrero (DV 1404) and the Carhuas-Comotrana Road (DV 5020; Figure 9G). Mollusks are dispersed throughout the sandstone but not uniformly, being present as scattered valves or packed beds of small arcids (Figure 9H), mactrids and venerids; valves of cup-and-flange oysters; concentrations of *T. cruzadoi*; or isolated specimens of *T. cepa*.

In the middle of the basal massive sandstone near Salinas de Otuma (DV 1132, 1133), Cerro Sombrero (DV 1107, 1365, 1366; Figure 10A), on both sides of the Carhuas-Comotrana Road (DV 395, 441, 2261, 5006, 5020, 8007, 8008; Figure 10B), and in a pair of amphitheater-shaped valleys between the Lomas Chilcatay and Playa del Morro (DV 8015, 8019, 8020, 8021; Figures 1D, 10C, 10D), a paleo-shoreline distance of 25 kilometers, a concretionary dolomitized sandstone occurs with large buccinid gastropods (*Misifulgur cruziana*) and abundant disarticulated bones and cranial endocasts of odontocetes – a horizon informally termed the "skull bed" (DV 395-11, 395-12, 441-14; Figure 4A). (The dolomitization of sediments that create bone-filled concretions has been attributed by Gariboldi et al. (2015) to the decomposition of cetacean carcasses.) Small boulders of CBR occur with the Salinas de Otuma vertebrate remains; similarly sized lithoclasts of hackly-weathering Otuma siltstone occur with the vertebrate remains above Playa del Morro (DV 8021).

Farther eastward, closer to the paleo-shoreline's intersection with the Carhuas-Comotrana Road (DV 1126), a correlative bed consists of iron-rich authigenic pebbles, lithoclastic boulders, shark teeth, and *Discinisca*. About two kilometers south of the same road, i.e., the southern end of Playa Sombrero, where the Chilcatay sea crossed from swales floored with Otuma strata (DV 4006, 4007) onto a faulted peneplain with blocks of CBR and unevenly eroded Otuma strata (DV 601, 8022, 8026), the basal Chilcatay sandstone has a higher proportion of oyster and barnacle fragments in a thicker section of massive *Thalassinoides*-burrowed sandstone. The bone-bearing dolomitized sandstone horizon, however, still occurs several meters above the unconformity (DV 601). Across shoals created by barely buried Otuma dolomite (DV 8027; Figure 10E), the dolomitzed Chilcatay bone bed is replaced with bioclastic gravelly sandstone with mud-filled barnacles (DV 8027; Figure 10F) and disarticulated cetacean bones.

No outcrops of the Chilcatay depositional sequence were found across the interior of the Quemado Peninsula. Chilcatay strata overlying Eocene strata are exposed in blocks successively down-dropped to the west on the paleo-peninsula's northwestern margin (e.g., DV 8019). Sections of the upper Chilcatay sequence and the entire Pisco sequence encroach on the paleo-peninsula's western rim (DV 1134, 5001), while farther inland, only small Cenozoic outcrops occur – upper Miocene coquina with oysters, barnacles, and pieces of *Concholepas kieneri* clustered around paleo-sea stacks composed of CBR (DV 3036).

4.3.2. Gran Tablazo Archipelago

Basal sands of the Chilcatay depositional sequence were deposited in the Gran Tablazo Archipelago across a rugged terrain of paleo-shoreline-parallel elongate islands, comparable in size to the modern Islas Ballestas and Isla Independencia (Figure 1C). The fault-bound, island-forming, CBR blocks had been uplifted and exposed subaerially between about 32 and 25 Ma, following the lithification of sediments deposited across the Otuma-age Bahía de Concha Roja (DeVries et al., 2017), a sequence of events evidenced by basal Chilcatay bioclastic sandstones lapping around outcrops of CBR that are themselves in fault contact with outcrops of Otuma sandstones (DV 5120).

The best exposed basal Chilcatay section in the Gran Tablazo Archipelago is found at the foot of southwest-facing slopes south of Cerros Colorados, on the informally named "Pampa El Cruce" (Figure 1E), where a bed of gravelly bioclastic sandstone (DV 2243, 4066, 4067, 4071, 7091, 7092) is separated by an angular unconformity (Figure 3B) from underlying indurated, brick-colored, tree trunk-bearing sandstone and soft-weathering white ashy sandstone of the Otuma sequence (DeVries et al., 2017). The basal Chilcatay bioclastic debris consists of large fragments of barnacles, oysters, small intact valves of *Chlamys*, *in situ* pholad bivalves in their burrows, and gastropods – naticids, giant specimens of *Turritella woodsi* (Figure 11A), nassariids, *Testallium cepa* (Figure 11B), *Olivancellaria tumorifera* (Figure 11C) – clumped in lenses. As many as four additional beds of bioclastic coarse-grained sandstone with a diverse assemblage of mollusks overlie the basal bioclastic bed, alternating with massive, bioturbated, wood-bearing sandstone (DV 1648, 2232, 2237, 2244, 4067, 4068, 4076, 7093).

Farther south, Chilcatay sediments onlap and wrap around a jagged hill of CBR (DV 7108), herein named "Cerro Geoglifo" (Figure 1E). At the hill's northern end, a nonconformity with CBR and an angular unconformity with the underlying Otuma sequence is covered with large oysters and CBR boulders (DV 2240). The boulders are overlain with oyster-barnacle sandy coquina interbedded with thick beds of oyster-bearing sandstone (DV 2239) and boulder horizons. Farther from the paleo-island (DV 2238),

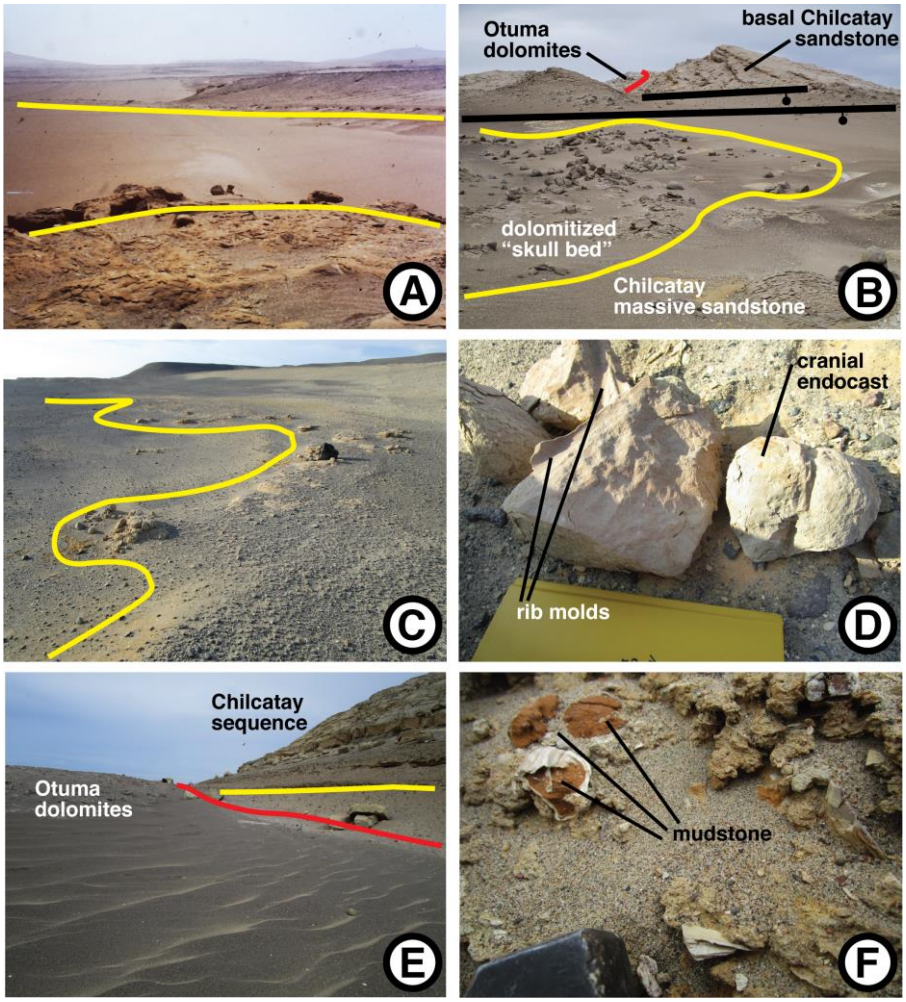

Figure 10. *"Skull bed" outcrops of odontocete bone concentrations along the early Miocene Playa Sombrero. Red lines mark sequence boundaries. Yellow lines mark the skull bed (A, C) or enclose it (B). A. Ledge of dolomitized skull bed east of Cerro Sombrero (DV 1366). B. Skull bed near Carhuas-Comotrana Road (DV 5020). Dolomitized bedding plane overlies massive sandstone, which in turn overlies alternating beds of massive and bioclastic sandstone, which are visible in the background across two faults; alternating beds also seen in Figure 9E. Skull bed also overlain by massive sandstone (Figure 9G). C. Ledge of skull bed above Playa del Morro (DV 8019). Most concretions enclose odontocete cranial endocasts or bones. Day pack for scale. D. Cranial endocast and rib molds of odontocete from skull bed above Playa del Morro (DV 8019). E. Bioclastic horizon with odontocete bones (yellow line), south of Lomas Chilcatay (DV 8027), correlative with dolomitized skull bed of Carhuas-Comotrana Road. Dolomitized Otuma beds produced several meters of relief that was nearly buried by basal Chilcatay massive sandstone and just barely covered by the bioclastic bone bed. Largest boulder at center right about one meter in diameter. F. Large barnacles filled with mudstone in clean-washed bioclastic coarse-grained sandstone, south of Lomas Chilcatay (DV 8027). Mudstone preserved inside barnacles indicates rapid transport from quieter depositional setting.*

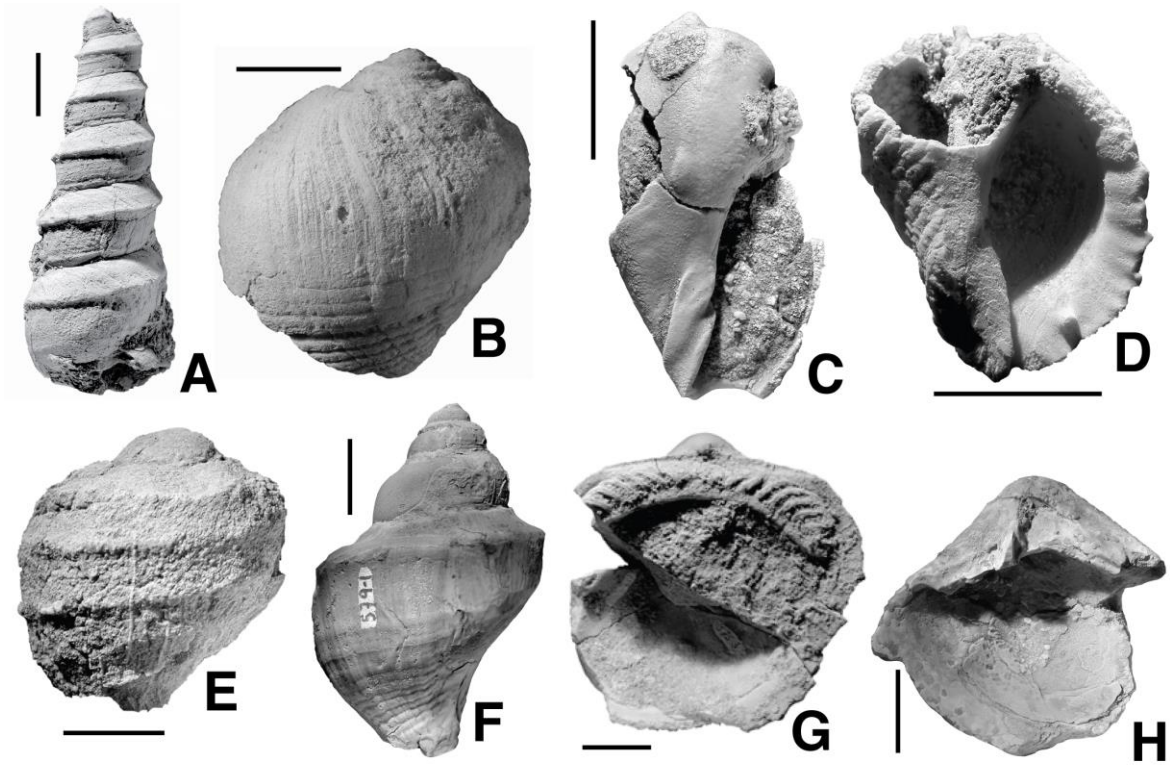

Figure 11. *Diagnostic molluscan taxa from the East Pisco Basin. Scale lines about one centimeter. A. Turritella woodsi Lisson, 1925. Otuma and basal Chilcatay sequences. See DeVries (2007) for discussion of species. B. Testallium cepa (Sowerby, 1846). Chilcatay and Pisco P1 sequences. See Vermeij and DeVries (1997) for discussion of species. C. Olivancellaria tumorifera Hupé, 1854). Chilcatay and Pisco P0 sequences. D. Acanthina katzi Fleming, 1972. Chilcatay and Pisco P0 and P1 sequences. See DeVries (2003) for discussion of species. E. Ficus distans (Sowerby, 1846). Chilcatay sequence. See DeVries (1997) for discussion of species. F. Misifulgur cruziana (Olsson, 1931). Chilcatay and Pisco P0 and P1 sequences. See DeVries (2016b) for discussion of species. G. Glycymeris ibari (Philippi, 1887). Chilcatay sequence. H. Tilicrassatella ponderosa (Philippi, 1887). Chilcatay and Pisco P0 sequences. See DeVries (2016a) for discussion of species.*

boulders become less common and the bioclastic beds have a more diverse molluscan fauna (DV 1648, 2237). At the southern end of the paleo-island, thick beds of oysters, barnacles, and angular boulders lap onto or against CBR on the basin side (DV 4077, 7105, 7108, 8037) and mainland side (DV 4048, 8048). Bioclastic beds on the mainland side are overlain by sandstone with lenses of barnacles, large oysters, *Chlamys*, large pieces of wood, and post-cranial bones and skulls of odontocetes. Comparable beds on the basin side (DV 2252, 2253, 7105, 7106) consist of oyster-barnacle bioclastic sandstone with cetacean and turtle bones and a diverse molluscan fauna (DV 8036).

Two kilometers southeast of Cerro Geoglifo, a basal bed of granitic boulders and bioclastic beds of cup-and-flange oyster-barnacle coquina unconformably overlie Otuma sandstone and lap onto the northern nose and basinward flank of another fault-bounded paleo-island of CBR, the informally designated "Cerro Macharé" (DV 4049, 4050; Figure 1E). The oyster banks extend for up to two kilometers in a basinward (southwest) direction, where basal Chilcatay strata consist of barnacle-oyster coquinas interbedded with massive thick-bedded sandstone and boulder horizons (DV 7111, 7112, 8049). Between indurated ridges of tilted Otuma sandstone (DV 8050, 8051), two-meter-deep ravinement depressions are filled with Chilcatay bioclastic sandstone containing barnacles, wood, valves of *Chlamys* and oysters, paired valves of the deep-burrowing infaunal bivalve, *Panopea*, and cetacean bones (DV 7112, 7113, 7114). Two kilometers southeast, on strike with the early Chilcatay shoreline and in the lee of two small paleo-islands, the informally named "Cerro Urbina" and "Cerro Casas" (Figure 1E), which themselves are ringed with coquinas of cup-and-flange oysters and barnacles (DV 5120, 8056, 8057), the diversity of gastropods in basal bioclastic sandstones (DV 8058, 8059) increases (trochids, *Natica*, *Sinum*, *Olivella*, *Conus*, turrids). One to four kilometers farther to the southeast, on Pampa Colorada (Figure 1E), where transgressive bioclastic sandstone beds pass from the protected lee of the informally designated "Cerro Esperante" (Figure 1E), small single and paired valves of *Chlamys* replace the diverse gastropod fauna (DV 1322, 1326, 5121, 8069; possibly DV 1324).

Outcrops of lower Chilcatay strata are less commonly encountered southeast of Cerro Macharé, i.e., past the northwestern end of the informally denominated "Cerro Ortlieb" (Figure 1E), either because the onlapping of Chilcatay strata on CBR commenced later or because Chilcatay strata were eroded prior to the onlap of Pisco strata across the landward face of Cerro Ortlieb (DV 4086). Southwest of Cerro Ortlieb, at the southeastern limit of Pampa Concha Roja, i.e., the Camino de los Burros (Figure 1E), Chilcatay strata (DV 1323, 1435) overlie Otuma strata that contain the Eocene gastropods, *Ficus chiraensis* and *Cristispira cochleiformis* (DeVries, 2007; DeVries et al., 2017).

Seaward of the Gran Tablazo Archipelago, outcrops of basal Chilcatay sandstone are preserved inside the half-grabens of Bajada del Diablo and Quebrada Perdida (DeVries et al., 2017). In the former, Otuma silty sandstones are overlain in angular unconformity by a lithoclastic boulder bed with shark teeth (DV 3023, 3024). At Quebrada Perdida, basal Chilcatay strata consist of up to six meters of gravel and conglomerate with shark teeth, barnacle fragments, and large lithoclasts of dolomitized siltstone (DV 1729, 2217, 3090, 3091).

4.3.3. Bahía de Ica Baja

Marine strata on the western side of the Río Ica from Cerro Tiza to Cerro La Bruja and outcrops of CBR on the northern and eastern side of the Río Ica from Ullujaya to the *Sula* Site (Figure 1F) bordered the early to middle Miocene Bahía de Ica Baja. The eastern margin of the Miocene bay was defined in part by the 40-km-long, high-angle, extensional Monte Grande Fault (DeVries, 2017; Figure 1F). Judging from the presence of gastropods (*Herminespina philippii* and *Acanthina obesa* at lower levels, *H. saskiae* and *A. triangularis* at higher levels (DeVries, 2003; DeVries and Vermeij, 1997) in coquinas interfingering with paleo-sea stacks at multiple elevations (Figure 2G), the footwall of the Monte Grande Fault (DV 1230, 1624, 1625, 5036) is inferred to have formed a west-facing parapet that plunged below sea level during the late Miocene and early Pliocene and perhaps earlier.

The basal lag bed of the Chilcatay sequence consists principally of bioclastic coarse-grained sandstone with cup-and-flange oysters, large oysters, *Chlamys*, *Acanthina katzi* (Figure 11D), and barnacles (DV 1640, 2001, 4032, 7023, 8104, 8121, 8124, 8125). Rounded lithoclastic boulders of dolomite and pumice occur on some surfaces (DV 4031), as do rounded and angular boulders of CBR (DV 1715, 4023, 4032, 8104). Iron-rich authigenic nodules encrust the Otuma-Chilcatay contact along the southwestern edge of the embayment (DV 5054, 5055). *Thalassinoides* burrows are cut into underlying Otuma sandstone (DV 2001). The basal lag is overlain at most localities by bedded or massive sandstone with relict laminae or hummocky cross-stratification (DV 1617). The massive beds often exhibit densely packed *Thalassinoides* burrows, rounded and angular cobbles, and lenses with barnacles, *Chlamys* valves, cup-and-flange oyster fragments (DV 1811), or a diverse assemblages of mollusks (naticids, epitoniids, *Crepidula*, *Ficus distans* (Figure 11E), *A. katzi*, *Misifulgur cruziana* (Figure 11F), venerids, lucinids, and scaphopods (DV 4031).

North of Fundo Santa Rosa (Figure 1F), basal Chilcatay sandstones unconformably overlie sandstone of the Los Choros Member of the middle Eocene Paracas Formation (Figure 3E). Los Choros sandstones contain the mollusks *Crassatella neorhynchus* and *Turritella lagunillasensis* (DV 7035). Swales filled with basal Chilcatay sandstone (DV 7036) contain valves of *Glycymeris ibari* (Figure 11G) and *Tilicrassatella ponderosa* (Figure 11H).

Most basal Chilcatay sections in Bahía de Ica Baja have a horizon, the Piedra Negra bed, with bioclastic conglomerate and black CBR boulders situated two to ten meters above the unconformity and usually underlain and overlain by massive bioturbated sandstone (Figure 12A). The Piedra Negra horizon extends from north of Cerro Tiza (DV 4031, 4032, 4033; Figures 1E, 1F) to the western edge of the Río Ica (DV 1639, 1640, 1811, 2001, 2205, 8131, 8137) and across the Río Ica (DV 1715) southward (DV

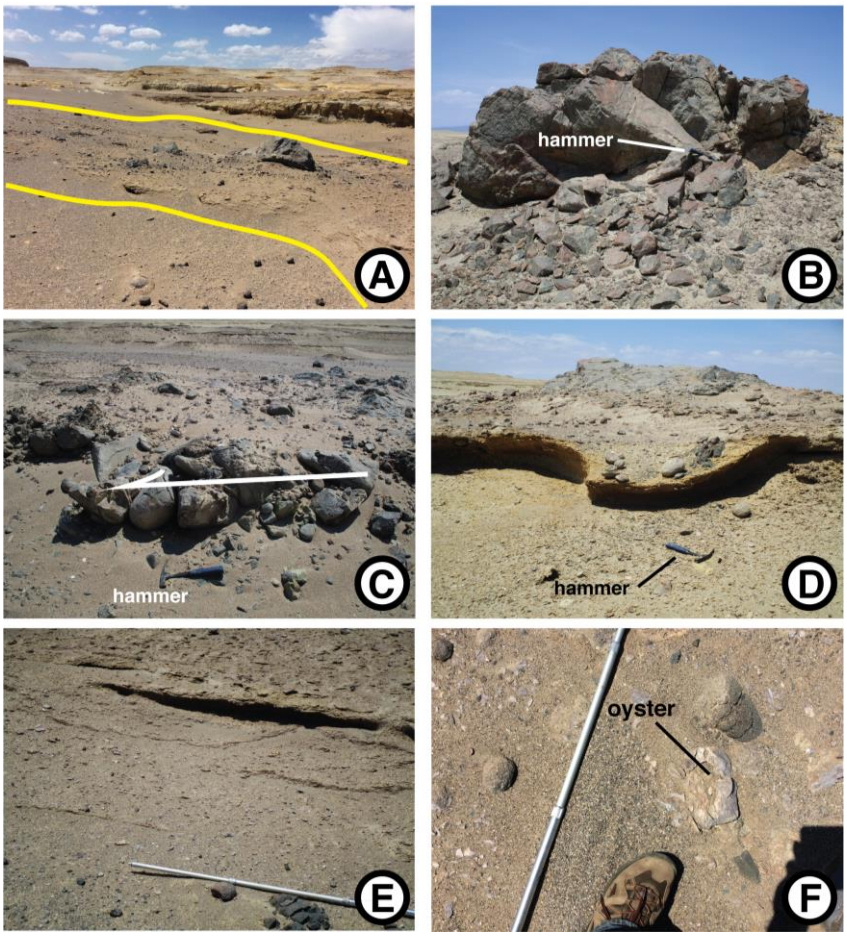

Figure 12. *Piedra Negra bed, lower Chilcatay depositional sequence (DV 8131). A. Bioclastic bed with CBR boulders and cobbles. Yellow lines marks abrupt transitions to massive sandstone above and below the boulder-bearing bed. Large CBR boulder about 1.5 meters long. B. Large CBR boulder resting on bioclastic sandstone and gravel base. Hammer for scale. C. Imbricate small boulders and cobbles. White arrow shows paleo-flow direction to southwest, away from the paleo-shoreline. D. Scoured base of bioclastic sandstone; channel is oriented northeast-southwest. Underlying unit is bioclastic massive sandstone. Channel with bioclastic fill is overlain by large CBR boulder. Hammer for scale. E. Successive scours and crossbedded fill in bioclastic portion of Piedra Negra bed. Jacob's staff for scale. F. Large undescribed oyster valve on conglomeratic upper surface of Piedra Negra bed. Not visible are fragments of echinoids, asteroids, ophiuroids, and crinoids. Jacob's staff for scale.*

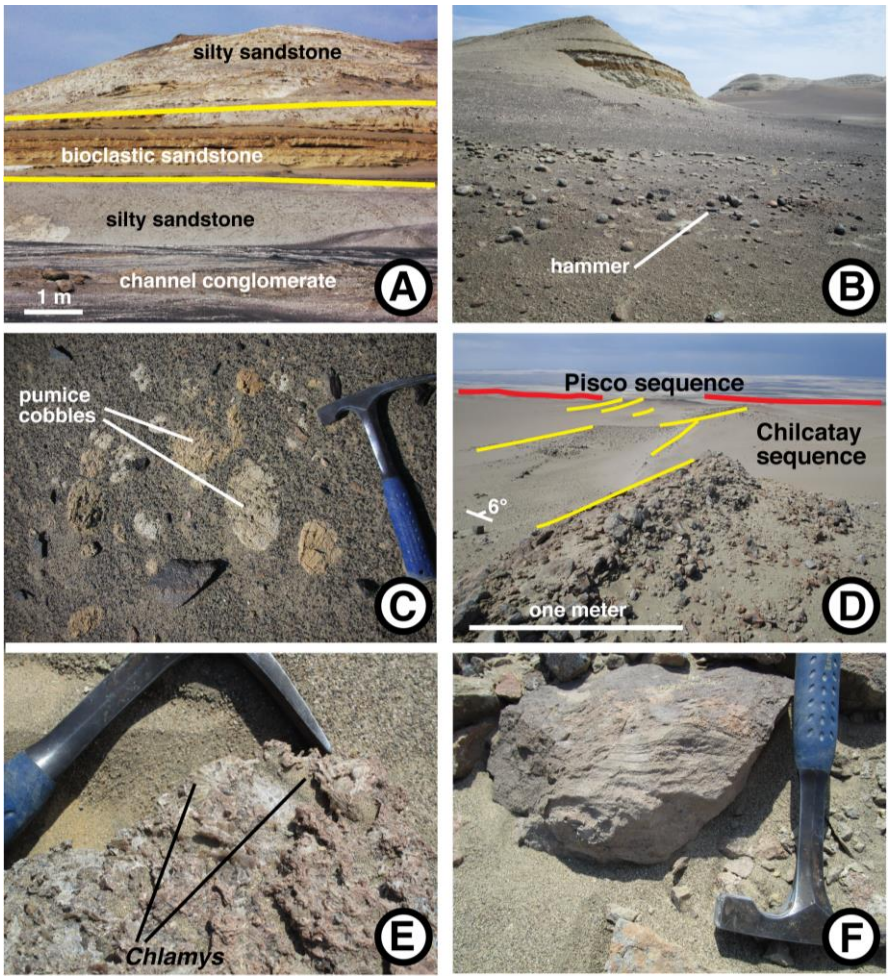

Figure 13. *Mid-Chilcatay shoaling event, parasequence, and channel-form deposits in Quebrada Chacaltana. A. Mid-Chilcatay parasequence in the Lomas Chilcatay (DV 396, 1817). Sediments above and below pair of yellow lines are silty sandstones with diatoms and scales of clupeoid fishes. Boulders from channel-form conglomerate with CBR and lithoclastic boulders in foreground. B. Bed of well rounded CBR cobbles and small boulders, mid-Chilcatay parasequence (DV 8084). Northern end of Cerros Colorados on the distant horizon. Hammer for scale. C. Well rounded pumice cobbles in mid-Chilcatay parasequence east of Cerro Geoglifo (DV 4082). D. Channel-form Chilcatay beds in Quebrada Chacaltana with basal fill of bioclastic debris and angular CBR cobbles and gravel (DV 8060). Channel bases (yellow lines dip steeply to the north; channels become smaller towards paleo-shoreline. Regional uplift dip (6° NE) at right angles to channel slopes. Red line marks base of Pisco sequence. E. Channel fill in Quebrada Chacaltana of bioclastic debris, including oysters and Chlamys, and gravel of CBR (DV 8060). Cement agatized at surface. F. Laminated coarse-grained sandstone in upper part of channel-fill deposits in Quebrada Chacaltana (DV 8060).*

1620, 8125) to Laberinto (DV 5054, 5055, 7023, 7030, 7032; Figure 1F).

Some boulders in the Piedra Negra bed, especially those farthest from the paleo-shoreline, exceed three meters in diameter (DV 1639, 1906; Figure 12B). At locality DV 8131, two- and three-meter boulders are interspersed among half-meter boulders. In some outcrops, the smaller boulders exhibit imbricate stacking (Figure 12C) that indicates a paleoflow azimuth of 210 degrees, i.e., directed offshore and perpendicular to the strike of the paleo-shoreline. Scoured troughs at the same horizon (Figure 12D) indicate comparable flow directions. The boulders are embedded within a bioclastic (oysters, *Chlamys*, barnacles) gravelly sandstone (Figure 12E), massively bedded or with small sets of crossbeds and scour surfaces. The Piedra Negra surface at DV 8131 was colonized by large oysters (Figure 12F) and an exceptional variety of echinoderms, including asteroids, echinoids, crinoids, and ophiuroids (R. Portell, written communication, July 2017).

The breadth of the Piedra Negra boulder field, the distal location of the largest boulders, the evidence of offshore flow at a distance of kilometers from the paleo-shoreline, and the incongruity of the boulder bed sandwiched between massive bioturbated inner shelf sandstones are consistent with a tsunami backwash deposit such as that produced by the Banda Aceh tsunami (Paris et al., 2010).

4.4. Mid-Chilcatay shoaling event

Throughout the East Pisco Basin, lithostratigrapic evidence points to the presence of a mid-Chilcatay parasequence that represents a shoaling event – coarse-grained sandstone, boulders, and shallow-water bioclastic debris (barnacles, oysters, echinoids) – overlying and underlying thick intervals of diatomaceous and clupeiod fish scale-bearing silty sandstone.

4.4.1. Playa Sombrero

Coarse-grained beds of the mid-Chilcatay parasequence sequence along Playa Sombrero are most evident in the type section of the Chilcatay Formation in the Lomas Chilcatay (DV 396, 443, 477, 478), where eleven meters of orange bioclastic sandstone contrast sharply with underlying and overlying thick sections of white silty sandstone (Figure 13A). The disconformable base of the coarse-grained interval is a thin lag of poorly sorted, black, quartzose sandstone with pebbles of CBR and barnacle fragments. Closer to the paleo-shoreline, large boulders of CBR occur in the basal bioclastic sandstone (DV 477), with barnacles shed from the boulders and a diverse molluscan fauna, including *Ficus distans*. The pebble lag at DV 396 is overlain by six meters of massive sandstone with relict laminae, fragments of barnacles, and in the upper portion, scattered invertebrates (large barnacles, *Crepidula*, *Olivancellaria tumorifera*), and *Thalassinoides* and *Gyrolithes* burrows. The allosequence pairing of pebble lag (and at DV 477, CBR boulders or cobbles) and massive sandstone repeats three more times in the overlying five meters. A fifth allosequence commences with a bed of coarse-grained oyster-barnacle sandstone with whole valves of *Chlamys*. The basal bed is overlain with massive sandstone, which then fines upward into tens of meters of silty sandstone with diatoms and clupeoid fish scales.

In an area less well studied, coarse-grained barnacle-bearing sandstone capping Cerros Las Salinas (DV 841; Figure 1D) and cobbly bioclastic gravel with cup-and-flange oysters on the ridge southwest of Salinas de Otuma (DV 2047, 2048) might represent the mid-Chilcatay shoaling event. Farther south, at the edge of Cuenca Sombrero, an outcrop (DV 1368) overlies lower Chilcatay sandstone and silty sandstone; it includes a horizon with lithoclastic cobbles of dolomitzed silty sandstone and lenses of coarse-grained bioclastic sandstone with barnacles, *Discinisca*, large oysters, small venerid and arcid bivalves, and odontocete bones. This bioclastic horizon is correlative with outcrops four kilometers north of the Carhuas-Comotrana Road (DV 5013, 5014), where six meters of barnacle-oyster sandstone are overlain by three meters of massive sandstone with cetacean bones, teeth of the shark, *Carcharocles megalodon*, and cup-and-flange oysters. The massive sandstone is overlain with boulders and crossbedded coquina with the clypeasteoid, *Abertella* (DV 5014, 5015, 5016, 5017; Figure 7C). The clypeasteroid beds are overlain by silty sandstone of the upper Chilcatay sequence (DV 507, 5015).

4.4.2. Gran Tablazo Archipelago

Much of the Chilcatay sequence deposited across the area once occupied by the Gran Tablazo Archipelago was eroded prior to or during the Pisco transgression. Silty sandstones of what remains of the upper Chilcatay sequence are most completely developed at the northeastern corner of Pampa El Cruce (DV 7089, 7090, 7095, 7096). In the same area, coarse-grained strata of the mid-Chilcatay parasequence – pumice cobbles (DV 7093) and horizons with boulders and well-rounded igneous and metamorphic cobbles (DV 2257, 7094, 8084; Figure 13B) – underlie the upper Chilcatay silty sandstone and overlie 40 meters of basal Chilcatay bioclastic sandstone (DV 4066, 4067, 7091, 7092, 7098, 7099) and an intervening wood-bearing medium-grained sandstone with *Testallium cepa* (DV 4069, 7093).

East of Cerro Geoglifo, a bed with CBR boulders (DV 4082, 4083, 8042, 8044) overlies lower Chilcatay oyster-bearing sandstone and pumice cobble beds (DV 4047, 4048; Figure 13C) that onlap the mainland side of the CBR hill and underlies silty sandstone of the upper Chilcatay sequence (DV 4083, 8043, 8076, 8078) and the boulder-bed lag at the base of the Pisco depositional sequence (DV 4044, 4083, 8075, 8077). Farther to the southeast, the boulder bed marking the mid-Chilcatay shoaling event merges with thick deposits of cup-and-flange oysters and barnacles that onlap the mainland side of Cerro Macharé (DV 4049, 4050).

A modern east-sloping valley, informally named "Quebrada Chacaltana" (Figure 1E), lies between the southeast end of Cerro Macharé and northwest end of Cerro Ortlieb. At the broad mouth of Quebrada Chacaltana lies a northeast-dipping bed of CBR boulders (DV 8059) that is correlative with the mid-Chilcatay boulder bed east of Cerro Geoglifo. Inside Quebrada Chacaltana, the northwestern and southeastern flanks consist of northeast-dipping bioclastic sandstone and oyster-barnacle coquinas that lap onto the mainland faces of

Cerros Macharé and Ortlieb (Figure 7D). In the middle of Quebrada Chacaltana, steeply inclined beds (Figure 13D) consisting predominantly of large sand grains of CBR and bivalves (oysters fragments, *Chlamys*; Figure 13E) are arranged in overlapping and anastomosing elongate (azimuth 210 degrees) channel-form outcrops (DV 8060), tens of meters long, ten meters wide, two to three meters thick, and asymmetrically preserved in a manner that all beds dip steeply to the northwest. The channel-form bodies are embedded in finer-grained oyster-barnacle bioclastic sandstone. Proceeding northeastward, i.e., down the modern Quebrada Chacaltana and towards the paleo-mainland, the channel-form deposits (DV 8061, 8062) become smaller, and the grain size becomes finer, and laminated coarse-grained sandstone becomes more common (Figure 13F). The elongate coarse-grained deposits are inferred to represent channels or the point-bars of channels that drained shallow marine waters behind Cerros Macharé and Ortlieb. They may be correlative with the nearby mid-Chilcatay boulder bed.

Farther to the southeast, beginning near Quebrada Chacaltana and passing Cerro Ortlieb toward Camino de los Burros, mid-Chilcatay boulders and upper Chilcatay fine-grained deposits disappear and are replaced by the basal boulder bed and overlying fine-grained sandstone of the Pisco depositional sequence (DV 8067), which also nonconformably overlies CBR (DV 4086). Even farther south, half grabens with CBR footwalls, CBR islands of the Gran Tablazo Archipelago, and marine strata at the northwestern edge of Bahía de Ica Baja meet in a structural nexus herein informally termed the "Nudo del Diablo" (Devil's Knot; Figure 1C). In this area, successive and overlapping channels are filled with poorly sorted conglomerates consist of CBR cobbles and lithoclasts of dolomitized and hackly silty sandstone (DV 2212; Figures 14A, 14B). The conglomerate-filled channels may represent the mid-Chilcatay shoaling event or might be contemporaneous with a lithoclast filled channel, ten meters deep, carved into and overlain by silty sandstones in the lower Chilcatay depositional sequence in the Lomas Chilcatay (DV 442, 1817; Figures 4A, 13A).

4.4.3. Bahía de Ica Baja

The mid-Chilcatay parasequence at the Viking Locality (DV 1615, 1636, 1637, 1638, 4022, 4023, 8126, 8127; Figure 1F) is represented by four beds with boulders of CBR, lithoclasts of dolomitized siltstone, and intercalated beds of coarse- and medium-grained bioclastic sandstone (Figure 14C). Exposures of the boulder beds (DV 8102, 8111, 8123) extend southwestward for eight kilometers towards the mouth of Quebrada Gramonal (Figures 14D, 14E). The bioclastic boulder beds overlie basal Chilcatay bioclastic oyster-barnacle sandstone and intervening silty sandstone and underlie a thick section of white-weathering silty sandstone (DV 8106) and medium-grained sandstone with *Misifulgur cruziana*, small shark teeth, fish skeletons, and large pieces of wood (DV 1615, 8109, 8110).

Mid-sequence Chilcatay boulder beds are present above Fundo Santa Rosa (DV 1023, 7034, 7039), associated with massive orange sandstone, bioclastic sandstone and coquina with broken barnacles and oysters. The boulder and bioclastic horizons trace southward into bioclastic sandstone (DV 7022) with broken barnacles, bryozoan nodules, and rare CBR boulders (DV 7024, 7031). At Laberinto, boulder beds and coarse-grained bioclastic sandstone (DV 5053, 5054, 5055) with barnacles, large oysters, *Chlamys* valves, and small odontocetes crop out in an extensively faulted area partly covered by modern sand dunes and a Pliocene non-marine lithoclastic debris flow (DV 5047, 5048, 7029). Three kilometers farther south, about one kilometer southwest of locality DV 5040, three boulder beds are intercalated with bioclastic sandstone that overlies and underlies silty sandstone (Figure 14F).

Boulder beds and barnacle- and oyster-bearing bioclastic sandstone of the mid-Chilcatay shoaling event within the inlandmost reaches of Bahía de Ica Baja, i.e., Yesera de Amara, Tinajones and Samaca West (Figures 1E, 1F), can be mistaken for the prominent lower Chilcatay Piedra Negra boulder bed. The mid-Chilcatay boulder beds, however, can be properly placed stratigraphically at DV 2203, 2204, 2206, and 8130. At locality DV 8130 and 8133, mid-Chilcatay CBR boulders occur together with glauconitic coarse-grained sandstone composed mostly of CBR grains.

4.5. Chilcatay clinoform allosequences

Clinoform allosequences, five to 50 meters thick and extending longshore and basinward for hundreds of meters to kilometers, are visible across the plains of Ullujaya West and Tinajones (DV 379, 1807, 4104, 8135; Figures 15A, 15B) and southward beyond the Viking Locality (DV 8108, 8109, 8110), but are most dramatically exposed transversely and longitudinally at Quebrada Gramonal (DV 1308; Figures 15C, 15D, 15E, 15F). An additional clinoform set crops out in Laberinto (DV 5050). By tracing clinoform allosequences and correlative strata from Quebrada Gramonal (DV 575) northward (DV 637, 8107, 8108) toward the Viking Locality (DV 1615) and across the Río Ica (DV 1642, 2207, 2210), it is apparent that the clinoform sets are developed only in the upper Chilcatay sequence. The allosequences interleave distally with silty diatomaceous sandstone (DV 598; Figure 15F) or medium-grained sandstone with *Thalassinoides* burrows, odontocete skulls, large pieces of wood, and rounded cobbles of pumice (DV 8134). Elsewhere in the East Pisco Basin, e.g., Playa Sombrero (DV 478, 5015) and the Gran Tablazo Archipelago (DV 7089, 7090), such silty and medium-grained sandstone constitutes the principal lithology of the upper Chilcatay sequence. Within Bahía de Ica Baja, the clinoform sets are absent at Cerro Tiza (DV 591), 14 kilometers basinward of the paleo-shoreline; absent at the Viking Locality (DV 1637), less than one kilometer from the paleo-shoreline; and rare at Laberinto (DV 5051, 5052), three to four kilometers from the paleo-shoreline.

At Quebrada Gramonal, oblique-tangential clinoform beds are arranged in stacked sets with sets decreasing in thickness up-section (Figure 15E). Foreset beds are continuous with topset beds in an inland direction, with bottomset beds in a basinward direction, and often truncated by an upper sequence boundary (DV 575, 1308, 4018). Foreset beds have dip azimuths of about 210 to 230 degrees, oblique to the course of the modern Quebrada

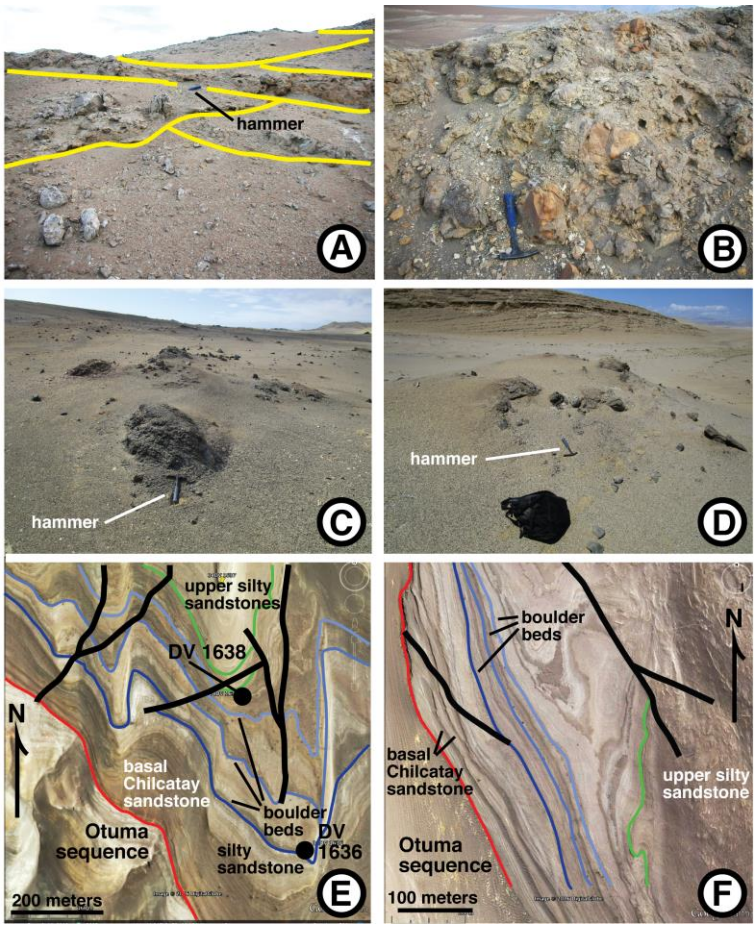

Figure 14. *Nudo del Diablo outcrops and mid-Chilcatay parasequence boulder beds in the Ica Valley. A. Successive cross-cutting channels in mid-Chilcatay sequence, Nudo del Diablo (DV 8126); channels marked with yellow lines. Channel fill of dolomitized siltstone lithoclasts, hackly siltstone lithoclasts, and bioclastic debris. Hammer for scale. B. Closeup of lithoclasts filling mid-Chilcatay channels in Nudo del Diablo (DV 8126). C. One of several CBR boulder beds comprising mid-Chilcatay parasequence, Viking Locality (DV 8126). Hammer for scale. D. Pile of CBR boulders at base of mid-Chilcatay parasequence between Viking Locality and the mouth of Quebrada Gramonal (DV 8123). Hammer for scale. E. Google Earth imagery showing multiple boulder beds (shades of blue) from the mid-Chilcatay parasequence near the Viking Locality. Red line is boundary between the Otuma and Chilcatay sequences. DV 1636 and DV 1638 shown for reference. F. Google Earth imagery showing multiple boulder beds (shades of blue) from the mid-Chilcatay parasequence west of the Sula Site. Red line is boundary between the Otuma and Chilcatay sequences. Locality DV 5040 is 400 meters northeast of upper right corner of image.*

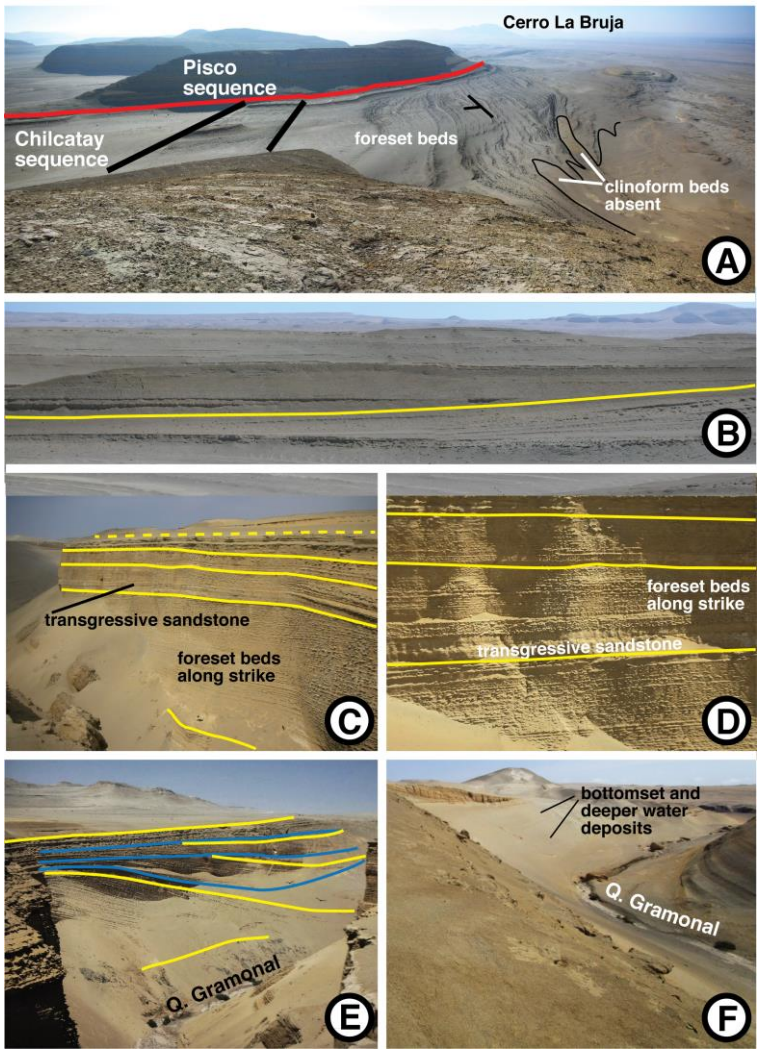

Figure 15. *Chilcatay clinoform allosequences. A. Foreset clinoform beds, dipping southwest (to the left in photo). Tinajones, view from DV 2032 northwestward towards Cerro La Bruja. Faults shown with thick black lines. Base of Pisco depositional sequence marked by red line. B. Clinoform foreset bed transitioning to left in photo to bottomset bed. Tinajones, DV 2207. Yellow line marks foreset/bottomset bed. C, D. Clinoform sets at Quebrada Gramonal, viewed along bedding strike from DV 4018. Yellow lines separate clinoform allosequences, each of which commences with a transgressive sandstone and culminates with progradative foreset beds. Thickness of section about 40 meters. E. Clinoform sets, Quebrada Gramonal, view of cliffs downstream from DV 1308. Yellow lines mark bases of sets' transgressive sandstone. Red lines mark erosive base of prograding foreset beds. F. Clinoform sets, Quebrada Gramonal, distal part of allosequences with foreset beds transitioning to bottomset beds and deeper water silty sandstones with diatoms and clupeoid fish scales between clinoform sets (DV 575).*

Gramonal but approximately perpendicular to the paleo-shoreline. Between Samaca and Yesera de Amara, clinoform sets are often offset, not always stacked (DV 2032), and vary in longshore width within and between allosequences (DV 1609). Clinoform beds have dip azimuths of 210 to 240 degrees, oblique to the course of the modern Río Ica but also approximately perpendicular to the paleo-shoreline. Similar dip azimuths characterize the clinoform sets between the Viking Locality and Laberinto.

The clinoform beds, which can dip as much as eight to ten degrees (DV 2208), consist of bioclastic sandstone and gravel-sized conglomerate with few cobbles or boulders. The invertebrate fauna consists of comminuted barnacles, echinoderms (disarticulated echinoid carapaces, sea urchin spines, and comatulid crinoids), and a diverse assemblage of gastropods and disarticulated bivalves. Vertebrate remains include shark teeth and partially disarticulated odontocete skulls and bones.

The Gramonal clinoform sets are separated landward by one to two meters of massive sandstone (DV 2034; Figures 15C, 15D) with *Thalassinoides* burrows, shark teeth, and partial skeletons of odontocetes. On the Ullujaya West pampa, clinoform sets are separated landward by massive sandstone (DV 8139) densely packed with *Thalassinoides* burrows; scoured channels filled with bioclastic sandstone and matrix-supported rounded igneous and metamorphic cobbles sourced from nearby pre-Chilcatay cobble conglomerates (DV 8141); boulders of pumice and CBR (Figures 16A, 16B); lenses and beds of barnacles, mollusks (*Glycymeris ibari*, *Tilicrassatella ponderosa*, *Turritella cruzadoi*, *Testallium cepa*, *Conus*) capped with veneers of transported oyster valves; small odontocetes; banks with *G. ibari*, *T. ponderosa*, *Crepidula*, *Calyptraea* (*Trochita*), *Acanthina katzi*, *T. cepa*, and *Olivancellaria tumorifera*; and mudstone with embedded cobbles (DV 1611, 1612, 4039, 4040). Basinward, the clinoform sets are separated by varying thicknesses of diatomaceous, fish scale-bearing, silty sandstone (DV 575, 598, 1022).

The uppermost clinoform allosequence in Quebrada Gramonal (DV 4018; Figure 16C) and Ullujaya/Tinajones (DV 1608, 2032, 2034; Figure 16D) is overlain with a few meters of massive, *Thalassinoides*-burrowed, odontocete- and shark tooth-bearing sandstone with thin-bedded intercalations of bioclastic sandstone, which in turn are overlain by thin beds of indurated dolomitized sandstone and silty sandstone with clupeoid fish scales, diatoms, and ash dated between 17 and 18 Ma (Belia et al., 2015); these beds have been designated informally in the field as the "Urbina beds."

4.6. Early Pisco transgressive phase

4.6.1. Bahía de Ica Baja (Yesera de Amara and Tinajones)

The Pisco transgression left its earliest mark in Bahía de Ica Baja, evidenced by the "P0" parasequence (terminology of Di Celma et al., 2017; previously named the "old Pisco beds" in the field) between Yesera de Amara and the Río Ica (Figure 17A). Towards Cerro La Bruja, P0 deposits onlap a peneplain of Precambrian granite (DV 489, 1605, 3081; Figure 17B; Montoya et al., 1994), as do the bioclastic strata (fragmented oysters, barnacles, and *Concholepas unguis*; DV 1605, 1606, 3081) of the overlying P1 parasequence. To the east, near the Río Ica (DV 2033), P0 and P1 deposits nonconformably overlie the previously unrecognized pre-Miocene conglomerate (DV 8141) and the metamorphic Precambrian Basal Complex (Montoya et al., 1994). One kilometer west of Yesera de Amara (DV 1608), the base of the P0 parasequence is marked by a lag of dolomitized lithoclasts (DV 1809; Figure 17C). Five kilometers farther west, at Zancones (DV 2211, 3042, 3043; Figure 17D), typical P0 mollusks are absent and a late Miocene ash bed (Di Celma et al., 2017) crops out just above the boulder-strewn base of the Pisco sequence.

In the Tinajones area, the basal P0 lag (DV 1180) contains one or more of the following: mollusks (*Miltha*, *Chionopsis*, *Ficus distans*, *Acanthina katzi*, *Misifulgur cruziana*), barnacle- and oyster-encrusted boulders, bioclasts of polychaete colonies, teeth of the shark *Carcharocles megalodon*, and bivalve-bored wood. The lag is overlain by massive sandstone with cetacean skeletons and paired valves of *Miltha*, *Chione* and *Chionopsis* (DV 1181, 1805). Closer to the high-stand P0 paleo-shoreline, a basal P0 lag of bioclastic sandstone with iron-rich authigenic nodules, barnacles, oysters, and *Testallium cepa* unconformably infills an irregular surface of tilted ridges of bored, dolomitized, Chilcatay sandstone (DV 2016; Figure 17E). The lag is overlain by bioturbated (*Thalassinoides*, *Gyrolithes*) massive sandstone with a horizon of paired *in situ Miltha* valves (Figure 6D), dispersed paired valves of *Chione* and *Chionopsis*, lenses of gastropods, bivalve-bored wood, and partial skeletons of cetaceans (DV 2014, 2015, 2016, 2017, 4065; Figure 17F). The massive bed is capped by a 30 cm-thick coquina (DV 2015, 2016, 4099, 4100, 4101) composed of barnacles and a diverse assemblage of mollusks (*Tilicrassatella ponderosa*, *Dosinia ponderosa*, *Chione*, *Turritella infracarinata*, *Muracypraea ormenoi*, *F. distans*). Exposures north of Yesera de Amara (DV 3087, 4102) show this coquina lies several meters below the boulder-bearing P0/P1 parasequence boundary. Between DV 4102 and Yesera de Amara, the faunally diverse coquina grades basinward into a venerid- and mactrid-bearing sandstone and farther basinward into gypsum beds with few mollusks (DV 4109).

Closest to the high-stand P0 paleo-shoreline, beds of poorly consolidated bioclastic sandy and gravelly conglomerate (DV 376, 2029, 2030, 2031, 2033, 7009) that cover CBR and pre-Miocene conglomerate consist of fragmented barnacles, oysters, crinoids, echinoids, the boring bivalve, *Petricola*, and the gastropods *Crepidula*, *A. katzi*, *Olivancellaria tumorifera*, *Olivella*, and *Conus* (DV 1613, 1614).

Farther to the southwest and farther from paleo-shorelines, the P0/P1 boundary throughout much of Tinajones has few boulders (DV 499); it is more often defined by a thick bed of bioclastic sandstone or coquina with mollusks (*Miltha*, *F. distans*; DV 1608, 2032). Just east of Yesera de Amara and Cerros Mama y Hija (Figures 1E, 1F), however, the P0/P1 contact is overlain by boulders and bioclastic debris, including shark teeth and balanopterid skeletons (DV 1801, 1802, 4064).

The P0/P1 boulder bed passes west of Yesera de Amara (DV 1017, 1809, 3088, 7018 (pebbles only) and north of Yesera de Amara (DV 1801, 1802, 4064, 4109) towards

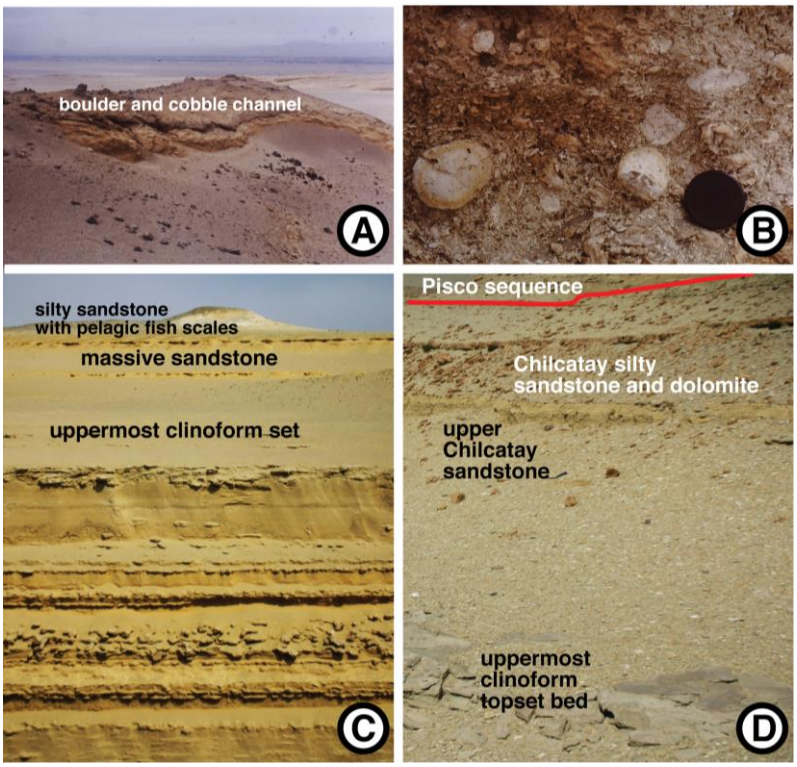

***Figure 16**. Upper Chilcatay sequence strata. A. Boulder- and cobble-filled channel cut into massive sandstone deposited between clinoform sets, Ullujaya West (DV 1612). Channel base about five meters wide. B. Close-up of channel fill debris: cobbles of pumice floating in matrix of barnacle coquina and bioclastic sandstone, Ullujaya West (DV 1612). Lens cap for scale. C. Uppermost Chilcatay sequence at Quebrada Gramonal, with white knoll at DV 4019. Uppermost clinoform set (viewed along strike of foreset beds) overlain with massive sandstone with cetacean bones, which in turn is overlain by deeper-water silty sandstones. Massive sandstones and silty sandstones are informally named the "Urbina beds". Width of view about seven meters. D. Uppermost Chilcatay sequence ("Urbina beds") overlying the uppermost clinoform set at the northern edge of Yesera de Amara (DV 2202).*

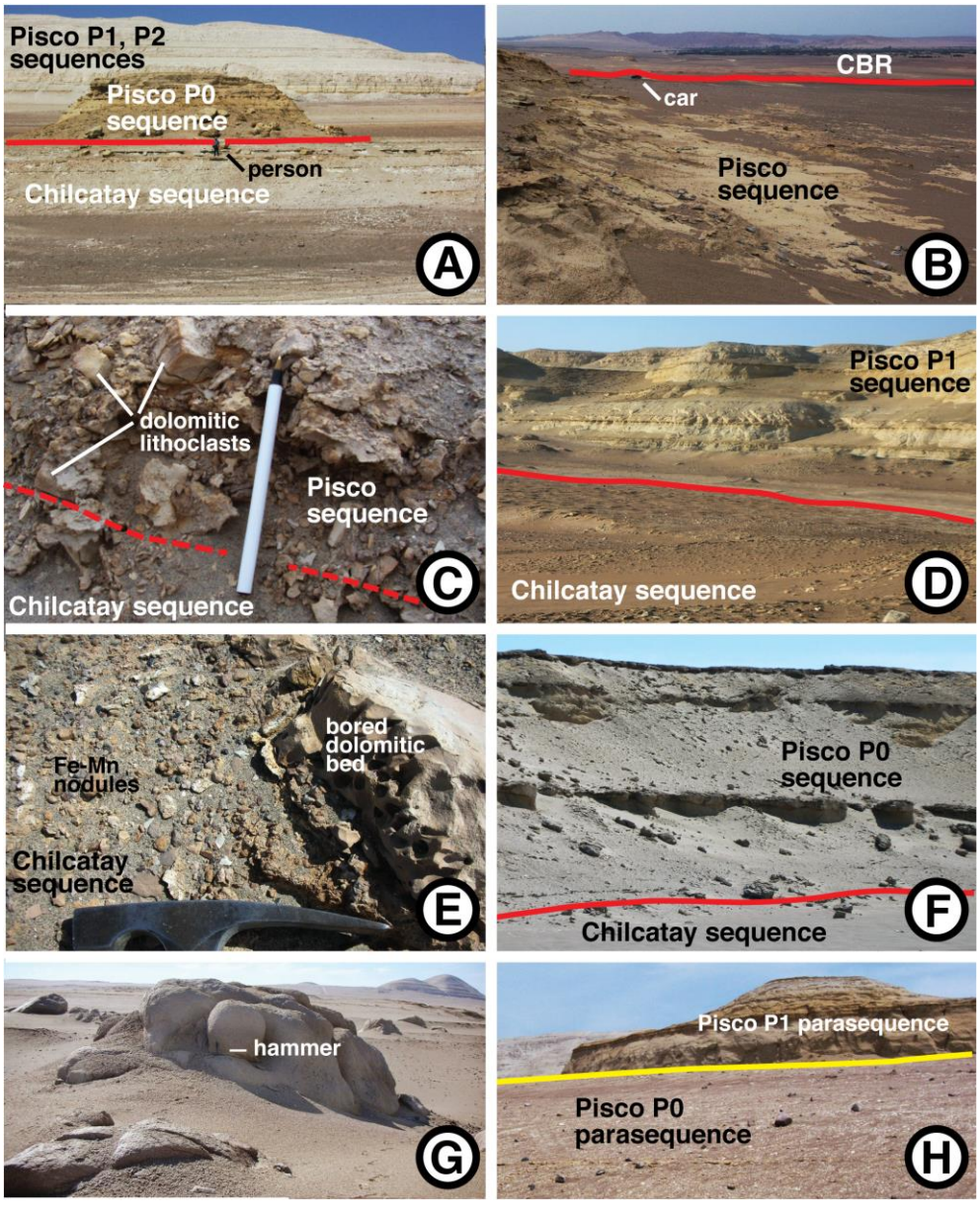

***Figure 17.** Lower Pisco depositional sequence. A. Upper Chilcatay sequence at base of knolls between Cerro Submarino and Yesera de Amara (DV 1510), overlain by boulder lag deposit and massive sandstone of Pisco P0 parasequence. Upper Chilcatay ash bed at person's feet dated between 17 and 18 Ma (Belia et al., 2015). Pisco P1 parasequence and younger allosequences in background. B. Massive sandstone of the Pisco P1 sequence lapping in distance onto CBR peneplain east of Cerro La Bruja. C. Dolomitized siltstone lithoclasts at base of Pisco sequence, west of Yesera de Amara (DV 1809). Lithoclasts overlie Chilcatay fine-grained deposits. D. Contact between Chilcatay and Pisco P1 sequence (red line), Zancones (DV 3042). The absence of Chilcatay-style mollusks indicates the absence of the Pisco P0 sequence in Zancones. E. Bored dolomitized Chilcatay siltstone underlying the Pisco P0 parasequence, Tinajones (DV 2016). F. Massive and bioclastic sandstone of the Pisco P0 parasequence, Tinajones (DV 2016). Width of view about six meters. G. Boulder bed on Pisco P0/P1 parasequence boundary, upper Tinajones towards Cerro La Bruja (DV 1613, 1614). CBR boulders several meters in diameter are stacked four meters high. Hammer for scale. H. Pisco P0/P1 parasequence boundary (yellow line) east of Yesera de Amara (DV 1182).*

Cerro La Bruja (DV 551, 1810, 3087, 7013, 7014, 7015, 7020; the lattermost locality has the gastropods *Crepidula*, *Acanthina katzi* and *Olivancellaria tumorifera*), where it eventually traverses the lower southeastern flank of that mountain (DV 2019, 3050, 3053, 3054) before turning eastward, passing downhill (DV 1613, 1614, 2018) between P0 and P1 bioclastic gravelly conglomerate to the floor of the Río Ica valley (DV 2029, 2030). At the head of Bahía de Ica Baja lie piles of boulders; most are granitic and some exceed four meters in diameter (DV 1613, 1614, 2018; Figure 17G).

East of Yesera de Amara, the boulders and cetacean bones at the P0/P1 boundary are overlain by 20 meters of massive, *Thalassinoides*- and *Gyrolithes*-burrowed, orange sandstone with dispersed pairs of *Chione*, *Chionopsis*, and *Dosinia*, cetacean bones, the turritellid *Incatella hupei*, and the middle Miocene-Pliocene *Ficus allemanae* (DV 542a, 549, 1182, 4064; Figure 17H). The massive sandstone is capped with a horizon of indurated sandstone with fish and cetacean bones and paired valves of middle Miocene *Anadara sechurana* and middle Miocene-Recent *Dosinia ponderosa*. The same *Anadara*-bearing horizon extends eastward to Cerro Submarino (DV 499, 3004). Westward and southward, the *Anadara* fauna is gradually replaced with an assemblage dominated by the bivalve, *Hybolophus* (DV 1806, 1809).

4.6.2. Bahía de Ica Baja (Quebrada Gramonal, Laberinto, Sula *Site)*

At the head of the canyon in Quebrada Gramonal, the lag at the base of the Pisco depositional sequence consists of a veneer of iron-rich authigenic nodules (DV 4018, 4019). Between Laberinto and the *Sula* Site, the same surface is covered with iron-rich authigenic nodules and varying proportions and sizes of dolomitized siltstone lithoclasts embedded in a matrix of coarse-grained bioclastic sandstone (DV 5038, 5039, 5040; Figure 18A). Lesser constituents include fragments of barnacles, cetacean bones, abraded shark teeth, and upended pairs of *Dosinia* resting on Chilcatay silty sandstone (DV 1021, 1309, 4019). Overlying the lag at Quebrada Gramonal are 15 meters of massive sandstone with partial skeletons of large balanopterids, tree trunks and other woody debris, and *Testallium cepa*. The sandstone is overlain by a horizon of large boulders of CBR (DV 377, 576, 699, 1021, 2034; Figure 18B) embedded in bioclastic gravelly sandstone that contains a diverse fauna of mollusks (*Tilicrassatella ponderosa*, *Ficus distans*, *T. cepa*, *Conus*, *Terebra*), bioclasts of polychaete colonies, large oysters, and barnacles. Based on the stratigraphic position of the boulder bed and the content of its fauna, the underlying massive sandstone is assigned to the P0 parasequence and the boulder bed is inferred to be the P0/P1 parasequence boundary. The absence of the older molluscan fauna and defining parasequence boundary farther south at the *Sula* Site indicates the P0 parasequence does not exist so far south or, perhaps, so close to the foot of the Monte Grande Fault.

At Quebrada Gramonal, an interval of massive wood-bearing sandstone, about 17 meters thick (DV 576, 1021, 2035, 4021), overlies the first boulder bed and in turn is overlain by a second boulder bed with fewer boulders (Figure 18C) but a similar molluscan fauna, although with a greater abundance of species (e.g., *Turritella infracarinata*) that most commonly occur in the P1 parasequence. Above the second boulder bed are 150 meters of massive wood-bearing sandstone (DV 1021, 2035, 7010, 7011) with intercalations of indurated 30-cm-thick beds of shell debris (with, in the lower 30 meters, accompanying widely spaced boulders of CBR; Figure 18C) containing a diverse fauna of small invertebrates, including the epitoniids *Scalina* and *Alora*, *Calyptraea* (*Trochita*), *T. infracarinata*, *Acanthina katzi*, *Concholepas unguis*, *Tactilispina vermeiji*, *T. cepa*, nassarids, turrids, odostomines, scaphopods, *Dosinia*, *Mulinia*, and paired *in situ* valves of *Panopea*. The vertebrate fauna includes partial skeletons of cetaceans, shark teeth, including those of *Carcharocles megalodon*, and complete skeletons of the shark, *Isurus hastalis* (DV 1301). Similar intercalated massive sandstones and shell lags with a diverse assemblage of small mollusks, comatulid crinoids, odontocetes, seabirds, shark teeth, and pieces of wood (DV 1653, 1654, 1655, 5043, 5044), crop out at the *Sula* Site (Figure 18D), although without boulders. The uppermost beds at Gramonal (DV 1021) contain specimens of *Concholepas chirotensis* and *Anadara sechurana*, but not *T. infracarinata*.

Between Quebrada Gramonal and the Sula Site are correlative outcrops (DV 1019, 1306, 1307, 5060) of scoured channels or point bars floored with lags containing the same diverse molluscan assemblage as seen in the intercalated shell lags north and south (Figure 18E).

4.6.3. Gran Tablazo Archipelago

Many of the *en echelon* ridges of CBR that formed Chilcatay islands of the Gran Tablazo Archipelago were no longer emergent or only barely so during early Pisco time, judged from the trace of the basal Pisco boulder bed onto the mainland flank of the paleo-islands (Figure 7D). The angularity of the unconformity between the Chilcatay and Pisco depositional sequences is substantial where north-dipping, bored, dolomitized silty sandstones of the upper Chilcatay sequence crop out (DV 1645, 2231) at the northern end of Cerros Colorados (DV 7090), persists to a lesser degree as far southeast as Cerro Geoglifo (DV 4043), and disappears in a welter of cup-and-flange oyster-barnacle coquina beds at the northwest end of Cerro Macharé (DV 4050).

The contact between the Chilcatay and Pisco depositional sequences at the northwest end of Cerros Colorados (DV 1645, 1646, 2231), four kilometers distant from Cerro Geoglifo, is blanketed by a veneer of iron-rich authigenic nodules, but no mollusks, cobbles, boulders, or lithoclasts (Figure 2A). Sandstones a few meters higher in the section (DV 1646) contain mollusks (*Anadara sechurana*, *Trachycardium*, *Dosinia ponderosa*, *Incatella hupei*) that are rare or absent in the P0 parasequence, but common in the P1 parasequence in Bahía de Ica Baja. Moving to the southeast along the base of the Pisco sequence, scattered boulders begin to appear with the authigenic nodules (DV 8083). Farther to the southeast, landward of Cerro Geoglifo (DV 4043, 4044, 8043, 8073, 8075, 8077, 8079, 8080, 8081, 8082), the two- and three-meter boulders become more

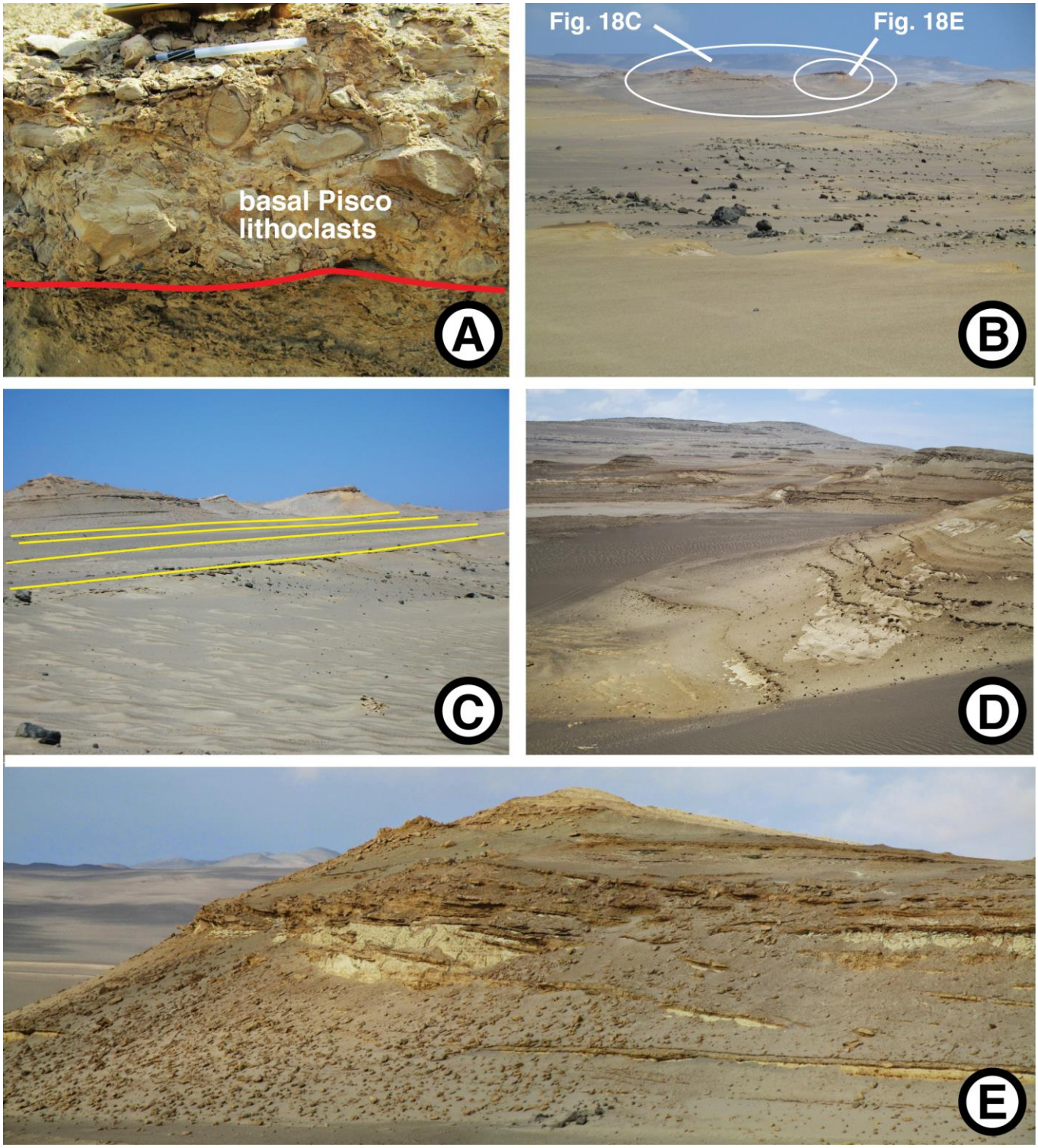

Figure 18. *Lower Pisco lithofacies from Quebrada Gramonal to the Sula Site. A. Dolomitic lithoclasts at base of Pisco sequence, overlying Chilcatay sandstones (DV 5038). B. Lowest and principal boulder bed of the Pisco sequence at Quebrada Gramonal, exposed as a bedding plane (DV 7011); inferred to be Pisco P0/P1 parasequence boundary based on molluscan fauna. Large boulder near center of photo about 1.5 meters in diameter. Location of outcrops shown in Figures 18C and 18E circled in white. C. Multiple boulder beds southeast of Quebrada Gramonal, east of road to Fundo Santa Rosa (DV 2034). Lowest bed inferred to be P0/P1 boundary. Boulder beds higher in section with fewer boulders and coinciding with fine bioclastic gravel; intervening sediments medium-grained to fine-grained sandstone with diverse molluscan fauna, cetacean bones, and entire skeletons of the shark, Isurus hastalis. D. Indurated bioclastic beds with cetaceans, seabirds, and a diverse invertebrate fauna, including scaphopods and crinoids, Sula Site (DV 5040). Bioclastic beds intercalated with soft-weathering fine- and medium-grained sandstone. E. Channel-form scours with basal lag of bioclastic coarse-grained sandstone (DV 5060) containing the same diverse molluscan fauna found in planar beds above Quebrada Gramonal and the Sula Site. Wall of the Monte Grande Fault in the background.*

closely spaced and set in a continuous pavement of gravel, rounded cobbles, and small boulders that underlie massive orange sandstone with large balanopterid whales (DV 4046). The boulder and cobble pavement continues southeastward behind Cerro Macharé and continues to Quebrada Chacaltana (DV 8067), where two- and three-meter boulders of granite rest on a thin bed of bioclastic sandstone that defines the Chilcatay/Pisco unconformity (Figure 8A). Overlying the boulder bed in Quebrada Chacaltana are several meters of massive orange sandstone (DV 8065, 8066) with lenticular accumulations and single paired valves of the middle Miocene *A*. *sechurana*, *Trachycardium*, and *D*. *ponderosa*, indicating that at the quebrada, too, the oldest Pisco beds of the P0 parasequence are absent and beds of the P1 parasequence directly rest upon Chilcatay strata. The same is true for *Dosinia*- and *Incatella*-bearing sandstones landward of Cerro Ortlieb (DV 4086, 4087), which overlie fine-grained beds of the Chilcatay sequence and lap onto CBR of that paleo-island; the P0 parasequence appears to be absent and the P1 parasequence directly overlies Chilcatay beds or CBR. The P1 parasequence, comprised of bioclastic sandstone with *Chlamys*, *Acanthina katzi*, and *Concholepas unguis*, directly ovelies Eocene strata south of Camino de los Burros (DV 1324, 1325).

At the western extremity of the Gran Tablazo Archipelago, in Quebrada Perdida, the base of the Pisco Formation consists of iron-rich authigenic nodules, small and large dolomitic lithoclasts, some bored on the top, rare rounded boulders of CBR, and small odontocetes (DV 1728, 2215, 2216). It is uncertain if these Quebrada Perdida beds represent a reappearance of the P0 parasequence.

4.6.4. Playa Sombrero

Southeast of Cerro Antivo (Figure 1D), several meters of bioclastic oyster-barnacle crossbedded sandstone with echinoids and *Discinisca* overlie a platform of CBR (DV 935, 1003, 1012, 1013, 1014). The presence of *Concholepas unguis*, also found at the *Sula* Site and on the upper slopes of Quebrada Gramonal, and the absence of molluscan taxa typical of the Chilcatay depositional sequence indicate an age younger than that of the P0 parasequence. On the southwestern side of Cerro Antivo, the same bioclastic sandstone (DV 1002, 1108) unconformably overlies dolomitized silty sandstone of the Chilcatay sequence (DV 1105).

Playa Sombrero had a more complex paleogeography beginning with early Pisco time, judging from the dramatic change in lithology and fauna from the pass at Cerro Antivo to an area seven kilometers to the northeast, where at localities DV 1004, 1007, and 1008, dense accumulations of the small bivalve, *Mulinia*, and the gastropod, *Turritella infracarinata*, occur in massive, bioturbated, medium-grained sandstone, surrounded by and presumably overlying CBR. These two species, together with *C*. *unguis* or *C*. *chirotensis*, *Crepidula*, *Nassarius*, a variety of small bivalves (*Tellina*, *Petricola*, venerids), and *Discinisca*, occur in discrete horizons between thick beds of crossbedded sandstone, which fines upward with a less diverse fauna of *Crepidula* and *Mulinia* (DV 1009, 1010, 1011).

Farther east, disarticulated and paired valves of *Mulinia* are the most abundant molluscan species in massive sandstone that unconformably overlies dolomitized, clupeoid scale-bearing, silty sandstone of the Chilcatay sequence in the Filudo Depression (DV 419, 420, 451, 452; Figure 1D). Other molluscan taxa include *Dosinia*, *Panopea*, *T*. *infracarinata*, and *Anadara sechurana*. No species typical of the Chilcatay or Pisco P0 parasequence occur in the basal beds. Although now in fault contact with western outcrops of CBR, the Filudo sediments probably accumulated in the lee of Cerros Antivo and Diablo, whereas correlative sediments, coarser grained and with an invertebrate fauna indicative of higher energy, accumulated on the exposed western side of that same Antivo CBR highland.

4.7. Cerro La Virgen Chilcatay deposits

Close to the Chilcatay paleo-shoreline of Playa Sombrero, at the latitude of Cerro La Virgen, a northwest-southeast trending, high-angle normal fault, herein informally named the "Gabriel Fault," juxtaposes a thick section of upper Chilcatay and Pisco sandstone (DV 480, 5031) to the south with a knobby peneplain of CBR draped with banks of cup-and-flange oysters and echinoid spines to the north (DV 391, 479, 4017; Figure 2C). The bioclastic banks are replaced farther from the paleo-shoreline (DV 5032) by a basal lag of boulders composed of CBR and dolomitized siltstone that rests on poorly exposed knobs of dolomitized siltstone of presumed Otuma age. The lag is overlain by three meters of interbedded barnacle-oyster-echinoid coquina and bioclastic sandstone, identical to beds seen near the base of the Chilcatay sequence farther west (DV 5019). The fault-warped basal bioclastic sandstone beds (DV 5032, 5033) are overlain by one meter of dolomitized sandstone with bivalve-bored wood and odontocete bones and four meters of medium-grained and silty sandstone. The silty sandstone is truncated by an overlying disconformable contact with Pisco beds. The Pisco erosional surface is covered with a 20-cm lag of bioclastic sandstone (large oysters, large overturned barnacles) with dolomitized bored lithoclasts and boulders of CBR (DV 5027, 5028, 5030). Several meters of alternating beds of bioclastic sandstone and coquina (DV 5029) grade upwards into sandstone and silty sandstone of the lower Pisco sequence (DV 4015, 5028), interrupted by a boulder bed 20 meters above the lower boundary of the Pisco sequence. The abundance of boulders increases to the north. Two kilometers to the south of DV 5028 and farther from a paleo-shoreline that appears to have wrapped from east of Cerro La Virgen (DV 5002) to the north (DV 5004, 8001) and northwest, near DV 8002 and 8003, the basal oyster-barnacle bioclastic sandstones are replaced with massive bioturbated sandstone (Figure 2B), capped with two closely spaced oyster-barnacle bioclastic beds, the lower with shark teeth, numerous vertebrate bones (fish, turtles, cetaceans) and bivalves (*Dosinia ponderosa*, *Anadara sechurana*; DV 4010). The bed corresponding to the boulder horizon under Cerro La Virgen is a *Discinisca* bioclastic sandstone with cetacean skulls (DV 4011); more cetacean skeletal remains occur a few meters higher in the section (DV 4012). Fine-grained tuffaceous sandstone appears in both the Cerro La Virgen section and a section

at DV 4011, about 50 meters above the base of the Pisco sequence.

A possible stratigraphic interpretation of the section below the lithoclastic lag at DV 5028 and DV 5030 is indicated by the presence of Chilcatay cup-and-flange oysters on the north side of the Gabriel Fault below Cerro La Virgen (DV 4017; Figure 2C), the presence of *A. sechurana* in massive sandstone above the basal Pisco lag deposit (DV 4010), and the bone-and-wood dolomitized bed. The lag/sandstone/siltstone interval is thought to be the base of the Chilcatay depositional sequence. If that is so, most of the Chilcatay sequence was evidently eroded prior to a middle Miocene transgression and the onset of Pisco P1 deposition. The Pisco P0 parasequence appears to be absent.

4.8. Bahía de Nazca

The Miocene-Pliocene Bahía de Nazca extended from the footwall of the high-angle normal, north-northwest-striking Monte Grande Fault (DeVries, 2017) eastward across Quebrada Huaricangana (Figure 1F) to the cliffs of Cerro Huaricangana (DeVries, 1988a), and perhaps farther south prior to the late Miocene. The bay was floored with pervasively faulted CBR (Montoya et al., 1994; Leon et al., 2008). Basement footwalls of half-grabens protected down-dropped continental and estuarine beds of the early to middle Eocene Caballas depositional sequence (DeVries, 2017), which crop out at Puerto Caballas and in the lower Río Grande valley (Leon et al., 2008; DeVries, 2017), and marine beds of the Paracas depositional sequence, which crop out in Quebrada Santa Cruz (Dunbar et al., 1990; Figure 1F) and across an amphitheater-shaped basin facing Puerto Caballas (DeVries, 2017). Gastropods (*Turritella lagunillasensis*, *Clavilithes lagunitensis*, *Surcula thompsoni*, *Andicula occidentalis*) from the mouth of Quebrada Santa Cruz (DV 585, 1959) are the same as those found in the Los Choros Member of the Paracas Formation on the Paracas Peninsula (DV 501), near Carhuas (DV 394), on the floor of Cuenca Sombrero (DV 1174, 1819), and in the Talara Basin of northern Peru (Woods, 1922; Olsson, 1928, 1929; Rivera, 1957; DeVries, 2007, 2017). These taxa indicate an age of middle to late Eocene. Nannofossils from Quebrada Santa Cruz also indicate an age of middle to late Eocene, consistent with the age of the Los Choros Member (Dunbar et al., 1990), or, if the identification of *Isthmolithus recurvus* is correct, a late Eocene and very early Oligocene age, consistent with the age of the Otuma depositional sequence (Dunbar et al., 1990; Stock, 1990; DeVries, 1998, 2004; DeVries et al., 2006, 2017; Shipboard Scientific Party, 2004).

In Quebrada Huaricangana, basal conglomeratic and bioclastic sandstones of Stock's (1990) "Unit A," contain specimens of *T. lagunillasensis* (mistakenly identified by this author in 1986 as *T. gilbertharrisi*; see Table I in Stock, 1990), which is known only from the middle Eocene Paracas Formation (DeVries, 1998, 2007). Horizons within Unit A, as well as overlying silty sandstone ("Unit B") that plausibly constitutes the upper middle Eocene Yumaque Member of the Paracas Formation (Dunbar et al., 1990, DeVries, 1998), contain nannofossils consistent with a late middle Eocene age, except for the presence of *Isthmolithus recurvus* (Marty, 1989).

Disconformably overlying Eocene strata on the eastern flank of Quebrada Huaricangana are coarse-grained sandstones of Stock's (1990) "Unit E." A clast-supported cobble conglomerate at about 100 meters in the measured section at Stock's locality QH87A2 contains abundant specimens of large *Turritella woodsi*, as do the same beds farther up Quebrada Huaricangana (DV 387, 581). While the presence of *T. woodsi* alone cannot distinguish beds of the Otuma from beds of the Chilcatay depositional sequences, the added presence of *Testallium cepa* in conglomeratic bioclastic sandstone deposited nonconformably on a peneplain of CBR at Pampa de Poroma, 40 km due east, on the landwardmost edge of Bahía de Nazca (DV 638, 1970) confirms a latest Oligocene to earliest Miocene age for the Pampa de Poroma deposit (Vermeij and DeVries, 1997) and points to a comparable age for the Huaricangana conglomeratic sandstone, i.e., the age of the Chilcatay depositional sequence. Silty sandstone overlying the *Turritella*-bearing sandstone of Quebrada Huaricangana, Stock's (1990) "Unit F," contains in sample RC-34 two radiolarian species, *Dorcadospyris ateuchus* and *Lychnocanoma elongata*, that are mistakenly attributed an early Oligocene age, but in fact, demonstrate a very late Oligocene or early Miocene age (Shipboard Scientific Party, 2004), i.e., consistent with the age of the Chilcatay depositional sequence.

Outcrops along the floor and high on the slopes of the Río Grande, along the western side of Bahía de Nazca include thick couplets of underlying orange sandstone and overlying soft-weathering white sandstone that are possible outcrops of Chilcatay beds, including bioclastic oyster- and echinoid-bearing sandstone at the foot of Cerro Terrestral (DV 522; Figure 1F; Leon et al., 2008).

Upper Miocene and Pliocene marine sandstones of the Pisco depositional sequence, to varying degrees tuffaceous and diatomaceous, disconformably overlie Chilcatay beds and underlie an inland-dipping marine terrace with a bioclastic veneer (DV 423) containing the extinct late Pliocene mollusks, *Acanthina triangularis* and *Trachycardium procerum domeykoana* (DeVries, 2003). In Quebrada Huaricangana, the base of the Pisco sequence (DV 421a, 422, 532) does not include the older Miocene molluscan fauna that characterizes the P0 parasequence of Bahía de Ica Baja, but rather species found in the P1 parasequence and younger Miocene strata, e.g., *Ficus allemanae* (DeVries, 1997), indicating the P0 sequence is absent in Bahía de Nazca.

On the western side of Bahía de Nazca, a thick section of tuffaceous and silty sandstone disconformably overlies older coarse-grained bioclastic strata (DV 522). Mollusks in the upper half of the section (*Crepipatella dilatata*, *F. allemanae*, *Dosinia ponderosa*, large *Chionopsis*) indicate a correlation with upper Miocene beds of the Río Ica valley.

Small outcrops of marine sandstone east and southeast San Juan de Marcona (DV 381, 468a) contain abundant, small, disarticulated *Chlamys* valves, indicative of the Chilcatay or Pisco P0 sequences, and at one locality, DV 1237, the taxa *Concholepas unguis*, *Acanthina katzi*, and *Tactilispina vermeiji,* which indicate a middle Miocene age, correlative with the lower P1 parasequence in Bahía de Ica

Baja. Nearby outcrops (82JM010B) contain a suite of diatom species indicating an early Miocene age, consistent with the Chilcatay depositional sequence (Macharé et al., 1988).

4.9. Chilcatay wood analysis

Permineralized plant material was found in massive and bioturbated sandstone overlying a bed of BCR boulders that forms the basal lag of the Chilcatay sequence. The 30-cm length of the horizontally deposited cylindrical piece of wood was encrusted on its underside with barnacles, indicating a lengthy period of transport in marine or brackish waters before burial. The following description constitutes the first documentation and identification of a plant megafossil from the Chilcatay depositional sequence.

The wood specimen displays fibrovascular bundles and fibrous rings scattered among ground tissue in transverse section. The general pattern of the fibrovascular bundles is *Cocos*-type (Figure 19A). The fibrovascular bundles have two (rarely up to 4) metaxylem elements each (Figures 19B, 19C) and are wider than long with reniforma-type dorsal caps (Figure 19D). The vascular zone of the fibrovascular bundles is excluded from the fibrous zone. Mean metaxylem element diameter is indeterminable because of compression, but assuming conservation of circumference, diameters of 160 µm are typical for bundles with two metaxylem elements (n = 3) (Figure 19B). Cellular structure in the ground parenchyma is poorly preserved. Based on these characters, this palm wood is thought to belong to the tribe Coryphodeae (Arecaceae) and is assigned to the genus *Palmoxylon* Schenk, 1882 (Tomlinson et al., 2011; Thomas and De Franceschi 2013; Thomas and Boura 2015). Extant species of Coryphoideae are found throughout the Neotropics (Eiserhardt et al. 2011).

The occurrence of this palm fossil provides some constraint on the coastal continental environment of the Pisco Basin during the early Miocene. The distribution of modern palms is limited generally to regions with mean cold-month temperatures >5 °C and mean annual temperatures >10 °C (Larcher and Winter, 1981; Greenwood and Wing 1995; Walther et al., 2007; Eiserhardt et al., 2011; Archibald et al. 2014; Royer et al., 2002). Palms are typically absent from desert and semi-desert regions, except where groundwater is regularly available near the surface (Tomlinson et al., 2011). The occurrence of *Palmoxylon* in the Chilcatay depositional sequence indicates either the existence of a wetter coastal climate during the early Miocene or, more likely, the presence along an arid coastline of riparian areas past which river water regularly flowed from the Andes, carrying woody debris to the coast.

5. Discussion

5.1. Recognition of depositional sequence boundaries

With a limited range of Cenozoic marine lithologies being prevalent in the East Pisco Basin, it is challenging to recognize a particular depositional sequence in the field. The combination of a ravinement surface in a forced regression context, lag deposit, and overlying massive sandstone is the best evidence for identifying the base of a depositional sequence. An angular unconformity is typically observed at the Otuma/Chilcatay contact, together with an uneven ravinement surface caused by differential erosion of soft-weathering and dolomitized silty sandstone beds. At the Chilcatay/Pisco contact, however, the angularity of the unconformity is usually imperceptible. Often, molluscan species from the lag deposit and overlying massive sandstone are the only means for confirming the identity of particular sequences, although in cases involving the Chilcatay and Pisco P0 parasequence, nearly identical faunas makes such a distinction more difficult.

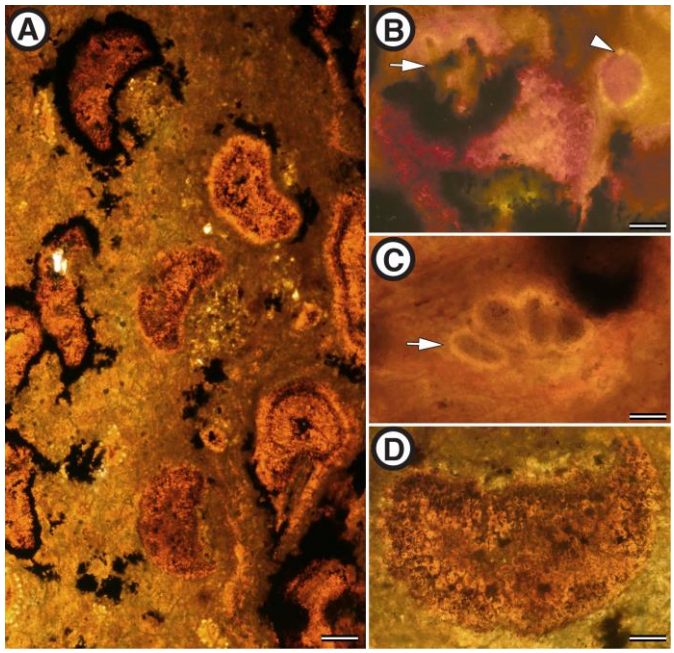

Figure 19. *Palmoxylon sp. (locality DV 8087-1) A. Cocos-type fibrovascular bundles, fibrous rings, and ground tissue. Note the fibrovascular bundles with cordata-type dorsal caps. B. Close up of a fibrovascular bundles and fibrous ring (at arrowhead). Note that the vascular zone contains two metaxylem elements (at arrow). C. Detail of the vascular zone of a bundle with four metaxylem elements (at arrow). D. Close up of a cordata-type dorsal cap. Scale bars: A = 200 µm; B and D = 125 µm; C = 100 µm.*

Index molluscan species (see DeVries (1995, 1997, 2003, 2007, 2016a, 2016b), DeVries et al. (2017), Nielsen and DeVries (2002), and Vermeij and DeVries (1997) for a discussion of some of these taxa) for the Paracas, Otuma, Chilcatay, Pisco P0, and Pisco P1 sequences are as follows:

Pisco, P1 and younger: *Ficus allemanae*, *Concholepas* spp., *Anadara sechurana*, *Trachycardium* aff. *T. procerum*, *Hybolophus* spp.

Chilcatay and P0: *Ficus distans*, *Turritella cruzadoi*, *Olivancellaria tumorifera*, cup-and-flange oysters, *Tilicrassatella ponderosa*, *Glycymeris ibari*.

Otuma: *Ficus chiraensis*, *Peruchilus culberti*, *Xenophora carditigera*, *Cardita newelli*, *Crassatella rafaeli*.

Paracas: *Turritella lagunillasensis*, *Cristispira paracasensis*, *Crassatella neorhynchus.*

Common species that are not restricted to one depositional sequence include *Turritella woodsi* (Otuma and Chilcatay), *Acanthina katzi* and *Misifulgur cruziana* (Chilcatay and Pisco), *Dosinia ponderosa* and *Turritella*

infracarinata (Pisco P0 and P1), and *Testallium cepa* (Chilcatay, Pisco P0, and lowermost Pisco P1).

Other surfaces with lag deposits or boulders include the Piedra Negra bed in the lower Chilcatay depositional sequence, within the mid-Chilcatay parasequence throughout the Pisco Basin, the Pisco P0/P1 contact in Bahía de Ica Baja and from Quebrada Gramonal to Laberinto, and successive boulder beds in the lower Pisco P1 sequence at Quebrada Gramonal. The origin of each of these boulder-bearing beds must be judged in their stratigraphic context. None of these examples is associated with an angular unconformity, hence none should be mistakenly identified as the basal Chilcatay ravinement surface and lag deposit. The Piedra Negra bed is ensconced within massive sandstone, a stratigraphic configuration that can only be compared in some cases with that of the Pisco P0/P1 contact. The latter, however, underlies by only a few meters or tens of meters sandstones with a Pisco P1 and younger molluscan fauna, whereas the former overlies by only a few meters the angular unconformity with Otuma strata.

5.2. Piedra Negra bed and tsunami deposits in the Pisco Basin

The Peruvian continental margin has been an active subduction zone from the Paleozoic to the present (Mamani et al., 2010). Tsunamis initiated by large subduction earthquakes along the Peruvian margin must have occurred throughout this time, and a geological record of tsunami events should exist where conditions were conducive to the preservation of tsunami deposits. In the East Pisco Basin, Eocene, Oligocene, and early to middle Miocene continental deposits are unknown. Thus, reports of modern, historic, and prehistoric tsunami deposits, including sediments carried inland during the Indian Ocean tsunami of 2004 and the Tohoku-oki tsunami of 2011 (e.g., Moore et al., 2006; Paris et al., 2007; Goto et al., 2015; Ishimura and Miyauchi, 2017) offer few insights regarding putative Miocene tsunami deposits in the the East Pisco Basin, other than to establish that shallow-water boulders four meters in length can be carried onshore hundreds of meters from exposed reef fronts (Goto et al., 2007).

Descriptions of modern offshore tsunami deposits are more likely to inform an analysis of the Piedra Negra bed and similar boulder beds in the East Pisco Basin. Tamura et al. (2015) identified thin sand beds at inner shelf depths carried seaward by the backwash of the Tohoku-oki tsunami, but also observed the similarity of these sand beds with storm-deposited sand and further commented that the tsunami sand horizons were likely being degraded by bioturbation and reworked by storm waves. Feldens et al. (2012) identified offshore tsunami deposits in the Indian Ocean down to a depth of 18 meters: sands resting on an erosional surface, poorly sorted and containing shell fragments, pieces of terrigenous rock, and plant debris. Sakuna et al. (2012) observed much the same, with terrigenous and anthropogenic debris in a coarse-grained layer at water depths to 15 meters and no evidence of a tsunami bed in sediments at a water depth of 57 meters.

The Piedra Negra boulder bed exhibits many of the features characteristic of offshore tsunami deposits (Sakuna et al., 2012) and offshore tsunami boulder beds in particular (Paris et al., 2010), including an erosive base, an extremely wide range of grain sizes and clast lithologies, very large boulders that are largest at the seaward limit of the deposit, imbricate clasts, and varied bedding structures. Not all these features have yet been associated with other boulder beds in the Chilcatay and Pisco depositional sequences. Mid-Chilcatay boulder beds from the Viking Locality to Laberinto and upper Pisco P1 boulder-bearing bioclastic sandstone beds above Quebrada Gramonal are not as densely packed with boulders of CBR as the Piedra Negra bed, nor are they as areally extensive. They do occur close to CBR sources, a black basement pampa southeast of Cerro Sechuito and the highlands east of the Monte Grande Fault (Figure 1F). North of Quebrada Gramonal, a Pisco P1 boulder bed laps onto that same black CBR pampa (DV 1232, 1234b). It remains unclear if these boulder beds represent tsunami backwash deposits or the transport of boulders away from CBR highlands by a combination of floods and storm waves.

Beds with origins attributed to tsunamis outside the East Pisco Basin include the middle Miocene Tsubutegaura conglomeratic horizons, which are embedded within alternating upper bathyal sandstone and siltstone in a paleo-embayment on the central coast of Japan (Shiki and Yamazaki, 1996; Tachibana and Tsuji, 2013). With respect to the largest boulder size (about three meters in diameter), the varied roundness (round to angular) of boulders, the great contrast in grain size between the conglomerate and the enclosing sedimentary strata, and the coarse-grained sandy texture of the conglomerate's matrix, the Japanese Miocene tsunamiite and the Piedra Negra bed are quite similar.

Correlative with the Piedra Negra bed along Playa Sombrero is a dolomitized horizon with numerous disarticulated skeletons of small odontocetes. If the Piedra Negra bed does record a catastrophic tsunami event, the correlative skull bed might represent mass mortalities involving pods of odontocetes that were trapped close to shore, killed and dismembered in the turbulence of the tsunami, pulled offshore in the tsunami backwash, and deposited just beyond wavebase. Although no submarine-backwash carcass accumulations have been reported in the modern literature, accounts of modern cetaceans carried inland do exist, as well as a description of pre-historic cetacean skeletons that may have been carried onshore by a tsunami affecting the Wellington area of New Zealand (Goff and Chagué-Goff, 2009).

5.3. Mid-Chilcatay shoaling event

In the middle of the Chilcatay depositional sequence, stacked allosequences of fining-up bioclastic sandstone overlying and underlying silty sandstone with fish scales and planktonic diatoms, point to a succession of short-lived shoaling events during mid-Chilcatay time. Bioclastic and crossbedded sandstone and coquina with fragments of oysters, barnacles, echinoderms, and mollusks predominate along Playa Sombrero, while boulders are

also an important clastic constituent in the Gran Tablazo Archipelago and Bahía de Ica Baja.

The lithostratigraphic evidence for mid-Chilcatay shoaling event in the East Pisco Basin spans areas with different tectonic styles and histories and 150 kilometers of shoreline, which argues against local uplift as a cause for the shoaling, but instead an extra-basinal mechanism, namely, fluctuating eustatic sea level. Diatom data from the type section of the Chilcatay Formation indicate the shoaling occurred around 19 Ma or 20 Ma, coinciding with an inferred rapid drop in sea level in the sea level curves of Haq et al. (1987), Hardenbol et al. (1998), Miller et al. (2005), and Kominz et al. (2008). That mid-early Miocene fall in global sea level is preceded and followed by two to five million years of rising or high-standing sea level in the sea level curves of Haq et al. (1987) and Hardenbol et al. (1998) and to a lesser extent, Miller et al. (2005), consistent with the thick interval of uninterrupted deeper water silty sandstone that underlies and overlies mid-Chilcatay bioclastic and boulder-bearing coarse-grained deposits.

5.4. Chilcatay clinoform allosequences

Clinoform allosequences in the upper Chilcatay depositional sequence in Bahía de Ica Baja derived their sediments from metamorphic rocks of the Precambrian "Basal Complex" (Montoya et al., 1994) and an unnamed pre-Miocene conglomerate with well rounded cobbles of metamorphic and igneous rocks (quartzite, greenstone, pumice) exposed today on the valley floor of the Río Ica at Ullujaya. These basement rocks formed northeastern paleo-highlands that stretched from the *Sula* Site to Ullujaya, flanked seaward at the latitudes of the *Sula* Site and Laberinto by a narrow coastal plain and at the latitudes of Ullujaya by a weakly inclined peneplain.

The geometry of the clinoform's top-, fore-, and bottomset beds and basinal setting (proximity of shoreline, inner shelf water depth, absence of point sources for sediment, longshore elongation of the clinoform body) are consistent with the sand-prone subaqueous delta model of Patruno et al. (2015). The thickness of the sets, sedimentary structures (relict laminae and ripples, pervasive diffused bioturbation), individual trace fossils (*Thalassinoides*, *Gyrolithes*), and the invertebrate fauna, diatom flora, and clupeoid fish fauna found within or between individual clinoform sets indicate that the deltas formed at inner shelf depths. Adopting the model of Patruno et al. (2015), it is proposed that southwestern swells from the Pacific Ocean set up northwest directed-longshore currents that transported sediment into the Bahía de Ica Baja, with an offshore component of the transport providing sediment for southwest-dipping clinoform beds forming below wavebase.

The presence in Bahía de Ica Baja of successive prograding clinoform allosequences of bioclastic sandstone separated by transgressive inner shelf bioturbated sandstone and even silty sandstone with outer shelf fish scales and diatoms indicates successive episodes of fluctuating relative sea level by tens of meters during the late early Miocene. The absence of clinoform allosequences in correlative strata elsewhere in the East Pisco Basin (Playa Sombrero, Gran Tablazo Archipelago) might result from more pronounced tectonism being localized along the course of the modern Río Ica, parallel to the Monte Grande Fault.

5.5. Pisco P0 parasequence

The Pisco P0 parasequence in Bahía de Ica Baja extends from Yesera de Amara to Quebrada Gramonal. A transgressive lag composed of boulders, lithoclasts, bioclasts, and/or iron-rich authigenic nodules is overlain by massive bioturbated inner shelf sandstone with articulated *in situ* venerid bivalves and cetacean bones; the sandstone is not overlain by deeper water silty sandstone. The lower boundary of the P0 parasequence is younger than the ~17.5 Ma ash from the top of the Chilcatay sequence and older than the ~14-12 Ma deeper-water diatomaceous silty sandstone (DV 549-P106) in the lower portion of the overlying P1 parasequence. The age of the lower boundary of the P1 parasequence is therefore also between 17.5 Ma and 14-12 Ma. The P0 and P1 lower parasequence boundaries coincide well with two closely timed major drops in global sea level between 17 and 14 Ma (Haq et al., 1987; Abreu and Anderson, 1998; Hardenbol et al., 1998; Miller et al., 2005).

5.6. Structural observations

The intent of this paper is not to describe the structural history of the East Pisco Basin. Nonetheless, the juxtaposition of outcrops of CBR and Cenozoic marine strata across fault contacts does provide independent evidence of tectonism that differs from evidence presented by Azalgara (1994) and Leon et al. (2008).

As is shown by Leon et al. (2008) and evident from this author's fieldwork and Google Earth imagery, the prevalent structural grain of the East Pisco Basin north of Laguna Grande is produced by parallel high-angle normal faults oriented in a NNE-SSW direction. These faults were active as early as the late Eocene, since uplifted blocks of CBR affected lithofacies of the lowermost Otuma depositional sequence differently than lithofacies of the older Paracas depositional sequence (DeVries et al., 2017). Blocks of *Turritella woodsi*-bearing basal Otuma sandstone in fault contact with blocks of CBR at Playa Talpo (DV 502), as well as a fault-ridden terrain southeast of the neck of the Paracas Peninsula (DV 560) and southeast of Playa Yumaque (DV 2043), where blocks of Otuma and Paracas strata are juxtaposed, (DeVries, 1998; DeVries et al., 2017) show that the NNE-SSW normal faults remained active or were reactivated after the earliest Oligocene. Late Miocene motion along the high-angle, east-dipping, NNE-SSW striking normal Santa Cruz Fault, east of Salinas de Otuma (Figure 1D), resulted in lower Miocene Chilcatay beds lying alongside broad expanses of CBR overlain by basal sandstone of the upper Eocene Otuma depositional sequence (DeVries, 1998; DeVries et al., 2017).

South of Laguna Grande, the prevalent structural grain across the remainder of the East Pisco Basin is produced by NW-SE high-angle normal faults. The Gran Tablazo Archipelago is characterized by NW-SE-fault-bounded blocks of CBR that became emergent after the early Oligocene deposition in the former Bahía Concha Roja and

before the latest Oligocene Chilcatay transgression, i.e., between 32 and 25 Ma. Otuma beds are also cut by complex sets of minor faults, not only in the area of the Gran Tablazo Archipelago, but also throughout the Bahía de Ica Baja and beneath Cerro Terrestral; very few of the faults penetrate the overlying Chilcatay and Pisco sequences.

5.7. A paleogeographic/paleoecological narrative

The East Pisco Basin hosted a diverse invertebrate and vertebrate fauna during the Miocene, with most species yet to be named and described. While the geographic and temporal distributions of these taxa were undoubtedly affected by regional and global evolutionary and paleoceanographic processes, the distributions might also reflect local differences in paleogeography and paleoecology that are recorded in the lithostratigraphy of the basin (Figures 20, 21A - 21E).

Field evidence indicates that early Chilcatay seas rose across a coastal plain of varied geography: a straight shoreline north of the modern Bahía de la Independencia (Playa Sombrero), a series of small islands of CBR near the modern Cerros Colorados (Gran Tablazo Archipelago), and a fault-controlled reentrant following the course of the modern Río Ica (Bahía de Ica Baja). The proximity and relief of the coastal plain determined the transgressive (intertidal?) substrate – boulders and cobbles of CBR, oyster banks, lithoclasts of dolomitized sandstone, or simply a thin layer of coarse-grained sand or authigenic iron-rich pebbles and nodules with reworked or *in situ* invertebrates. A greater uniformity of depositional environment prevailed as the Chilcatay transgression progressed and as depositional water depths along Playa Sombrero and the Bahía de Ica Baja moved below wave base, which resulted in the accumulation of massive bioturbated sand with an infauna of crustaceans and venerid bivalves, the likely prey of the predatory/scavenging buccinid, *Misifulgur*. At comparable depths around the islands of the Gran Tablazo Archipelago, oyster and barnacle banks throughout much of the lower Chilcatay sequence point to high energy environments or a ready source of shallow-water bioclastic debris. Farther from the shores of paleo-islands, a diverse molluscan epibenthic fauna inhabited coarse-grained sandy substrates.

The relative tranquility of the inner shelf appears to have been violently interrupted around 22 Ma by a tsunami powerful enough to have flushed from the narrowed confines of Bahía de Ica Baja three-meter boulders of CBR that then traveled several kilometers seaward (Figure 21A) and, more speculatively, to have smashed and washed seaward from the shores of Playa Sombrero the carcasses of hundreds or thousands of small odontocetes (Figure 21E). Only in the area of the Gran Tablazo Archipelago does the tsunami signal fail to stand out.

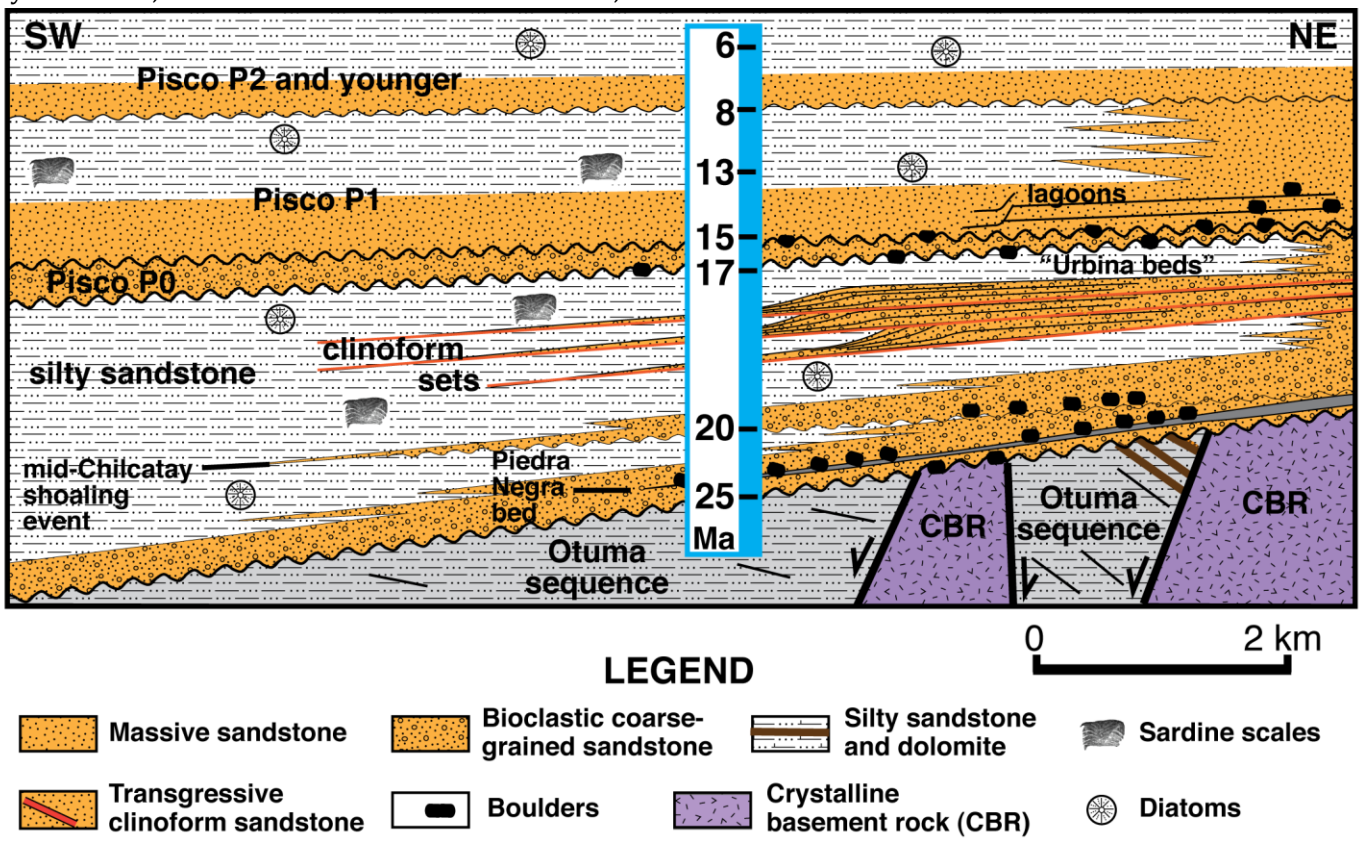

Figure 20. *Composite schematic NE-SW cross-section of the Chilcatay and lower Pisco depositional sequences as they appear in the Río Ica valley. The clinoform sets, Pisco P0 parasequence, and lagoons do not appear outside Bahía de Ica Baja. The Piedra Negra boulder bed is replaced along Playa Sombrero with an odontocete-bearing dolomitized siltstone bed. Pisco allosequences/parasequences younger than P1 have been described by Di Celma et al., (2017). Approximate ages are given for major lithostratigraphic boundaries. CBR = crystallline basement rock. The youngest age (6 Ma) approximates ages obtained with ^{40}Ar-^{39}Ar throughout the Río Ica valley (Dunbar et al., 1990; Brand et al., 2011, with analyses of samples DV 494-5Snee (Cerro Blanco, 82m in measured section) and DV 505 3Snee (Hueco La Zorra, 114m in measured section) by L. Snee; ^{40}Ar-^{39}Ar ages communicated to Esperante et al. (2015) by K. Nick; and one unpublished ^{40}Ar-^{39}Ar date from the Río Ica valley analyzed by L. Snee (DV 456-1Snee, east of Ocucaje, 6.16 Ma).*

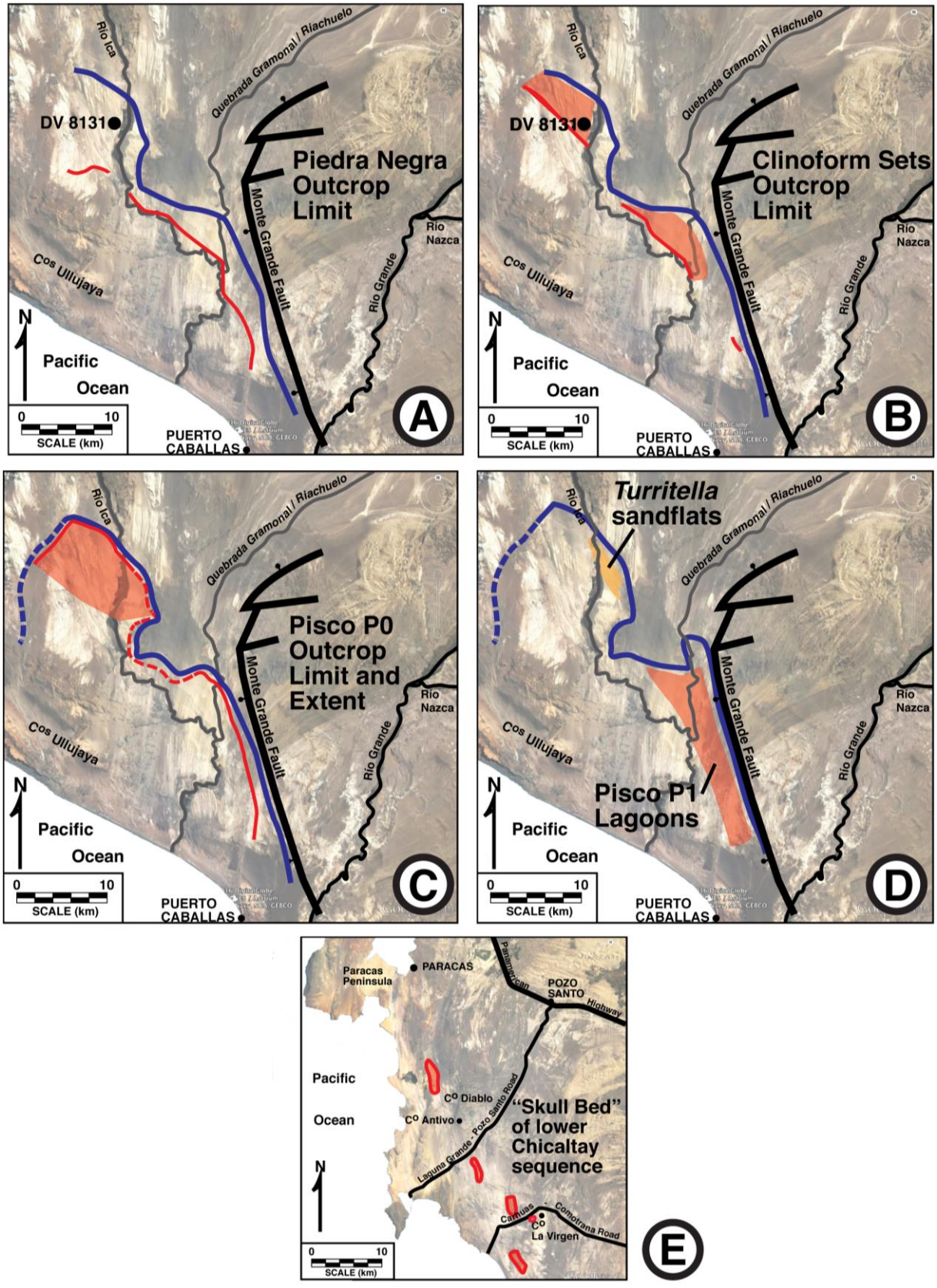

Figure 21. *Paleogeographic maps. Blue lines denote estimated position of paleo-shoreline contemporaneous with Miocene deposit being shown. A. Western extent of lower Chilcatay Piedra Negra bed, Bahía de Ica Baja. Red line marks limit of outcrop, which is probably close to true limit of deposit only on western side of Río Ica. B. Outcrops of upper Chilcatay clinoform sets, Bahía de Ica Baja (shaded pale red). Western limit of outcrop (red line) approximately coincides with true limit of the clinoforms. . C. Pisco P0 parasequence in Bahía de Ica Baja. Extent (pale red) and shoreline limit (red line) is supportd by exposures in Río Ica valley. The shoreline limit only is supported by outcrop along Quebrada Gramonal and is inferred for Laberinto and the Sula Site. D. Pisco P1 lagoons extending from Quebrada Gramonal to the Sula Site, indicated by red shading. Channel-form scours filled with bioclastic deposits containing the same diverse fauna found above Quebrada Gramonal and the Sula Site occur near the western edge of the mouth of Quebrada Gramonal. Correlative beds with vast numbers of Turritella infracarinata are indicated with orange shading. Purple line is estimated paleo-shoreline. E. Outcrops of the lower Chilcatay "skull bed," marked in red, between Salinas de Otuma and the Lomas Chilcatay.*

At about 20 Ma, the East Pisco Basin experienced a shoaling event (maybe as many as five successive lesser events comprising one long interval of relative sea level instability) that is defined today by a forced regression surface and an influx of boulders along those stretches of the paleo-shoreline in Bahía de Ica Baja that were close to subaerial outcrops of CBR. All other parts of the East Pisco Basin were also affected. The composition and diversity of the molluscan fauna, however, was unchanged by the shoaling event.

While most of the East Pisco Basin was buried during late Chilcatay time by a hundred meters of fine-grained sedimentary sediment with a complement of foraminifera, diatoms, and fish scales indicative of outer shelf environments, the eastern margin of Bahía de Ica Baja repeatedly experienced the spilling over of coarse-grained bioclastic sands into deeper water, with an inner shelf gradient thereby steepened by foreset beds dipping steeply seaward (Figure 21B). If the Patruno et al. (2015) sub-aqueous delta model is applicable to the Chilcatay clinoform allosequences, it may be postulated that longshore currents directed by the increased vertical offset of the Monte Grande Fault in interaction with an ocean swell from the southwest created the conditions for these deltas. The clinoform substrates were atypically coarse-grained for such shelf depths, which might have created peculiar conditions for the invertebrates and vertebrates dwelling on or above the clinoform sands.

The oldest Pisco sediments in the East Pisco Basin, now designated the Pisco P0 allosequence (herein, parasequence) by Di Celma et al. (2017), blanketed fine-grained Chilcatay sediments and ridges of dolomitized sandstone in the fault-ridden Bahía de Ica Baja (Figure 21C) but do not seem to have crossed the folded paleo-hills of Chilcatay sedimentary rocks around Zancones nor passed across exposures of tilted Chilcatay sediments of the Gran Tablazo Archipelago. The innermost floor of Bahía de Ica Baja was covered with boulders, cobbles, bioclastic debris, and a diverse infaunal bivalve fauna of *Tilicrassatella*, venerids, and large mactrids and an epibenthic invertebrate fauna dominated by echinoids, barnacles, oysters, pectinids (*Chlamys*), crepidulids, and brachiopods (*Discinisca*), which were preyed upon by the gastropods *Acanthina* and *Olivancellaria*.

A forced regression surface that separates the Pisco P0 from Pisco P1 surface may have overlapped in time with another tsunami event, judging from the large boulders of diverse igneous and metamorphic lithology scattered and stacked along the P0/P1 contact and an accumulation of balanopterid skeletons below the eastern cliffs of Cerros Mama y Hija. Increasing water depths associated with the Pisco P1 transgression led to the deposition and preservation of massive bioturbated sand, a reprise of the same early Chilcatay lithofacies, but with a more diverse bivalve infauna, represented in outcrop by *in situ* paired valves of *Miltha*, *Chione*, *Chionopsis*, and *Dosinia*, as well as the semi-infaunal *Anadara sechurana*. *Misifulgur cruziana* was still the principal epibenthic predator/scavenger.

On the eastern side of Bahía de Ica Baja, a succession of lagoons evolved in the lee of the Monte Grande Fault and an inferred uplifted highland (Figure 21D). The lagoons, which emptied into the broader Bahía de Ica Baja embayment, supported an diverse invertebrate fauna, both infaunal and epifaunal, on soft sandy substrates – as diverse as the older Chilcatay invertebrate fauna that lived on coarser-grained substrates in the waters surrounding the Gran Tablazo Archipelago. The shallow lagoonal waters were occupied by sharks (*Isurus hastalis*, among others), rays, and cetaceans, and visited by seabirds (*Sula*). Both within the eastern lagoons and on protected sand flats farther inside Bahía de Ica Baja, vast numbers of *Turritella infracarinata* often dominated the epibenthic invertebrate fauna. Similarly protected sand flats in the Filudo Depression, in the lee of Cerros Antivo and Diablo, inboard of Playa Sombrero, were also inhabited by large numbers of *T*. *infracarinata*. The Filudo infauna was dominated by a small species of the mactrid bivalve, *Mulinia*; other bivalve taxa included *Anadara sechurana* and *Panopea*.

5.8. Evidence for an Oligocene-Miocene Golfo de Pisco

Brand et al. (2004) proposed the concept of a Miocene bay that encompassed part of the East Pisco Basin, an embayment herein termed the "Golfo de Pisco." Their arguments for a late Miocene embayment were sedimentological and taphonomic, stemming from a consideration of the excellent preservation of hundreds of balanopterid whale skeletons throughout the upper Pisco sequence. Key evidence included (1) a prevalence of winnowing, scouring, and rippling in beds of tuffaceous and diatomaceous silty sandstone, indicating deposition at depths shallower than storm wave base and (2) a high degree of articulation for the pristine cetacean skeletons, despite a lack of evidence for anoxia, hypoxia, or algal mats, which would have protected the bones from scavenging. This led Brand et al. (2004) to infer high rates of sedimentation and rapid burial of the skeletons, presumably at shallow depths not subject to the effects of open ocean swell or strong longshore currents.

That this evidence supports the existence of a protected embayment, i.e., a late Miocene Golfo de Pisco, can be disputed. Anoxia, hypoxia, and blue-green bacterial mats occur on the modern continental margin of Peru (McCaffrey et al., 1989) together with evidence of winnowing and erosion (DeVries, 1980; Levin et al., 2002). Diatomaceous sediments, which during the Quaternary achieved their greatest thicknesses offshore of the East Pisco Basin at outer shelf and upper slope water depths of 200 to 600 meters (DeVries, 1980; DeVries and Schrader, 1981; DeVries and Pearcy, 1982), can also accumulate in shallow water, well above wave base and very close to shore, whether an embayment is involved (the late Miocene Bahía de Nazca, where diatomaceous silty sand accumulated within a few hundred meters of the mountainous slopes of the Miocene manifestation of Cerro Huaricangana (DV 531; DeVries, 1988a) or not (the coast of Namibia, where a modern diatomaceous mud belt, 740 kilometers long, has an average water depth at its shoreward margin of 31 meters; Bremner, 1980).

Should a late Miocene Golfo de Pisco be inferred from the criteria of Brand et al. (2004), the gulf would have extended from Corre Viento, where at least one horizon exists with numerous balanopterid skeletons (DV 1318, 3044, 3045), to Yesera de Amara, inland to Cerro Ballena, and across the

modern Río Ica to similar deposits north and south of Ullujaya (DV 572). Beyond those confines, i.e., northward to Cerro Lechuza and south to Cerro Huaricangana, sedimentological and textural characteristics of the upper Miocene silty sandstone are similar, but well preserved balanopterid skeletons are much less common.

Skeletal remains of balanopterids are concentrated on or near the P0/P1 parasequence contact in the lowermost Pisco depositional sequence at Yesera de Amara (DV 1180) and remains of other cetaceans occur throughout the older Chilcatay depositional sequence, but less commonly than is the case for upper Pisco strata and more often in coarse-grained deposits. Thus, criteria for an late Miocene embayment set forth by Brand et al. (2004) are not met in the East Pisco Basin for the early Miocene. Although the preservation of clinoform allosequences in the upper Chilcatay sequence might be considered evidence for a protected Golfo de Pisco, the sub-aqueous deltaic model of Patruno (2015), in which the clinoform sets form at and below wave base, would not require a protected shallow environment to form.

Whereas sedimentological and paleontological evidence for a Golfo de Pisco may be equivocal, offshore subsurface data indicates that the early to late Miocene continental shelf may have been configured differently than it is today. Seismic profiles of the West Pisco Basin (Azalgara, 1994) indicate substantial erosion, probably subaerial, during the middle to late Miocene. If so, a land mass of unknown size and continuity might have existed tens of kilometers seaward of the present coastline, affecting marine depositional environments across the East Pisco Basin. One compelling piece of evidence exists for an offshore landmass, albeit for the middle Eocene: a clinoform set of coarse-grained sandstone beds (DV 8116), configured much like those of Quebrada Gramonal and Tinajones, with a down-dip azimuth of 080 degrees, i.e., towards the South American landmass. The clinoform set, embedded within the Los Choros Member of the Paracas Formation, overlies sandstones with spatangoid (heart sea urchin) carapaces (DV 8114) and clusters of *Turritella lagunillasensis* (DV 8115) and underlies archeocete-bearing fine-grained sandstones of the Yumaque Member of the Paracas Formation. The sediment source for the Los Choros clinoform beds was likely the extensive outcrop of CBR that forms the modern Cerros Ullujaya (Figure 1F).

6. Conclusions

6.1. Comparative Cenozoic lithofacies development in the East Pisco Basin

The distribution of sediments throughout the East Pisco Basin during the early and middle Miocene can be viewed in the context of depositional patterns in the same basin throughout the Cenozoic (Dunbar et al., 1990; DeVries, 1998, 2017; Leon et al., 2008; DeVries et al., 2017). In one sense, sediment sources and processes have not changed since the middle Eocene, either close to shore or at outer shelf depths. Sandstone (coarse-grained sand, conglomerate) and silty sandstone or siltstone predominate in the Paracas, Otuma, Chilcatay, and Pisco depositional sequences. The two lithologies each vary mostly by the degree of bioclastic content (in the former case) or tuffaceous and diatomaceous content (in the latter case). Boulders of CBR appear in coarse-grained strata of all four marine sequences, while dolomitized horizons appear in deeper water deposits of the same four sequences.

The Chilcatay sequence resembles the Paracas sequence in that the respective transgressive seas crossed a topographically complex coastal plain that had long been emergent and subject to protracted periods of tectonism and subaerial erosion. The Paracas sequence, however, is unique, at least in parts of the basin (the Paracas Peninsula, Fundo Santa Rosa) for its thick basal sandstone, which can attain thicknesses of 50 to 100 meters.

The Chilcatay shoreline was divided into segments in a fashion similar to the Otuma shoreline (DeVries et al., 2017). Both shorelines had an archipelago and embayment, although the two features were situated at different places along the coast. The Otuma-age Paracas Archipelago was on the north side of the Quemado Peninsula, while the Chilcatay-age Gran Tablazo Archipelago was on the south side of that peninsula. The Otuma-age Bahía Concha Roja was much farther north than the Chilcatay-age Bahía de Ica Baja, and only in the Otuma embayment was the depositional environment substantially different than the depositional environments seen along the rest of the contemporaneous shoreline.

Relatively little time passed, i.e., between one million years (Bahía de Ica Baja) and five million years (Zancones for example) between late Chilcatay deposition and the onset of a transgression that intiated the development of the Pisco depositional sequence. Sedimentary strata of the two sequences are quite similar, reflecting the continuity of sedimentary sources and depositional processes since the middle Eocene as well as a more closely shared post-Oligocene diagenetic history. The distribution of lithofacies was more uniform during Pisco time, however, since much of the post-Oligocene coastal plain topography had already been covered and smoothed by Chilcatay sediments.

6.2. Directions for further research

In the East Pisco Basin, much more is unknown than known regarding the depositional and structural history and distribution of Cenozoic fauna and flora. The following two research topics are of both specific and general interest and thus are recommended for further study.

1. Biostratigraphy. Biostratigraphic data from the East Pisco Basin have always been collected piecemeal and thus have had limited utility. A comprehensive microfossil biostratigraphic data set with sampling of the full thickness of entire depostional sequences would greatly improve our understanding of lithostratigraphic and paleobiological events. Such a data set would also provide insights regarding the prevailing paleoeanographic regimes and might provide evidence for the large-scale configuration of the East and West Pisco basins, inasmuch as the outer basin's submergent or emergent status might have affected the distribution and taxonomic composition of pelagic and neritic components of plankton preserved in East Pisco Basin sediments.

2. Faunal diversity. The East Pisco Basin has a remarkable complement of invertebrate and vertebrate fossils. Working within an improved biostratigraphic and lithostratigraphic framework, questions of biodiversity, evolution, extinction, and biogeography could be addressed with greater sophistication. Local distribution patterns of fauna, particularly vertebrates, which might only reflect outcrop availability, collecting effort, or small-scale paleogeographic features, could be distinguished from patterns induced by regional or global processes, whether tectonic, thermal or circulational.

Acknowledgements

I was introduced to the the Pisco and Sacaco basins by Christian de Muizon (then with the Institut Français des Études Andines, Lima, Peru) in 1983 and to remote parts of the Pisco Basin, e.g., the newly upgraded Carhuas-Comotrana Road and roads to Quebrada Gramonal and Puerto Caballas, by Rob Dunbar (then with Rice University, Houston, Texas USA) and Paul Baker (Duke University, Chapel Hill, North Carolina, USA) in 1986. Hans Schrader and his student, Peter Rønning (both then with Oppgave Geologisk Institutt Avdeling B, Universitetet I, in Bergen, Norway) provided field assistance in 1987, as did Todd Thornburg and Larry Snee (both then with Oregon State University, Corvallis, Oregon, USA, in the School of Oceanography and Department of Geology, respectively). José Macharé (then with the Instituto Geofísico del Perú, Lima, Peru) provided advice during the 1980s regarding his former dissertation field area and was instrumental in a meeting at the Hotel El Carmelo, in Ica, where in 1989 a decison was reached to apply the 'Chilcatay' name to the Oligocene-Miocene depositional sequence of sediments that José had first identified. Vera Alleman (Universidad Ricardo Palma, Lima, Peru) provided logistical help in the 1990s. Dr. Macharé also provided helpful advice in the preparation of this manuscript. Marcelo Stucchi, then recently graduated from the Universidad Ricardo Palma, provided valuable field assistance in Caravelí in 1999. From 2013 to the present, Raul Esperante (Loma Linda University, Loma Linda, California, USA) and Claudio Di Celma (Università degli Studi di Camerino, Camerino, Itlay) have offered valuable sedimentological insights. Echinoderms were identified by Roger Portell (Museum of Natural History, University of Florida, Gainesville, Florida, USA). Aldo Marcelo Benites Palomino (currently with the Smithsonian Tropical Research Institute, Balboa, Ancón, Panama) kindly provided the Spanish translation of the abstract.

Of special significance has been the incomparable collaboration in the field since 2001 with Mario Urbina-Schmitt (Departamento de Paleontología de Vertebrados, Museo de Historia Natural Javier Prado, Universidad Nacional Mayor de San Marcos, Lima, Peru), a collaboration precipitated by a fraught midnight encounter in August, 1999, on the stoop of Josefina and Carlos Martin, Sr.'s house in Sacaco.

References

Abreu, V.S., Anderson, J.B. 1998. Glacial eustacy during the Cenozoic: Sequence stratigraphic implications. American Association of Petroleum Geologists (AAPG) Bulletin, v. 82, p. 1385-1400.

Adams, G.I. 1906. Caudal, procedencia y distribucíon de aguas de los Departamentos de Lima y Ica. Boletín del Cuerpo de Ingenieros de Minas del Perú, v. 37, p. 1-94.

Adams, G.I. 1909. An outline review of the geology of Peru. Reports of the Smithsonian Institution for 1908, p. 385-430.

Akiba, F. 1986. Middle Miocene to Quaternary diatom biostratigraphy in the Nankai Trough and Japan Trench, and modified lower Miocene through Quaternary diatom zones for middle-to-high latitudes of the North Pacific. In: Initial Reports of the Deep Sea Drilling Project, Kagami, H., Karig, D.E., Coulbourn, W.T., et al. (editors), Deep Sea Drilling Project, Washington, DC, v. 87, p. 393-481.

Andrews, G.W. 1988. A revised marine diatom zonation for Miocene strata of the southeastern United States. United States Geological Survey Professional Paper, number 1481, 29 p.

Anthonissen, D.E., Ogg, J.G. 2012. Cenozoic and Cretaceous biochronology of planktonic foraminifera and calcareous nannofossils. In: The Geologic Time Scale 2012, Gradstein, F.M., Ogg, J.G., Schmitz, M.D., Ogg, G.M. (editors), Elsevier Publishing, Amsterdam, The Netherlands, p. 1083-1128.

Archibald, S.B., Morse, G.E., Greenwood, D.R., Mathewes, R.W. 2014. Fossil palm beetles refine upland winter temperatures in the early Eocene climatic optimum. Proceedings of the National Academy of Sciences of the United States of America, v. 111(22), p. 8095-8100.

Azalgara, C. 1994. Structural evolution of the offshore forearc basins of Peru, including the Salaverry, Trujillo, Lima, West Pisco and East Pisco Basins. Masters thesis, Rice University, Houston, Texas, USA, 178 p.

Baldauf, J.G, Barron, J.A. 1991. Diatom biostratigraphy: Kerguelen Plateau and Prydz Bay regions of the Southern Ocean. In: Proceedings of the Ocean Drilling Program, Scientific Results, Barron, J. A., Larsen, B., et al. (editors), Ocean Drilling Program, College Station, Texas, USA, v. 119, p. 547-598.

Banerjee, I., Kidwell, S.M. 1991. Significance of molluscan shell beds in sequence stratigraphy: an example from the Lower Cretaceous Mannville Group of Canada. Sedimentology, v. 38, p. 913-934.

Baqueiro C., E., Aldana A., D. 2000. A review of reproductive patterns of bivalve mollusks from Mexico. Bulletin of Marine Science, v. 66, p. 13-27.

Barron, J.A. 1983. Latest Oligocene through early middle Miocene diatom biostratigraphy of the eastern tropical Pacific. Marine Micropaleontology, v. 7, p. 487-515.

Barron, J.A. 1985. Late Eocene to Holocene diatom biostratigraphy of the equatorial Pacific Ocean, Deep Sea Drilling Project Leg 85. In: Initial Reports of the Deep-sea Drilling Project, Mayer, L., Theyer, F., Thomas, E., et. al. (editors), Deep Sea Drilling Project, Washington, DC, USA, v. 85, p. 413-456.

Barron, J.A. 1992. Neogene diatom datum levels in the equatorial and North Pacific. In: The Centenary of

Japanese Micropaleontology, Ishizaki, K., Saito, T. (editors), Terra Scientific Publishing Company, Tokyo, p. 413-425.

Barron, J.A. 2006. Diatom biochronology of the early Miocene of the equatorial Pacific. Stratigraphy, v. 2, p. 281-309.

Barron, J.A., Browning, J., Sugarman, P., Miller, K.G. 2013. Refinement of late-early and middle Miocene stratigraphy for the East Coast of the United States. Geosphere, v. 9(5), p. 1286-1302.

Barron, J.A., Fourtanier, E., Bohaty, S. 2004. Oligocene and earliest Miocene diatom stratigraphy of ODP Leg 199 Site 1220, equatorial Pacific. In: Proceedings of the Ocean Drilling Program, Scientific Results, Wilson, P.A., Lyle, M., Janecek, T.R., Firth, J.V. (editors), Ocean Drilling Program, College Station, Texas, USA, v. 199, p. 1-25.

Barron, J.A., Keller, G., Dunn, D.A. 1985. A multiple microfossil biochronology for the Miocene. In: The Miocene Ocean: Paleoceanography and Biogeography, Kennett, J.P. (editor), Memoir of the Geological Society of America, v. 163, p. 21-36.

Belia, E., Nick, K. 2016. Miocene calcareous nannofossil biostratigraphy from low latitudes, Pisco Basin, Peru. Geological Society of America Abstracts with Program, v. 48(4), doi: 10.1130/abs/2016CD-274218.

Belia, E.R., Nick, K., Bedoya Agudelo, E., Concheyro, A. 2015. Late Oligocene-early Miocene calcareous nannofossils from basal Pisco Formation, Pisco Basin, Peru. Journal of Nannofossil Research, v. 35, p. 22.

Benton, M.J., Harper, D.A.T. 1997. Basic Palaeontology. Addison Wesley Longman, Harlow, Great Britian, 342 p.

Berggren, W.A., Kent, D.V., Swisher, C.C., III, Aubry, M.-P. 1995. A revised Cenozoic geochronology and chronostratigraphy. In: Geochronology, Time Scales and Global Stratigraphic Correlation, Berggren, W.A., Kent, D.V., Aubry, M.-P., Hardenbol, J. (editors), Society of Economic Paleontologists and Mineralogists (SEPM), Special Publication, v. 54, p. 129-212.

Berti, M., Genevois, R., Simoni, A., Tecca, P.R. 1999. Field observations of a debris flow event in the Dolomites. Geomorphology, v. 29, p. 265-274.

Bhattacharya, J.P. 2005. Allostratigraphy vs. sequence stratigraphy. AAPG Hedberg Research Conference (Aug. 26-29, 2005), Dallas, Texas, USA, p. 18.

Bianucci, G., Urbina, M., Lambert, O. 2015. A new record of *Notocetus vanbenedeni* (Squalodelphinidae, Odontoceti, Cetacea) from the early Miocene of Peru. Comptes Rendus Palevol, v. 14, p. 5-13.

Brand, L.R., Esperante, R., Chadwick, A.V., Poma P., O., Alomía, M. 2004. Fossil whale preservation implies high diatom accumulation rate in the Miocene–Pliocene Pisco Formation of Peru. Geology, v. 32, p. 165-168.

Brand, L., Urbina, M., Chadwick, A.V., DeVries, T.J., Esperante, R. 2011. A high-resolution framework for the remarkable fossil cetacean assemblage of the Miocene/Pliocene Pisco Formation, Peru. Journal of South American Earth Sciences, v. 31, p. 414-425.

Bremner, J.M. 1980. Physical parameters of the diatomaceous mud belt off South West Africa. Marine Geology, v. 34, p. M67–M76.

Cantalamessa, G., Di Celma, C. 2005. Sedimentary features of tsunami backwash deposits in a shallow marine Miocene setting, Mejillones Peninsula, northern Chile. Sedimentary Geology, v. 178, p. 259–273.

Catuneanu, O., Abreu, V., Bhattacharya, J.P., et al. 2009. Towards the standardization of sequence stratigraphy. Earth-Science Reviews, v. 92, p. 1-33.

Clarke, J.A., Sepka, D.T., Salas-Gismondi, R., Altamirano, A.J., Shawkey, M.D., D'Alba, L., Vinter, J., DeVries, T.J., Baby, P. 2010. Fossil evidence for evolution of the shape and color of penguin feathers. Science, v. 330, p. 954-957.

Clarke, J.A., Sepka, D.T., Stucchi, M., Urbina, M., Giannini, N., Bertelli, S., Narvaez, Y., Boyd, C.A. 2007. Paleogene equatorial penguins challenge the proposed relationship between biogeography, diversity, and Cenozoic climate change. Proceedings of the National Academy of Sciences of the United States of America, v. 104, p. 11545-11550.

Clemens, S.C., Kuhnt, W., LeVay, L.J., Anand, P., Ando, T., et al. 2016. Expedition 353 methods. In: Proceedings of the International Ocean Discovery Program, Clemens, S.C., Kuhnt, W., LeVay, L.J., and the Expedition 353 Scientists (editors), International Ocean Discovery Program, College Station, Texas, USA, v. 353, http://dx.doi.org/10.14379/iodp.proc.353.102.2016.

Dávila M., D. 1989. Estratigrafía Cenozoica del valle del Río Grande, Cuenca de Pisco, Perú. Boletín de la Sociedad Geológica del Perú, v. 80, p. 65-75.

Dávila M., D., Torres, A., Sanchez, W., Rodriguez, W., Escalante, A. Bustamante, D. 1987. Litoestratigrafía y sedimentología del Terciario del Río Grande-Palpa. Resúmenes del VI Congreso Peruano de Geología, v. S-2, p. 88.

DeVries, T.J. 1980. Nekton remains, diatoms, and Holocene upwelling off Peru. Masters thesis, Oregon State University, Corvallis, Oregon, USA, 85 p.

DeVries, T.J. 1986. Geology and paleontology of tablazos of northern Peru. Ph.D. dissertation, Ohio State University, Columbus, Ohio, USA, 964 p.

DeVries, T.J. 1988a. Paleoenvironments of the Pisco Basin. In: Cenozoic geology of the Pisco Basin; a guidebook to accompany a regional IGCP 156 field workshop; "Genesis of Cenozoic phosphorites and associated organic-rich sediments; Peruvian continental margin" (May 16-25, 1988), Dunbar, R.B., Baker, P.A. (editors), Rice University, Houston, Texas, USA, p. 41-50.

DeVries, T.J. 1988b. Chilcatay sections of the Caballas formation. In: Cenozoic geology of the Pisco Basin; a guidebook to accompany a regional IGCP 156 field workshop; "Genesis of Cenozoic phosphorites and associated organic-rich sediments; Peruvian continental margin" (May 16-25, 1988). Dunbar, R.B., Baker, P.A. (editors), Rice University, Houston, Texas, USA, p. 185-195.

DeVries, T.J. 1995. *Concholepas* Lamarck, 1801 (Neogastropoda:Muricoidea): A Neogene genus native to South America. Veliger, v. 38, p. 284-297.

DeVries, T.J. 1997. Neogene *Ficus* (Mesogastropoda: Ficidae) from the Pisco basin (Peru). Boletín de la Sociedad Geológica del Perú, v. 86, p. 11-18.

DeVries, T.J. 1998. Oligocene deposition and Cenozoic sequence boundaries in the Pisco Basin. Journal of South American Earth Sciences, v. 3, p. 217-231.

DeVries, T.J. 2003. *Acanthina* Fischer von Waldheim, 1807 (Gastropoda: Muricidae), an ocenebrine genus endemic to South America. Veliger, v. 46, p. 332-350.

DeVries, T.J. 2004. Eocene mollusks from the Pisco Basin (southern Peru): Evidence for re-evaluating the age of the Otuma Formation. XII Congreso Peruano de Geología, Lima, Peru, October, 2004. Sociedad Geológica del Perú, Resúmenes Extendidos, Publicación Especial, v. 6, p. 436-439.

DeVries, T.J. 2007. Cenozoic Turritellidae (Gastropoda) from southern Peru. Journal of Paleontology, v. 81, p. 331-351.

DeVries, T.J. 2008. Pliocene and Pleistocene *Fissurella* Bruguiere, 1789 (Gastropoda: Fissurellidae) from southern Peru. Veliger, v. 50, p. 129-148.

DeVries, T.J. 2016a. Fossil Cenozoic crassatelline bivalves from Peru: New species and generic insights. Acta Palaeontologica Polonica, v. 61, p. 661-688.

DeVries, T.J. 2016b. Latest Oligocene and Miocene whelks (Gastropoda: Neogastropoda: Buccinidae) from Peru. The Nautilus, v. 130(3), p. 101-115.

DeVries, T.J. 2017. Eocene stratigraphy and depositional history near Puerto Caballas (East Pisco Basin, Peru). Boletín de la Sociedad Geológica del Perú, v. 112, p. 39-52.

DeVries, T.J., Narváez, Y., Sanfilippo, A., Malumian, N., Tapia, P. 2006. New microfossil evidence for a late Eocene age of the Otuma Formation (southern Peru). XIII Congreso Peruano de Geología, Lima, Peru, October, 2006, Sociedad Geológica del Perú, Publicación Especial, v. 7, p. 615-618.

DeVries, T.J., Pearcy, W.G. 1982. Fish debris in sediments of the upwelling zone off central Peru: a late Quaternary record. Deep-Sea Research, v. 28(1A), p. 87-109.

DeVries, T.J., Schrader, H. 1981. Variation of upwelling/oceanic conditions during the latest Pleistocene through Holocene off the central Peruvian coast: a diatom record. Marine Micropaleontology, v. 6, p. 157-167.

DeVries, T.J., Schrader, H. 1997. Middle Miocene marine sediments in the Pisco basin (Peru). Boletín de la Sociedad Geológica del Perú, v. 87, p. 1-13.

DeVries, T.J., Urbina, M., Jud, N.A. 2017. The Eocene-Oligocene Otuma depositional sequence (East Pisco Basin, Peru): Paleogeographic and paleoceanographic implications of new data. Boletín de la Sociedad Geológica del Perú, v. 112, p. 14-38.

DeVries, T.J., Vermeij, G. 1997. *Herminespina*: new genus of Neogene muricid gastropod from Peru and Chile. Journal of Paleontology, v. 71, p. 610-615.

Di Celma, C. Malinverno, E., Bosio, G., Collareta, A., Gariboldi, K., Gioncada, A., Molli, G., Basso, D., Varas-Malca, R., Pierantoni, P.P., Villa, I.M., Lambert, O., Landini, W., Sarti, G., Cantalamessa, G., Urbina, M., Bianucci, G. 2017. Sequence stratigraphy and paleontology of the upper Miocene Pisco Formation along the western side of the lower Ica valley (Ica Desert, Peru). Rivista Italiana di Paleontologia e Stratigrafia, v. 123(2), p. 255-273.

Dott, R.H., Jr., Bourgeois, J. 1982. Hummocky stratification: significance of its variable bedding sequences. Geological Society of America Bulletin, v. 93, p. 663-680.

Doweld, A.B. 2017. (2548) Proposal to conserve the name *Palmoxylon* against *Fasciculites* and *Perfossus* (fossil Arecales). *Taxon*, v. *66*(4), p. 989–991.

Dunbar, R.B., Marty, R.C., Baker, P.A. 1990. Cenozoic marine sedimentation in the Sechura and Pisco basins, Peru. Palaeogeography, Palaeoclimatology, Palaeoecology, v. 77, p. 235-261.

Dworschak, P.C., Rodrigues, S. de A. 1997. A modern analogue for the trace fossil *Gyrolithes*: burrows of the thalassinidean shrimp *Axianassa australis*. Lethaia, v. 30, p. 41-52.

Ehret, D.J., MacFadden, B.J., Jones, D.S., DeVries, T.J., Foster, D.A., Salas-Gismondi, R. 2012. Origin of the white shark *Carcharodon* (Lamniformes: Lamnidae) based on the recalibration of the upper Neogene Pisco Formation of Peru. Palaeontology, v. 55, p. 1139-1153.

Eiserhardt, W., Svenning, J.-C., Kissling, W.D., Balslev, H. 2011. Geographical ecology of the palms (Arecaceae): Determinants of diversity and distributions across spatial scales. Annals of Botany, v. 108(8), p. 1391-1416.

Esperante, R., Brand, L.R., Chadwick, A.V., Poma P., O. 2015. Taphonomy and paleoenvironmental conditions of deposition of fossil whales in the diatomaceous sediment of the Miocene/Pliocene Pisco Formation, southern Peru: a new fossil-Lagerstatte. Palaeogeography, Palaeoclimatology, Palaeoecology, v. 417, p. 337-370.

Feldens, P., Schwarzer, K., Sakuna, D., Szczucinski, W., Sompongchaiyakul, P. 2012. Sediment distribution on the inner continental shelf off Khao Lak (Thailand) after the 2004 Indian Ocean tsunami. Earth Planets and Space, v. 64, p. 875-887.

Fourtanier, E. 1991. Diatom biostratigraphy of equatorial Indian Ocean Site 758. In: Proceedings of the Ocean Drilling Program, Scientific Results, Weissel, J., Pierce, J., Taylor, E., Alt, J., et al. (editors), Ocean Drilling Program, College Station, Texas, USA, v. 121, p. 189-208.

Gariboldi, K., Gioncada, A., Bosio, G., Malinverno, E., Di Celma, C., Chiara, T., Cantalamessa, G., Landini, W., Urbina Schmitt, M., Bianucci, G. 2015. The dolomitic nodules enclosing fossil marine vertebrates in the East Pisco Basin, Peru: Field and petrographic insights into their genesis and role in preservation. Palaeogeography, Palaeoclimatology, Palaeoecology, v. 438, p. 81-95.

Gilkinson, K.D., Gagnon, J.M. 1991. Substratum associations of natural populations of Iceland scallops, *Chlamys islandica* Muller 1776, on the northeastern Grand Bank of Newfoundland. American Malacological Bulletin, v. 9, p. 59-67.

Goff, J., Chagué-Goff, C. 2009. A brief communication: Cetaceans and tsunamis – whatever remains, however improbable, must be the truth? Natural Hazards and Earth Systems Sciences, v. 9, p. 855-857.

Goto, K., Chavanich, S.A., Imamura, F., Kunthasap, P., Matsui, T., Minoura, K., Sugawara, D., Yanagisawa, H. 2007. Distribution, origin, and transport process of boulders deposited by the 2004 Indian Ocean tsunami at Pakarang Cape, Thailand. Sedimentary Geology, v. 202, p. 821-837.

Goto, K., Satake, K., Sugai, T., Ishibe, T., Harada, T., Murotani, S. 2015. Historical tsunami and storm deposits during the last five centuries on the Sanriku coast, Japan. Marine Geology, v. 367, p. 105-117.

Greenwood, D.R., Wing, S.L. 1995. Eocene continental climates and latitudinal temperature gradients. Geology, v. 23(11), p. 1044-1048.

Gutierrez A., D. 1948. Estudio de algunos fósiles del Terciario de Paracas. Senior thesis, Universidad Nacional Mayor de San Marcos, Lima, Peru. Pagination unknown.

Gutierrez-Mas, J.M. 2011. *Glycymeris* shell accumulations as indicators of recent sea-level changes and high-energy events in Cadiz Bay (SW Spain). Estuarine, Coastal and Shelf Science, v. 92, p. 546-554.

Haas, H., Rowe, N.P. 1999. Thin sections and wafering. In: Fossil Plants and Spores: Modern Techniques, Jones, T.P., Rowe, N.P. (editors), Geological Society of London, Bath, United Kingdom, p. 76-81.

Haq, B.U., Hardenbol, J., Vail, P.R. 1987. Chronology of fluctuating sea levels since the Triassic. Science, v. 235, p. 1156-1167.

Hardenbol, J., Thierry, M.B., Farley, M.B., Jacquin, T., Graciansky, P.C. de, Vail, P.R. 1998. Mesozoic and Cenozoic sequence chronostratigraphic framework of European basins. In: Mesozoic and Cenozoic Sequence Stratigraphy of European Basins, Graciansky, P.C., et al. (editors), Society of Economic Paleontologists and Mineralogists (SEPM), Special Publication, v. 60, p. 3-13.

Hartley, A., Howell, J., Mather, A.E., Chong, G. 2001. A possible Plio-Pleistocene tsunami deposit, Hornitos, northern Chile. Revista Geológica de Chile, v. 28, p. 117-125.

Harwood, D., Maruyama, T. 1992. Oligocene to Pleistocene diatom biostratigraphy of Southern Ocean sediments from the Kerguelen Plateau. In: Proceedings of the Ocean Drilling Program, Scientific Results, Wise, S.W., Jr., Schlich, R. (editors), Ocean Drilling Program, College Station, Texas, USA, v. 120, p. 683-733.

Ibaraki, M. 1993. Eocene to early Miocene planktonic foraminifera from the south of Paracas, central Peru. Shizuoka University, Report of the Faculty of Sciences, v. 27, p. 77-93.

Ishimura, D., Miyauchi, T. 2017. Holocene environmental changes and paleo-tsunami history in Onuma on the southern part of the Sanriku Coast, northeast Japan. Marine Geology, v. 386, p. 126-139.

Kato, M. 1996. The unique intertidal subterranean habitat and filtering system of a limpt-like brachiopod, *Discinisca sparselineata*. Canadian Journal of Zoology, v. 74, p. 1983-1988.

Katz, T., Ginat, H., Eyal, G., Steiner, Z., Braun, Y., Shalev, S., Goodman-Tchernov, B.N. 2015. Desert flash floods form hyperpycnal flows in the coral-rich Gulf of Aqaba, Red Sea. Earth and Planetary Science Letters, v. 417, p. 87-98.

Kominz, M.A., Browning, J.V., Miller, K.G., Sugarman, P.J., Mizintseva, S., Scotese, C.R. 2008. Late Cretaceous to Miocene sea-level estimates from the New Jersey and Delaware coastal plain coreholes: an error analysis. Basin Research, v. 20, p. 211-226.

LaBarbera, M. 1985. Mechanisms of spatial competition of *Discinisca strigata* (Inarticulata: Brachiopoda) in the intertidal of Panama. Biological Bulletin (Woods Hole, Massachusetts), v. 168, p. 91-105.

Laharie, R. 1976. Recherches géomorphologiques sur le néogène du sud du Pérou. Bulletin de l'Institut Français d'Études Andines, v. 5, p. 9-37.

Lambert, O., Bianucci, G., Post, K., Muizon, C. de, Salas-Gismondi, R., Urbina, M., Reumer, J. 2010. The giant bite of new raptorial sperm while from the Miocene Epoch of Peru. Nature, v. 466, p. 105-108.

Larcher, W., Winter, A. 1981. Frost susceptibility of palms: Experimental data and their interpretation. Principes, v. 25, p. 143-152.

Leckie, R.M., Farnham, C., Schmidt, M.G. 1993. Oligocene planktonic foraminifer biostratigraphy of Hole 803D (Ontong Java Plateau) and Hole 628A (Little Bahama Bank), and comparison with the southern high latitudes. In: Proceedings of the Ocean Drilling Program, Scientific Results, Berger, W.H., Kroenke, L.W., Mayer, L.A., et al. (editors), Ocean Drilling Program, College Station, Texas, USA, v. 130, p. 113-136.

León, W., Rosell, W., Aleman, A., Torres, V., Cruz, O. de la. 2008. Estratigrafía, sedimentología, y evolución tectónica de la Cuenca Pisco Oriental. Instituto Geológico Minero y Metalúrgico (INGEMMET), Estudios Regionales, Serie D, Boletín, v. 27, 154 p.

Le Roux, J.P. 2015. A critical examination of evidence used to re-interpret the Hornitos mega-breccia as a mass-flow deposit caused by cliff failure. Andean Geology, v. 42, p. 139-145.

Levin, L.A., Gutíerrez, D., Rathburn, A., Neira, C., Sellanes, J., Muñoz, P., Gallardo, V.A., Salamanca, M. 2002. Benthic processes on the Peru Margin: A transect across the oxygen minimum zone during the 1997–98 El Niño. Progress in Oceanography, v. 53, p. 1-27.

Loutit, T.S., Hardenbol, J., Vail, P.R., Baum, G.R. 1988. Condensed sections: the key to age determination and correlation of continental margin sections. Society of Economic Paleontologists and Mineralogists (SEPM), Special Publication, v. 42, p. 183-213.

Macharé, J. 1987. La marge continentale du Pérou: Régimes tectoniques et sédimentaires cénozoiques de l'avant-arc des Andes centrales. Ph.D. dissertation, Université de Paris XI, Orsay, France, 391 p.

Macharé, J., DeVries, T., Barron, J., Fourtanier, E. 1988. Oligo-Miocene transgression along the Pacific margin of South America: new paleontological and geological evidence from the Pisco basin (Peru). Géodynamique, v. 3, p. 25-37.

Macharé, J., Fourtanier, E. 1987. Datation des formations Tertiaires du bassin de Pisco (Perou) à partir d'associations de diatomé. Académie des Sciences (Paris), Comptes Rendus, Séries II, v. 305, p. 407-412.

Mamani, M., Woerner, G., Sempere, T. 2010. Geochemical variations in igneous rocks of the Central Andean Orocline (13°S to 18°S); tracing crustal thickening and magma generation through time and space. Geological Society of America Bulletin, v. 122 (1-2), p. 162-182.

Marocco, R., Muizon, C. de. 1988. Le Bassin Pisco, bassin cénozoïque d'avant arc de la côte du Pérou central; analyse géodynamique de son remplissage. Géodynamique, v. 3, p. 3-19.

Martinez-Córdova, L.R. 1996. Contribución al conocimiento de la fauna malacológica de cuatro lagunas costeras del estado de Sonora, México. Ciencias Marinas, v. 22, p. 191-203.

Marty, R.C. 1989. Stratigraphy and chemical sedimentology of Cenozoic biogenic sediments from the Pisco and

Sechura basins, Peru. Ph.D. dissertation, Rice University, Houston, Texas, USA, 268 p.

Maruyama, T. 2000. Middle Miocene to Pleistocene diatom stratigraphy of Leg 167. In: Proceedings of the Ocean Drilling Program, Scientific Results, Lyle, M., Koizumi, I., Richter, C., Moore, T.C., Jr. (editors), Ocean Drilling Program, College Station, Texas, USA, v. 167, p. 1-48.

Marx, F.G., Lambert, O., Muizon, C. de. 2017. A new Miocene baleen whale from Peru deciphers the dawn of cetotherids. Royal Society Open Science, v. 4, 170560. http://d.doi.org/10.1098/rsos.170560, 22 p.

McCaffrey, M.A., Farrington, J.W., Repeta, D.J. 1989. Geochemical implications of the lipid composition of *Thioploca* spp. from the Peru upwelling region—15°S. Organic Geochemistry, v. 14, p. 61-68.

Miller, K.G., Kominz, M.A., Browning, J.V., Wright, J.D., Mountain, G.S., Katz, M.E., Sugarman, P.J., Cramer, B.S., Christie-Blick, N., Pekar, S.F. 2005. The Phanerozoic record of global sea-level change. Science, v. 310, p. 1293-1298.

Miller, K.G., Mountain, G.S., Browning, J.V., Kominz, M., Sugarman, P.J., Christie-Blick, N., Katz, M.E., Wright, J.D. 1998. Cenozoic global sea level, sequences, and the New Jersey transect: results from coastal plain and continental slope drilling. Review of Geophysics, v. 36, p. 569-601.

Montoya, M., Garcia, W., Caldas, J. 1994. Geología de los cuadrángulos de Lomitas, Palpa, Nasca, y Puquio. Instituto Geológico Minero y Metalúrgico (INGEMMET), Boletín, Series A, Carta Geológica Nacional, v. 53, 100 p.

Moore, A., Nishimura, Y., Gelfenbaum, G., Kamataki, T., Triyono, R. 2006. Sedimentary deposits of the 26 December 2004 tsunami on the northwest coast of Aceh, Indonesia. Earth, Planets and Space, v. 58(2), p. 253-258.

Moore, H.B., López, N.N. 1970. A contribution to the ecology of the lamellibranch *Dosinia elegans*. Bulletin of Marine Science, v. 20, p. 980-986.

Muizon, C. de. 1988. Les vertébrés fossiles de la formation Pisco (Pérou): biostratigraphie, corrélations et paléoenvironnement. Géodynamique, v. 3, p. 21-24.

Muizon, C. de, DeVries, T.J. 1985. Geology and paleontology of late Cenozoic marine deposits in the Sacaco area (Peru). Geologisches Rundschau, v. 74, p. 547-563.

Netto, R.G., Buatois, L.A., Mangano, M.G., Balistieri., P. 2007. *Gyrolithes* as a multipurpose burrow: an ethologic approach. Revista Brasileira de Paleontologia, v. 10, p. 157-168.

Newell, N.D. 1956. Reconocimiento geológico de la región Pisco-Nazca. Boletín de la Sociedad Geológica del Perú, v. 30, p. 261-295.

Nielsen, S.N. 2003. Die marinen Gastropden (exklusive Heterostropha) aus dem Miozän von Zentralchile. Ph.D. dissertation, Universität Hamburg, Hamburg, Germany, 229 p.

Nielsen, S.N., DeVries, T.J. 2002. Tertiary Xenophoridae of western South America. The Nautilus, v. 116(3), p. 71-78.

Niitsuma, S., Ford, K.H., Iwai, M., Chiyonobu, S., Sato, T. 2006. Data report: magnetostratigraphy and biostratigraphy correlation in pelagic sediments, ODP Site 1225, eastern equatorial Pacific. In: Proceedings of the Ocean Drilling Program, Scientific Results, Jørgensen, B.B., D'Hondt, S.L., Miller, D.J. (editors), Ocean Drilling Program, College Station, Texas, USA, v. 201, p. 1-19.

Noble, D.C., Sebrier, M., Megard, F., McKee, E.H. 1985. Demonstration of two pulses of Paleogene deformation in the Andes of Peru. Earth and Planetary Science Letters, v. 73, p. 345-349.

Olsson, A.A. 1928. Contributions to the Tertiary paleontology of northern Peru. Part 1, Eocene Mollusca and Brachiopoda. Bulletins of American Paleontology, v. 14, p. 47-164.

Olsson, A.A. 1929. Contributions to the Tertiary paleontology of northern Peru. Part 2, Upper Eocene Mollusca and Brachiopoda. Bulletins of American Paleontology, v. 15, p. 67-116.

Olsson, A.A. 1932. Contributions to the Tertiary paleontology of northern Peru. Part 5, The Peruvian Miocene. Bulletins of American Paleontology, v. 19, p. 1-272.

Paine, R.T. 1962. Filter-feeding pattern and local distribution of the brachiopod, *Discinisca strigata*. Biological Bulletin (Woods Hole, Massachusetts), v. 123(3), p. 597-604.

Paris, R., Fournier, J., Poizot, E., Etienne, S., Morin, J., Lavigne, F., Wassmer, P. 2010. Boulder and fine sediment transport and deposition by the 2004 tsunami in Lhok Nga (western Banda Aceh, Sumatra, Indonesia): a coupled offshore-onshore model. Marine Geology, v. 268, p. 43-54.

Paris, R., Lavigne, F., Wassmer, P., Sartohadi, J. 2007. Coastal sedimentation associated with the December 26, 2004 tsunami in Lhok Nga, west Banda Aceh (Sumatra, Indonesia). Marine Geology, v. 238 (1-4), p. 93-106.

Patruno, S. 2015. Quantitative characterisation of deltaic and subaqueous clinoforms. Earth-Science Reviews, v. 142, p. 79-119.

Pecho G., V. 1983. Geología de los cuadrángulos de Pausa y Caravelí 31-p, 32-p. Instituto Geológico Minero Metalúrgico (INGEMMET), Serie A (Carta Geológica Nacional), Boletín, v. 3, 125 p.

Petersen, G. 1954. Informe preliminar sobre la geología de la faja costanera del Departamento de Ica. Boletín Técnico de la Empresa Petrolera Fiscal (Lima), v. 1, p. 33-34.

Philippi, R.A. 1887. Los fósiles terciarios i cuartarios de Chile. Brockhaus, Leipzig, 312 p.

Posamentier, H.W., James, D.P. 1993. An overview of sequence-stratigraphic concepts: uses and abuses. In: Sequence Stratigraphy and Facies Associations, Posamentier, H.W., Summerhayes, C.P., Haq, B.U., Allen, G.P. (editors), Blackwell, Oxford, Great Britain, p. 3-18.

Ramsey, A.T.S., Baldauf, J.G. 1999. A reassessment of the Southern Ocean biochronology. Geological Society of London, Memoir, v. 18, 122 p.

Rivera, R. 1957. Moluscos fósiles de la formación Paracas, departamento de Ica. Boletín de la Sociedad Geológica del Perú, v. 32, p. 165-219.

Rønning, P.O. 1990. Evolution and paleoceanography of the Pisco Basin (Peru). Masters thesis, Oppgave Geologisk Institutt Avdeling B, Universitetet I, Bergen, Norway, 135p.

Royer, D.L., Osborne, C.P., Beerling, D.J. 2002. High CO_2 increases the freezing sensitivity of plants: Implications for

paleoclimatic reconstructions from fossil floras. Geology, v. 30(11), p. 963-966.

Rüegg, W. 1948, Investigación geológica preliminar en la Península de Paracas y región de Pisco. Instituto Geológico del Perú con mapas y perfiles, Lima, Inédito.

Rüegg, W. 1956. Geologie zwischen Cañete-San Juan (13°00'-15°24') Südperu. Geologische Rundschau, v. 45, p. 775-858.

Sakuna, D., Szczucinski, W., Feldens, P., Khokiattiwong, S. 2012. Sedimentary deposits left by the 2004 Indian Ocean tsunami on the inner continental shelf offshore of Khao Lak, Adaman Sea (Thailand). Earth, Planets and Space, v. 64, p. 931-943.

Salas, R., Stucchi, M., DeVries, T.J. 2003. The presence of Plio-Pleistocene *Palaeolama* sp. (Artiodactyla: Camelidae) on the southern coast of Peru. Bulletin de l'Institut Français d'Études Andines, v. 32, p. 347-359.

Savrda, C.E. 1995. Ichnologic applications in paleoceanographic, paleoclimatic, and sea-level studies. Palaios, v. 10, p. 565-577.

Schenk, A. von. 1882. Die Perfossus-Arten Cotta's. In: Botanische Jahrbücher für Systematik, Pflanzengeschichte und Pflanzengeographie, Engler, A., v. 3(5), p. 483-486.

Schoene, B.R., Flessa, K.W., Dettman, D.L., Roopnarine, P.D. 2002. Sclerochronology and growth of the bivalve mollusks *Chione* (*Chionista*) *fluctifraga* and *C.* (*Chionista*) *cortezi* in the northern Gulf of California, Mexico. Veliger, v. 45, p. 45-54.

Shiki, T., Yamazaki, T. 1996. Tsunami-induced conglomerates in Miocene upper bathyal deposits, Chita Peninsula, central Japan. Sedimentary Geology, v. 104, p. 175-188.

Shipboard Scientific Party, 2000. Leg 186 explanatory notes. In: Proceedings of the Ocean Drilling Program, Initial Reports, Sacks, I.S., Suyehiro, K., Acton, G.D., et al. (editors), Ocean Drilling Program, College Station Texas, USA, v. 186, p. 1-37.

Shipboard Scientific Party, 2004. Leg 207 Explanatory notes. In: Proceedings of the Ocean Drilling Program, Initial Reports, Erbacher, J., Mosher, D.C., Malone, M.J., et al. (editors), Ocean Drilling Program, College Station Texas, USA, v. 207, p. 1-94.

Sivan, D., Potasman, M., Almogi-Labin, A., Bar-Yosef Mayer, D.E., Spanier, E., Boaretto, E. 2006. The *Glycymeris* query along the coast and shallow shelf of Israel, southeast Mediterranean. Palaeogeography, Palaeoclimatology, Palaeoecology, v. 233, p. 134-148.

Spiske, M., Bahlburg, H., Weiss, R. 2014. Pliocene mass failure deposits mistaken as submarine tsunami backwash sediments: An example from Hornitos, northern Chile. Sedimentary Geology, v. 305, p. 69-82.

Stainforth, R., Rüegg, W. 1953. Mid-Oligocene transgression in southern Peru. American Association of Petroleum Geologists (AAPG), Bulletin, v. 37, p. 568-569.

Steinmann, G. 1930. Geología del Perú. Carl Winter, Heidelberg, 462 p.

Stock, C.E. 1990. Tertiary geology of the Quebrada Huaricangana area, East Pisco Basin, southern Peru: Late Paleogene to Neogene transgressive sedimentation within a forearc basin. Masters thesis, Rice University, Houston, Texas, USA, 228 p.

Stucchi, M. 2003. Los piqueros (Aves: Sulidae) de la formación Pisco, Perú. Boletín de la Sociedad Geológica del Perú, v. 95, p. 75-91.

Stucchi, M. 2007. Los pinguinos de la Formación Pisco (Neógeno), Peru. Cuadernos del Museo Geominero (Madrid, Spain), v. 8, p. 367-373.

Stucchi, M., Varas-Malca, R.M., Urbina-Schmitt, M. 2016. New Miocene sulid birds from Peru and considerations on their Neogene fossil record in the Eastern Pacific Ocean. Acta Palaeontologica Polonica, v. 61, p. 417-427.

Suess, E., von Huene, R. 1988. Ocean Drilling Program Leg 112, Peru continental margin: Part 2, Sedimentary history and diagenesis in a coastal upwelling environment. Geology, v. 16, p. 939-943.

Tachibana, T., Tsuji, Y. 2013. Geological and hydrological examination of the bathyal tsunamigenic origin of Miocene conglomerates in Chita Peninsula, central Japan. Pure and Applied Geophysics, v. 168, p. 997-1014.

Tamura, T., Sawai, Y., Ikehara, K., Nakashima, R., Hara, J., Kanai, Y. 2015. Shallow-marine deposits associated with the 2011 Tohoku-oki tsunami in Sendai Bay, Japan. Journal of Quaternary Science, v. 30(4), p. 293-297.

Thomas, R., Boura, A. 2015. Palm stem anatomy: Phylogenetic or climatic signal? Botanical Journal of the Linnean Society, v. 178(3), p. 467-88.

Thomas, R., De Franceschi, D. 2013. Palm stem anatomy and computer-aided identification: The Coryphoideae (Arecaceae). American Journal of Botany, v. 100(2), p. 289-313.

Tomlinson, P.B., Horn, J.W., Fisher, J.B. 2011. The anatomy of palms: Arecaceae - Palmae. Annals of Botany, v. 108(8), 276 p.

van Wagoner, J.C., Posamentier, H.W., Mitchum, R.M., Vail, P.R., Sarg, J.F., Loutit, T.S., Hardenbol, J. 1988. An overview of the fundamentals of sequence stratigraphy and key definitions. In: Sea-level Changes: an Integrated Approach, Wilgus, CK., Hastings, B.S., Kendall, C.G.St.C., Posamentier, H.W., Ross, C.A., Van Wagoner, J.C., (editors), Society of Economic Paleontologists and Mineralogists (SEPM), Special Publication, v. 42, p. 39-45.

Varas-Malca, R.M., Valenzuela-Toro, A.M. 2011. A basal monachine seal from the middle Miocene of the Pisco Formation, Peru. Ameghiniana, v. 48, p. R216-R217.

Vargas-Zamora, J.A., Sibaja-Cordero, J.A. 2011. Molluscan assemblage from a tropical estuarine sand-mud flat, Gulf of Nicoya, Pacific, Costa Rica (1984-1987). Revista de Biología Tropical, v. 59, p. 1135-1148.

Vermeij, G., DeVries, T.J. 1997. Taxonomic remarks on Cenozoic pseudolivid gastropods from South America. The Veliger, v. 40, p. 23-28.

Vokes, H.E. 1969. Observations on the genus *Miltha* (Mollusca: Bivalvia) with notes on the type and the Florida Neogene species. Tulane Studies in Geology and Paleontology, v. 7(3), p. 94-126.

Walther, G.-R., Gritti, E.S., Berger, S., Hickler, T., Tang, Z., Sykes, M.T. 2007. Palms tracking climate change. Global Ecology and Biogeography, v. 16(6), p. 801-809.

Woods, H. 1922. Mollusca from Eocene and Miocene deposits of Peru. In: Geology of the Tertiary and Quaternary Periods in the northern part of Peru, Bosworth, T.O., Macmillan, London, p. 51-113.

Zettler, M.L., Bochert, R., Pollehne, F. 2009. Macrozoobenthos diversity in an oxygen minimum zone off northern Namibia. Marine Biology, v. 156, p. 1949-1961.

Appendix I.

Locality latitude and longitude coordinates. Localities of DeVries are preceded in the text with the letters "DV." Localities of José Macharé are preceded with two numbers and the letters "JM."

376	14°35'15”S	75°37'22”W
377	14°45'45”S	75°30'27”W
379	14°35'01”S	75°40'54”W
381	15°23'24"S	73°03'26"W
387	14°58'44"S	75°19'23"W
391	14°10'18"S	76°05'43"W
394	14°11'54"S	76°08'41"W
395	14°10'04”S	76°07'05”W
396	14°11'20”S	76°06'23”W
397	14°11'15”S	76°05'35”W
411	13°53'51"S	76°09'22"W
417	13°56'46”S	76°05'09”W
419	13°57'28”S	76°06'59”W
420	13°57'48”S	76°07'18”W
421a	14°57'08"S	75°18'06"W
422	14°56'06"S	75°17'35"W
423	14°56'44"S	75°18'59"W
441	14°11'31”S	76°06'56”W
442	14°11'27"S	76°06'29"W
443	14°11'21”S	76°06'24”W
451	13°57'19”S	76°07'19”W
452	13°57'49”S	76°07'12”W
456	14°22'42"S	75°36'27"W
467	15°23'22"S	75°09'06"W
468a	15°17'58"S	75°08'26"W
477	14°11'16"S	76°05'55"W
478	14°11'23”S	76°06'23”W
479	14°10'49"S	76°05'25"W
480	14°11'30”S	76°04'50”W
484	14°35'38"S	75°40'10"W
489	14°32'23”S	75°39'31”W
494	14°25'22"S	75°41'12"W
499	14°34'57”S	75°39'46”W
501	13°54'39"S	76°21'29"W
502	13°48'15"S	76°20'43"W
505	14°26'39"S	75°40'55"W
507	14°38'02"S	75°38'27"W
517	15°34'14"S	74°43'33"W
522	14°50'19"S	75°21'50"W
531	14°58'14"S	75°17'58"W
532	14°55'06"S	75°15'33"W
542	14°35'31”S	75°40'15”W
542a	14°35'31”S	75°40'15”W
549	14°36'44”S	75°40'31”W
551	14°34'08”S	75°40'40”W
560	13°52'57"S	76°14'46"W
572	14°31'11"S	75°35'02"W
574	14°45'13"S	75°30'39"W
575	14°45'54”S	75°30'53”W
576	14°45'38”S	75°30'21”W
581	14°58'09"S	75°19'16"W
585	14°55'50"S	75°29'07"W
591	14°40'28”S	75°41'03”W
598	14°45'46”S	75°30'58”W
601	14°11'38”S	76°06'38”W
614	14°54'36"S	75°08'55"W
637	14°45'25”S	75°01'04”W
638	15°00'36"S	74°59'04"W
699	14°45'15”S	75°30'42”W
841	13°59'28”S	76°13'33”W
935	14°03'49”S	76°08'58”W
937	13°57'59"S	76°08'04"W
1002	14°04'05”S	76°09'18”W
1003	14°03'42”S	76°08'04”W
1004	14°00'58”S	76°08'14”W
1007	14°00'17”S	76°08'11”W
1008	14°00'27”S	76°07'57”W
1009	14°01'45”S	76°05'03”W
1010	14°01'42”S	76°04'51”W
1011	14°01'37”S	76°04'42”W
1012	14°02'42”S	76°05'03”W
1013	14°03'32”S	76°05'15”W
1014	13°58'49”S	76°06'57”W
1017	14°35'13”S	75°35'29”W
1019	14°45'50”S	75°30'22”W
1021	14°44'19”S	75°31'02”W
1022	14°45'43”S	75°30'59”W
1023	14°47'19”S	75°30'29”W
1101	14°01'33”S	76°13'38”W
1105	14°05'00”S	76°09'58”W
1107	14°05'53”S	76°09'44”W
1108	14°04'08”S	76°09'17”W
1126	14°00'55”S	76°14'22”W
1129	14°00'54”S	76°13'10”W
1130	14°00'02”S	76°13'24”W
1131	13°59'48”S	76°13'38”W
1132	13°59'53”S	76°13'24”W
1133	14°05'40”S	76°13'12”W
1134	14°15'15”S	76°01'40”W
1174	14°08'37"S	76°10'16"W
1180	14°35'41”S	75°40'14”W
1181	14°35'41”S	75°40'15”W
1182	14°35'39”S	75°40'23”W
1183	14°35'37"S	75°40'04"W
1230	14°40'45”S	75°29'20”W
1232	14°42'11"S	75°31'04"W
1234b	14°41'43"S	75°32'45"W
1237	15°18'29"S	75°07'27"W
1251	15°48'42"S	74°21'24"W
1256	15°56'27”S	73°19'40”W
1258	15°56'35”S	73°19'19”W
1259	15°58'44”S	73°18'07”W
1260	15°58'37”S	73°18'21”W
1265	16°23'59"S	73°12'42"W
1266	16°24'00"S	73°12'41"W
1301	14°45'19”S	75°30'40”W
1306	14°45'45”S	75°30'23”W
1307	14°45'48”S	75°30'23”W
1308	14°45'36”S	75°30'43”W
1309	14°45'25”S	75°30'43”W
1318	14°28'58"S	75°44'02"W
1322	14°26'04”S	75°51'00”W
1323	14°27'08”S	75°52'19”W
1324	14°27'35”S	75°51'32”W
1325	14°27'44”S	75°50'29”W
1326	14°26'34”S	75°50'24”W
1365	14°05'35”S	76°09'58”W
1366	14°05'56”S	76°09'45”W
1368	14°05'35”S	76°09'10”W
1372	15°33'58"S	74°51'02"W
1403	14°05'49”S	76°11'08”W
1404	14°05'57”S	76°09'44”W
1435	14°27'11”S	75°52'28”W
1456	14°51'21"S	75°25'47"W

1510	14°35'41"S	75°40'05"W
1605	14°31'11”S	75°39'43”W
1606	14°31'06”S	75°39'31”W
1608	14°35'24”S	75°38'18”W
1609	14°35'22”S	75°38'22”W
1611	14°34'52”S	75°38'40”W
1612	14°34'49”S	75°38'41”W
1613	14°33'45”S	75°38'58”W
1614	14°33'24”S	75°39'11”W
1615	14°41'32”S	75°35'16”W
1617	14°41'56”S	75°35'25”W
1620	14°41'52”S	75°35'42”W
1624	14°40'48”S	75°29'02”W
1625	14°40'47”S	75°29'35”W
1636	14°41'47”S	75°35'49”W
1637	14°41'27”S	75°35'55”W
1638	14°41'36”S	75°35'53”W
1639	14°38'13”S	75°37'45”W
1640	14°38'07”S	75°37'53”W
1642	14°37'37"S	75°37'53"W
1645	14°20'52”S	75°54'23”W
1646	14°20'37”S	75°54'18”W
1648	14°22'25”S	75°53'52”W
1653	14°50'16”S	75°27'29”W
1654	14°50'07”S	75°27'32”W
1655	14°50'26”S	75°27'38”W
1715	14°37'17"S	75°35'46"W
1728	14°33'22"S	75°52'49"W
1729	14°34'00”S	75°53'53”W
1801	14°35'39”S	75°40'16”W
1802	14°35'34”S	75°40'31”W
1805	14°35'33”S	75°40'18”W
1806	14°35'27”S	75°41'06”W
1807	14°35'01”S	75°40'55”W
1808	14°35'04"S	75°41'27"W
1809	14°35'44”S	75°41'33”W
1810	14°35'52”S	75°41'01”W
1811	14°38'45”S	75°37'59”W
1817	14°11'23"S	76°06'26"W
1819	14°08'40"S	76°10'27"W
1906	14°38'58"S	75°38'57"W
1959	14°55'53"S	75°29'07"W
1965	14°51'56"S	75°25'07"W
1970	14°59'59"S	75°59'01"W
2001	14°38'07”S	75°38'25”W
2012	14°36'24"S	75°34'26"W
2013	14°36'44"S	75°34'49"W
2014	14°33'50”S	75°40'11”W
2015	14°34'12”S	75°40'02”W
2016	14°34'11”S	75°39'59”W
2017	14°34'06”S	75°40'02”W
2018	14°33'12”S	75°39'42”W
2019	14°33'24”S	75°39'49”W
2028	14°34'22"S	75°36'51"W
2029	14°34'47”S	75°37'13”W
2030	14°34'54”S	75°37'32”W
2031	14°34'54”S	75°37'37”W
2032	14°35'56”S	75°38'04”W
2033	14°34'54”S	75°37'28”W
2034	14°45'24”S	75°30'40”W
2035	14°45'23”S	75°30'32”W
2043	13°55'39"S	76°16'52"W
2047	14°00'57”S	76°14'35”W
2048	14°00'48”S	76°15'01”W
2202	14°36'32"S	75°38'28"W
2203	14°37'45”S	75°38'00”W
2204	14°37'45”S	75°38'04”W
2205	14°38'00”S	75°38'02”W
2206	14°37'43”S	75°38'02”W
2207	14°37'30”S	75°38'15”W
2208	14°37'22”S	75°38'14”W
2209	14°37'29"S	75°38'07"W
2210	14°36'55”S	75°38'50”W
2211	14°34'06”S	75°43'47”W
2212	14°36'46”S	75°45'49”W
2215	14°33'17"S	75°53'23"W
2216	14°33'29"S	75°52'59"W
2217	14°33'48”S	75°53'46”W
2231	14°20'52”S	75°54'23”W
2232	14°22'47”S	75°53'58”W
2237	14°22'30”S	75°53'46”W
2238	14°22'34”S	75°53'45”W
2239	14°22'42”S	75°53'45”W
2240	14°22'49”S	75°53'36”W
2243	14°22'59”S	75°53'55”W
2244	14°22'47”S	75°53'58”W
2249	14°23'02"S	75°53'59"W
2252	14°23'44”S	75°53'24”W
2253	14°23'43”S	75°53'20”W
2257	14°21'47”S	75°53'57”W
2261	14°10'46”S	76°08'00”W
3004	14°34'36"S	75°39'55"W
3018	14°06'38"S	76°10'01"W
3021	14°22'58"S	75°57'02"W
3023	14°27'58”S	75°55'32”W
3024	14°27'41”S	75°55'41”W
3036	14°16'29”S	75°57'13”W
3042	14°34'07”S	75°43'39”W
3043	14°34'16”S	75°43'41”W
3044	14°30'39"S	75°43'57"W
3045	14°30'34"S	75°43'59"W
3050	14°33'35”S	75°39'59”W
3053	14°33'33”S	75°39'48”W
3054	14°33'34”S	75°39'51”W
3081	14°31'11”S	75°39'43”W
3087	14°34'16”S	75°40'33”W
3088	14°35'25”S	75°41'08”W
3090	14°39'55”S	75°53'42”W
3091	14°33'46”S	75°53'45”W
4006	14°11'15”S	76°07'07”W
4007	14°11'17”S	76°07'01”W
4010	14°11'01"S	76°05'32"W
4011	14°11'10"S	76°05'30"W
4012	14°11'11"S	76°05'31"W
4015	14°10'43”S	76°05'19”W
4017	14°10'50”S	76°05'23”W
4018	14°45'24”S	75°30'46”W
4019	14°45'18”S	75°30'46”W
4021	14°43'43”S	75°31'04”W
4022	14°40'47”S	75°36'32”W
4023	14°41'15”S	75°36'12”W
4031	14°39'02”S	75°39'54”W
4032	14°39'18”S	75°38'32”W
4033	14°39'44”S	75°39'59”W
4039	14°34'34”S	75°38'46”W
4040	14°34'34"S	75°38'31"W
4041	14°33'35"S	75°39'48"W
4043	14°21'58”S	75°53'28”W
4044	14°22'28”S	75°53'03”W
4046	14°22'18”S	75°52'50”W
4047	14°23'13”S	75°52'59”W
4048	14°23'18”S	75°53'17”W
4049	14°24'05”S	75°52'28”W
4050	14°24'06”S	75°52'08”W
4064	14°35'35”S	75°40'28”W
4065	14°34'11”S	75°40'02”W
4066	14°21'49”S	75°54'23”W
4067	14°21'46”S	75°54'21”W

4068	14°21'44"S	75°54'18"W
4069	14°21'43"S	75°54'16"W
4071	14°22'58"S	75°53'55"W
4076	14°22'55"S	75°53'52"W
4077	14°23'33"S	75°53'54"W
4082	14°23'06"S	75°52'58"W
4083	14°22'54"S	75°52'53"W
4086	14°25'38"S	75°50'26"W
4087	14°25'04"S	75°49'59"W
4099	14°34'08"S	75°40'09"W
4100	14°34'25"S	75°40'07"W
4101	14°34'27"S	75°40'12"W
4102	14°34'18"S	75°40'29"W
4104	14°34'01"S	75°40'57"W
4109	14°35'18"S	75°40'38"W
5001	14°12'18"S	76°05'58"W
5002	14°09'59"S	76°04'44"W
5004	14°09'09"S	76°04'38"W
5006	14°09'37"S	76°08'09"W
5012	14°09'17"S	76°08'13"W
5013	14°09'07"S	76°07'58"W
5014	14°09'01"S	76°07'50"W
5015	14°08'53"S	76°07'43"W
5016	14°08'58"S	76°07'32"W
5017	14°09'17"S	76°07'11"W
5019	14°10'29"S	76°07'31"W
5020	14°10'31"S	76°07'33"W
5021	14°10'22"S	76°07'47"W
5027	14°10'34"S	76°05'31"W
5028	14°10'20"S	76°05'27"W
5029	14°10'09"S	76°05'24"W
5030	14°10'11"S	76°05'34"W
5031	14°10'34"S	76°06'05"W
5032	14°10'30"S	76°06'09"W
5033	14°10'20"S	76°06'24"W
5036	14°40'46"S	75°28'25"W
5038	14°50'05"S	75°28'44"W
5039	14°50'18"S	75°28'12"W
5040	14°50'30"S	75°28'07"W
5043	14°50'24"S	75°27'34"W
5044	14°50'22"S	75°27'33"W
5047	14°50'04"S	75°29'45"W
5048	14°49'43"S	75°29'36"W
5050	14°49'06"S	75°29'16"W
5051	14°49'13"S	75°29'23"W
5052	14°49'13"S	75°29'21"W
5053	14°49'37"S	75°29'39"W
5054	14°49'31"S	75°29'40"W
5055	14°49'30"S	75°29'43"W
5060	14°45'56"S	75°30'22"W
5120	14°26'13"S	75°52'58"W
5121	14°27'06"S	75°51'51"W
7009	14°34'47"S	75°37'15"W
7010	14°44'38"S	75°30'47"W
7011	14°44'39"S	75°30'50"W
7013	14°34'12"S	75°40'51"W
7014	14°34'22"S	75°40'46"W
7015	14°34'19"S	75°40'46"W
7017	14°34'19"S	75°41'13"W
7018	14°34'31"S	75°41'05"W
7020	14°33'35"S	75°39'59"W
7022	14°48'24"S	75°29'58"W
7023	14°48'20"S	75°30'17"W
7024	14°48'16"S	75°30'03"W
7029	14°49'19"S	75°29'54"W
7030	14°49'18"S	75°29'57"W
7031	14°48'56"S	75°29'57"W
7032	14°48'57"S	75°30'00"W
7034	14°47'29"S	75°30'21"W
7035	14°47'31"S	75°30'28"W
7036	14°47'29"S	75°30'34"W
7039	14°47'28"S	75°30'17"W
7041	14°47'28"S	75°29'50"W
7089	14°21'05"S	75°54'54"W
7090	14°21'10"S	75°54'37"W
7091	14°21'36"S	75°54'26"W
7092	14°21'40"S	75°54'25"W
7093	14°21'38"S	75°54'18"W
7094	14°21'36"S	75°54'16"W
7095	14°21'05"S	75°55'10"W
7096	14°20'18"S	75°55'10"W
7098	14°21'46"S	75°54'32"W
7099	14°21'44"S	75°54'29"W
7105	14°23'33"S	75°53'26"W
7106	14°23'44"S	75°53'19"W
7108	14°23'10"S	75°53'30"W
7111	14°24'24"S	75°52'51"W
7112	14°24'53"S	75°53'12"W
7113	14°24'51"S	75°53'18"W
7114	14°24'50"S	75°53'18"W
8001	14°07'27"S	76°05'07"W
8002	14°08'18"S	76°06'47"W
8003	14°08'17"S	76°06'40"W
8007	14°08'51"S	76°06'59"W
8008	14°08'54"S	76°07'02"W
8015	14°13'20"S	76°06'22"W
8019	14°13'22"S	76°06'33"W
8020	14°13'09"S	76°06'45"W
8021	14°13'07"S	76°06'43"W
8022	14°12'06"S	76°06'21"W
8026	14°12'25"S	76°06'10"W
8027	14°12'21"S	76°06'15"W
8031	14°11'13"S	76°07'08"W
8036	14°23'38"S	75°53'18"W
8037	14°23'35"S	75°53'18"W
8042	14°23'06"S	75°52'43"W
8043	14°22'55"S	75°52'48"W
8044	14°23'09"S	75°52'56"W
8048	14°23'17"S	75°53'19"W
8049	14°24'58"S	75°53'09"W
8050	14°24'59"S	75°53'10"W
8051	14°25'03"S	75°53'14"W
8056	14°25'56"S	75°52'49"W
8057	14°25'51"S	75°52'37"W
8058	14°25'52"S	75°52'29"W
8059	14°25'45"S	75°52'19"W
8060	14°25'08"S	75°51'44"W
8061	14°24'58"S	75°51'39"W
8062	14°24'41"S	75°51'35"W
8065	14°24'18"S	75°51'23"W
8066	14°24'17"S	75°51'27"W
8067	14°24'21"S	75°51'35"W
8069	14°26'30"S	75°52'02"W
8073	14°22'47"S	75°53'00"W
8075	14°22'20"S	75°53'03"W
8076	14°22'21"S	75°53'19"W
8077	14°22'12"S	75°53'22"W
8078	14°22'06"S	75°53'30"W
8079	14°21'54"S	75°53'29"W
8080	14°21'49"S	75°53'40"W
8081	14°21'43"S	75°53'40"W
8082	14°21'39"S	75°53'45"W
8083	14°21'36"S	75°53'48"W
8084	14°21'06"S	75°54'09"W
8087	14°23'42"S	75°54'50"W
8089	14°23'45"S	75°54'32"W
8090	14°23'48"S	75°54'32"W
8102	14°43'18"S	75°33'39"W

8104	14°42'56"S	75°33'56”W
8106	14°42'41"S	75°33'51”W
8107	14°42'16"S	75°33'46”W
8108	14°42'07"S	75°34'05”W
8109	14°42'15"S	75°34'11”W
8110	14°42'17"S	75°34'09”W
8111	14°42'38"S	75°34'13”W
8114	14°44'34"S	75°32'50"W
8115	14°44'31"S	75°32'55"W
8116	14°44'26"S	75°32'54"W
8121	14°44'14"S	75°32'32”W
8123	14°44'09"S	75°32'27”W
8124	14°41'40"S	75°36'00”W
8125	14°41'45"S	75°36'00”W
8126	14°41'35"S	75°35'56”W
8127	14°41'27"S	75°35'55”W
8130	14°36'23"S	75°37'37”W
8131	14°36'57"S	75°37'40”W
8133	14°36'49"S	75°37'44”W
8134	14°36'44"S	75°37'45”W
8135	14°36'21"S	75°37'40”W
8137	14°35'57"S	75°37'21”W
8139	14°35'41"S	75°37'31”W
8141	14°34'46"S	75°37'18”W
82JM010b	15°18'30"S	75°07'00"W
84JM407	14°11'30"S	76°07'00"W